May 2013

Methods in Metallomics, Proteomics, and Toxicology: Development and Applications of Laser Ablation Inductively Coupled Plasma Mass Spectrometry and Native SDS-PAGE

William John Wobig
University of Wisconsin-Milwaukee

METHODS IN METALLOMICS, PROTEOMICS, AND TOXICOLOGY: DEVELOPMENT AND APPLICATIONS OF LASER ABLATION INDUCTIVELY COUPLED PLASMA MASS SPECTROMETRY AND NATIVE SDS-PAGE

by

William J. Wobig

A Thesis Submitted in
Partial Fulfillment of the
Requirements for the Degree of

Master of Science
in Chemistry

at

The University of Wisconsin-Milwaukee
May 2013

ABSTRACT

METHODS IN METALLOMICS, PROTEOMICS, AND TOXICOLOGY: DEVELOPMENT AND APPLICATIONS OF LASER ABLATION INDUCTIVELY COUPLED PLASMA MASS SPECTROMETRY AND NATIVE SDS-PAGE

by

William J. Wobig

The University of Wisconsin-Milwaukee, 2013
Under the Supervision of Dr. David H. Petering

Polyacrylamide gel electrophoresis (PAGE) is a bio-analytical method used to separate proteins in solution into an array of individual bands of proteins in a gel matrix. Current PAGE methods, however, have severe limitations in simultaneously maintaining a protein's native structure and association with transition metals while providing adequate resolution. Laser Ablation Inductively Coupled Plasma Mass Spectrometry (LA-ICP-MS) provides a means to perform trace to ultra-trace level inorganic analysis of solid samples such as dried PAGE gels containing metallo-protein arrays. Current LA-ICP-MS methods involving the analysis of PAGE gels, however, have been limited in their effective use by inadequate limits of detection to effectively detect trace level metallo-proteins on dried PAGE gels, and to date, have been mostly utilized as proof of principle experiments. The goal of this investigation was to develop a LA-ICP-MS method to provide adequate detection limits for trace level analysis of isolated metallo-protein

bands on dried PAGE gels, and to develop a native PAGE method to adequately resolve protein bands from complex protein mixtures in solution. In addition, a LA-ICP-MS method was developed to detect trace level amounts of toxic metals in organisms to provide a means of performing “top-down” experiments involving toxic metal trafficking from organism exposure, to protein targets of toxic metals. Data are presented in support of the newly developed PAGE-LA-ICP-MS, Native Sodium Dodecyl Sulfate PAGE method (NSDS-PAGE), and toxic metal analysis of organisms, which together provide the means to separate and detect metallo-proteins from complex proteomic samples, and locate toxic metal binding sites in organisms. These findings and new methods provide, for the first time, the means to effectively study complex protein mixtures in the context of metallomics, and identify toxic metal binding sites in organisms.

To my wife and family,

Your love, support, and encouragement enabled me to succeed.

To all of the science educators I have learned from and worked with,

Your passion for teaching inspired my passion for science.

TABLE OF CONTENTS

LIST OF FIGURES

LIST OF TABLES

LIST OF ABBREVIATIONS

AA	Amino Acid
ADH	Alcohol Dehydrogenase
AAS	Atomic Absorption Spectroscopy
β-ME	2-Mercaptoethanol
BN-PAGE	Blue Native Polyacrylamide Gel Electrophoresis
CA	Carbonic Anhydrase
DEAE	Diethylaminoethyl
ICP-MS	Inductively Coupled Plasma Mass Spectrometry
IEF	Isoelectric focusing
IEX	Ion Exchange Chromatography
LA	Laser Ablation
NSDS-PAGE	Native Sodium Dodecyl Sulfate Polyacrylamide Gel Electrophoresis
PMSF	Phenylmethanesulfonyl fluoride
SDS-PAGE	Sodium Dodecyl Sulfate Polyacrylamide Gel Electrophoresis
SOD	Superoxide Dismutase
TPEN	N,N,N’,N’-Tetrakis-(8-p-toluenesulfonamido)quinoline
TSQ	6-methoxy-(8-p-toluenesulfonamido)quinoline

1. Introduction

There are two major emerging fields of study in biochemistry which rely on numerous analytical techniques to explore their respective biochemical phenomena [1-17]. One field is proteomics, which is a branch of biotechnology concerned with applying the techniques of molecular biology, biochemistry, and genetics to analyzing the structure, function, and interactions of the proteins produced by the genes of a particular cell, tissue, or organism, with organizing the information in databases, and with applications of the data [18]. A second field metallomics, is a study of the metallome, interactions, and functional connections of metal ions and other metal species with genes, proteins, metabolites, and other biomolecules in biological systems [2]. There are a variety of analytical techniques that can be utilized, which begin at the cellular level of analysis, and terminate at the biomolecular and elemental level (Figure 1.1) [3-8, 11].

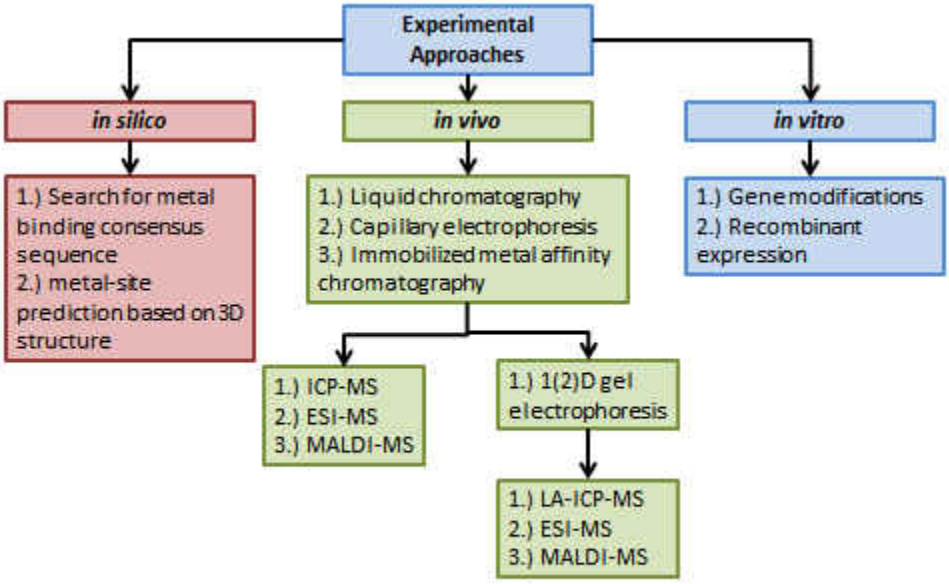

Figure 1.1. Flow chart of analytical techniques utilized in the study of proteomics and metallomics [3].

Numerous approaches for studying proteins in the aforementioned "-omics" are available involving direct or indirect analysis of protein samples. Indirect analysis of protein samples can be performed using *in silico* experiments. *In silico* analysis involves the utilization of genomic data bases and protein crystal structure information to determine hypothetical metal binding sites in proteins based upon their three dimensional structure and amino acid sequences [3,19-21]. Direct analysis of protein samples can be performed using *in vitro* experiments. Experiments which involve *in vitro* analysis, utilize gene modifications or recombinant expression of genes to determine their effect on metal binding proteins and regulation of the organism's

metallome[3]. A second approach in the direct analysis of protein samples can be performed using *in vivo* experiments. There are a variety of analytical approaches to performing *in vivo* experiments, all of which begin with either tissues or cell cultures [3-8]. These tissues and cell cultures are then homogenized to release the biomolecules from the cells into solution. The complex biomolecular solutions are then reduced in complexity using various liquid chromatographic techniques which separate the biomolecules based on size such as capillary electrophoresis, or their affinity for various metals using immobilized metal affinity chromatography. If adequate separation is achieved using liquid chromatography alone, the inorganic information of the biomolecules can be obtained using Inductively Coupled Plasma Mass Spectrometry (ICP-MS). In addition, the identity of the biomolecule can be determined using Electrospray Ionization Mass Spectrometry (ESI-MS) and/or Matrix Assisted Laser Desorption/Ionization Mass Spectrometry (MALDI-MS) [3,5]. If adequate separation cannot be achieved using liquid chromatography alone, a second separation step is necessary. Gel electrophoresis can be performed to separate the biomolecules in solution into an array of biomolecules in a gel. The inorganic information can then be obtained using X-ray absorption spectrometry or Laser Ablation Inductively Coupled Plasma Mass Spectrometry (LA-ICP-MS). In addition, the identity of the biomolecule can also be determined by the aforementioned ESI-MS and/or MALDI-MS techniques [3,5]. One analytical method progression for studying the proteins in the aforementioned "-omics" includes the experimentation with whole organisms or cell cultures, followed by homogenization of the tissue or cell culture, various liquid chromatography

separations of homogenized samples, separation of liquid chromatography fractionated samples on a polyacrylamide gel using polyacrylamide gel electrophoresis, and ultimately inorganic analysis using Laser Ablation Inductively Coupled Plasma Mass Spectrometry and/or identification using LC-MS coupled to genomic data base searches. Experiments utilizing this flow of experimental analysis have demonstrated promising results, yet often lack critical evaluation of results, and refinement of the methods utilized [4,5,7,11].

Polyacrylamide gel electrophoresis (PAGE) is an analytical method used to separate large biomolecules, typically proteins, in solution, into arrays of proteins in a polyacrylamide gel matrix [1,4-7,12-17]. The method employs the use of separated conductive buffers, and an applied electric potential to generate an electrochemical potential between the two separated conductive buffers. The polyacrylamide gel mediates this potential, which causes proteins coated with charged reagents to migrate through the gel. As the proteins permeate through the polyacrylamide gel, they are separated based upon size in the case of sodium dodecyl sulfate PAGE (SDS-PAGE) and Blue Native PAGE (BN-PAGE). The proteins in these gels can then be imaged by staining using various reagents including Coomassie R-250 and silver. The proteins molecular weight can be estimated by running markers containing proteins of known size for direct comparison [6]. Further analysis can also be performed such as identification of the proteins by LC-MS analysis coupled to genomic data base searches [3,5].

Current commercially available PAGE methods have substantial limitations for their utilization in isolating individual proteins from complex proteomic mixtures. BN-PAGE is widely known to have the capability of separating proteins in their native conformations [4]. However, upon critical evaluation, BN-PAGE provides poor resolution, making the separation of numerous proteins in a complex mixture difficult [12-14]. On the other end of the spectrum, SDS-PAGE, widely known to provide excellent resolution in the separation of numerous proteins in a complex mixture, also, denatures them in the process, making the study of their native metal complement difficult [4,15-17]. This particularly limits the use of SDS-PAGE in the study of metallomics, where the denaturation of proteins makes any evaluation of a protein's transition metal content problematic. These critical evaluations of PAGE methods prompt the need to develop a new PAGE method capable of separating complex protein mixtures, while maintaining their native complement of transition metals, in order to effectively study the metallo-proteome of a cell. Many of these proteins utilize transition metal cofactors to support their tertiary and quaternary structures, and in catalysis, including zinc, iron, and copper [4,19,20]. In addition, many of these proteins and metallo-proteins have been shown to react with heavy metals such as cadmium [22-25]. Cadmium has been shown to react with cysteine amino acid residues, as shown by the reaction of cadmium with the cysteine rich protein metallothionein, which have toxic effects on cells [25]. This further emphasizes the need for a PAGE method capable of resolving proteins in a complex mixture while maintaining their complement of native and/or toxic metals for further analysis.

Laser ablation utilizes a low wavelength, micro-focused, pulsed laser, in conjunction with a precisely controlled, motorized, sealed sample stage to ablate solid samples to an aerosol. This aerosol in then transported to an ICP-MS via carrier gases, typically helium and argon, for subsequent analysis [26,27]. ICP-MS utilizes a high energy and temperature ionization source to completely atomize and ionize samples for inorganic analysis [28]. The coupling of laser ablation and inductively coupled plasma mass spectrometry allows for the inorganic analysis of solid samples [26,27]. In the past decade, Laser Ablation Inductively Coupled Plasma Mass Spectrometry has emerged in the study transition metals in biological tissues and proteins [4,5,7]. Many of these experiments have only been proof of principle experiments, without focus being put into the development of robust and sensitive LA-ICP-MS methods for the analysis of transition metals in biological samples, especially proteins separated by PAGE [4,5]. Poor detection limits of 0.35 and 3.15 ppm for copper and zinc respectively determined from one such proof of principle experiment are not suitable for the analysis of complex protein mixtures containing trace levels of transition metals. Moreover, unspecified transition metal interferences have limited the use of LA-ICP-MS in its application to proteomics [4]. A calculation of the necessary amount of proteome needed to detect a single zinc protein can be performed using the previously determined detection limit of 3.15 ppm zinc as a benchmark for the analytical performance of the LA-ICP-MS technique. It has been estimated that there are possibly 2,800 ±400 different zinc proteins in human proteome [19], therefore one would need 8.82 mg of zinc from cells to image single zinc protein. This calculation assumes equal expression and quantities of all possible zinc proteins, and that there is

1.54×10^{-14} g of zinc per cell in LLC-PK_1 cells [9]. From this calculation, one would need 5.72×10^{11} cells to image single zinc protein (200 L of cell cultures).

Current LA-ICP-MS methods need critical evaluation and further refinement to achieve higher sensitivity to be practical for zinc-proteomic studies, and other studies in metallomics, proteomics, and toxic metal experiments where transition metals are present at trace levels. LA-ICP-MS has also been utilized to determine metallomic information in tissues, cells, and organisms [7,8]. Starting with the use of LA-ICP-MS to perform analysis of organisms and/or tissues for metallomic and toxic metal studies, one identify particular organs or cells which accumulate the metal of interest. Further analysis utilizing PAGE gels on which proteomes from these organs and/or tissues are separated, can provide the biomelucular information on which proteins bind a parcular metal of interest. This top down approach can provide a thorough understanding and link between observations at the tissue and cellular level to underlying biochemical causes and mechanisms at the proteomic level. Our experiments should elucidate many biochemical phenomena including, in proteomics and metallomics, identifying which proteins are being expressed that subsequently bind a variety of transition metals including zinc, copper, and iron. In metallomics, identifying specifically which zinc proteins from cellular microscopic images and proteome are reactive with TSQ [9,29]. TSQ (6-methoxy-(8-p-toluenesulfonamido)quinolone) is a zinc sensor, which upon binding zinc, exhibits a fluorescent enhancement [29]. Experiments where zinc proteomes were reacted with TSQ, showed that TSQ bound to zinc proteins and formed ternary

adducts and subsequently fluoresced [9,29]. In toxic metal experiments, where cells were exposed to cadmium, LA-ICP-MS could show which specific proteins are reactive to cadmium other than metallothionein [11,22-25]. In addition, LA-ICP-MS could show where in zebra fish, a model for development and behavioral studies, methyl mercury binds [30].

In summary, the fields of proteomics, metallomics, and toxic metal exposure, experiments rely on a wide variety of bio-analytical methods that are largely not optimized for effective study in the aforementioned fields. PAGE-LA-ICP-MS methods provide a promising route for the elucidation of many biochemical mechanisms in the aforementioned fields. For that reason, the following project goals were set for an investigation into the optimization of PAGE and LA-ICP-MS for their application in proteomics, metallomics, and toxic metal exposure studies.

Project Goals

1. Develop a high resolution, native PAGE method for the separation of complex proteome samples.

2. Develop a sensitive, quantitative, LA-ICP-MS method for the analysis of PAGE gels containing trace levels of transition metals.

3. Develop a sensitive, robust, LA-ICP-MS method for the analysis of mercury in dried zebra fish embryos.

2. Methods

2.1. *Culture of LLC- PK_1 Cells*

LLC-PK_1 cells (transformed kidney epithelial cells from *Sus scrofa* (pig)) were purchased from the American Tissue Culture Company (ATCC CL 101). Frozen LLC-PK_1 cells at -80°C were rapidly thawed and transferred into 10 mL M199 media (Sigma) containing 4% fetal calf serum (FCS) and 50 mg/L penicillin G and 50 mg/L streptomycin. After 48 hours media was decanted and 15 mL of M199 supplemented with antibiotics and 4% FCS was added to adherent cell culture. Subsequently, media was changed every 48 hours. The flask was incubated under 5% CO_2 at 37 °C. The cultures were divided using trypsin/EDTA every 5-7 days to avoid over-confluence and cell layering. All of the cell manipulations were carried out in a sterile hood and all culture-ware and chemicals were purchased sterile, autoclaved or filter sterilized using Falcon 0.22 µm filters.

2.1.1. Preparation of LLC-PK1 cell cytosol

Cells were grown for chromatography, electrophoresis, and LA-ICP-MS in batches of culture plates. Cell suspensions of approximately 2 x 10^5 cells per milliliter were prepared and 10 mL of cell suspension solution was transferred onto each 100 cm^2 cell culture plate. Cells were subsequently incubated for 5-10 days to achieve confluence, while changing the media every 48 hours. After cells reached confluence, the media was decanted from the plates, and the adherent cells on the culture plates were rinsed three times with PBS prepared as follows: 4.7 g of Na_2HPO_4, 1.0 g of NaH_2PO_4 , 32.3 g of NaCl, and 25.3 g of Choline Chloride were transferred to a 4.0 L container and diluted to

volume with MilliQ™ water. The plates were subsequently drained, and 1.0 mL of DPBS (Sigma) was transferred onto each 1.0 mL cell culture plate. Adherent cells were detached from the cell culture plates using a cell scraping tool, and the cell suspension was transferred into 50 mL Falcon tubes. Since cell suspensions prepared from scraping cells are unable to be counted using a hemocytometer due to cell aggregation, one plate of cells per experiment was prepared in the same manner with the following exception: cells were detached from culture plates by adding 0.5 mL of trypsin/EDTA solution to the culture plate, incubating the cell culture plate for 5 minutes, then evenly suspended and transferred to a hemocytometer to perform a cell count. Cell counts were then extrapolated to the number of plates prepared during the experiment. Typically, 1.0 x 10^9 – 3.0 x 10^9 cells provided enough cytosolic proteome for analysis of subsequent fractions using PAGE and LA-ICP-MS after DEAE ion exchange chromatography. The cells were then centrifuged for 4 minutes at 680 xg and re-suspended in 10 mL of homogenization buffer prepared by the following formulation: pH 7.5, 50 mM Tris-Cl 0.25 M sucrose, 5 mM $MgSO_4$, 1 mM PMSF, 5 mM β-ME. 500 units Benzonase, a nonspecific exonuclease (Sigma), was then added to the cell suspension to remove DNA and RNA contamination. The cell suspension was homogenized using a Potter-Elvehjem homogenizer at 1,000 rpm making 50 passes. The cell homogenate was subsequently centrifuged for 60 minutes at 100,000 xg using a Beckman Ultra Centrifuge. The supernatant was referred to as proteome and used in subsequent experiments.

2.2. Quantification of Zinc and Cadmium by Atomic Absorption Spectroscopy

The metal content of solutions was measured by flame atomic absorption spectroscopy. The GBC AAS instrument was fitted with an acetylene torch using an 80:20 mixture of compressed air and acetylene. Measurements were obtained using a zinc or cadmium element lamp and a deuterium background lamp. Data were acquired in running mean mode and the instrument was calibrated prior to analyzing each sample set using standards of 0.5 ppm, 1.0 ppm. and 2.0 ppm zinc or cadmium solutions.

2.3. DEAE Ion Exchange Chromatography

The starting conductivity of proteome sample solutions was measured, with typical values of approximately 5.0 mS. Proteome sample solutions were then diluted from 10 mL to 15 mL using DEAE ion exchange chromatography starting buffer (degassed 10 mM Tris-Cl,pH 8.0, conductivity = 0.1 mS) in 15 mL Amicon® Ultra 3,000 MWCO centrifugal filtration tubes. Samples were then centrifuged at 12,000 xg for 60 minutes to remove as much buffer as possible with typical proteome sample solution volumes after centrifugation of 5.0 mL. Proteome sample solutions were again diluted to 15 mL with DEAE ion exchange chromatography starting buffer and the conductivity was measured again. Proteome sample solutions were centrifuged again in 15 mL Amicon® Ultra 3,000 MWCO centrifugal filtration tubes at 12,000 xg for 60 minutes. The process was repeated until the conductivity of the sample was less than 1 mS to allow for proper binding to the DEAE column. A Bio-Rad™ Bio-Scale™ DEAE Mini-Macro-Prep® 5 mL column was used for ion exchange chromatography with a 100 mL buffer gradient

consisting of degassed 10 mM Tris-Cl, pH 8.0, 0.1 mS conductivity starting buffer, and 10 mM Tris-Cl + 1 M NaCl, pH 8.0, 86 mS conductivity final buffer. Proteome sample solutions were recirculated over the DEAE column for six hours at 4 °C, at a flow rate of 1 mL/min using a peristaltic pump to allow adequate time for the proteins in solution to bind to the column. The peristaltic pump was then connected to the buffer reservoirs and 20 drop fractions (approximately 1 mL) were collected at a flow rate of 1 mL/minute.

2.3.1. TSQ Activity of DEAE IEX Proteome Fractions

Fractions from DEAE ion exchange chromatography were analyzed for TSQ (AnaSpec) activity using a Hitachi F4500 spectrofluorimeter, to determine if any of the zinc from the proteome fractions was reactive to TSQ. Fractions were placed directly in the cuvette and the fluorescence was recorded. Fractions were analyzed by adding TSQ to a final concentration of 20 µM and were allowed to react for 30 minutes. Fluorescence was measured by exciting at 370 nm and monitoring the emission profile from 400 – 600 nm. Background fluorescence was first subtracted, then fluorescence was integrated and reported as the integrated fluorescence.

2.3.2. Reaction of Cadmium with DEAE IEX Proteome Fractions

Select LLC-PK_1 proteome fractions from DEAE ion exchange chromatography were divided into two 0.5 mL aliquots. One aliquot was reacted with cadmium in a 1:1 ratio

based on the fraction's zinc content, determined by AAS, for one hour at 4 °C prior to subsequent experiments.

2.4. Blue Native Polyacrylamide Gel Electrophoresis

2.4.1. BN-PAGE of Select Proteome Fractions from DEAE IEX

Select fractions from DEAE ion exchange chromatography of LLC-PK_1 proteome prepared per section 2.3 were concentrated using centrifugal filtration in 0.5 mL Amicon® Ultra 3,000 MWCO tubes. Samples were centrifuged for 30 minutes at 12,000 xg at 4 °C. 15 µL of each of the concentrated proteome fraction was then combined with 5 µL of Invitrogen™ Native PAGE® Sample Buffer (4X). 10 µL of each sample was then loaded onto duplicate Invitrogen™ 4-16% Bis-Tris Novex® NativePAGE™ gels and electrophoresis was performed using an Invitrogen™ XCell SureLock® Mini cell with reagents from Invitrogen™ as summarized in Table 2.1.

	Invitrogen™ BN-PAGE Conditions
Voltage	150 V Constant
Temperature	Ambient
Run Buffer (Cathode)	50 mM BisTris 50 mM Tricine 0.002% Coomassie G-250 pH 6.8
Run Buffer (Anode)	50 mM BisTris 50 mM Tricine pH 6.8
Sample Buffer	50 mM BisTris 6 N HCl 50 mM NaCl 10% w/v Glycerol 0.001% Ponceau S pH 7.2

Table 2.1. Summary of BN-PAGE electrophoresis conditions and reagents.

Typical electrophoresis times were approximately 75 minutes.

2.4.2. BN-PAGE of Model Proteins

Bovine zinc carbonic anhydrase (Sigma), yeast zinc alcohol dehydrogenase (Sigma), and Zinc-Copper Superoxide Dismutase (Sigma) lyophilized proteins were dissolved in degassed 20 mM Tris-Cl pH 7.4. 7.5 µg, 5.0 µg, and 2.5 µg of each protein was then combined with 5 µL of Invitrogen™ NativePAGE™ Sample Buffer (4X), and adjusted to a final volume of 20 µL using MilliQ™ water. 10 µL of each sample was then loaded onto duplicate Invitrogen™ 4-16% Bis-Tris Novex® NativePAGE™ gels and electrophoresis was performed using an Invitrogen™ XCell SureLock® Mini cell with reagents from Invitrogen™ as summarized in Table 2.1.

2.5. Sodium Dodecyl Sulfate Polyacrylamide Gel Electrophoresis

2.5.1. SDS-PAGE of Select Proteome Fractions from DEAE IEX

Select fractions from DEAE ion exchange chromatography of LLC-PK1 proteome prepared per section 2.3 were concentrated using centrifugal filtration in 0.5 mL Amicon® Ultra 3,000 MWCO tubes. Samples were centrifuged for 30 minutes at 12,000 xg at 4 °C. 15 µL of each of the concentrated proteome fraction was then combined with 5 µL of Invitrogen™ NuPAGE™ LDS Sample Buffer (4X). Samples were then heated to 70 °C for 10 minutes. 10 µL of each sample was then loaded onto duplicate Invitrogen™ 12% Bis-Tris Novex® NuPAGE™ gels and electrophoresis was

performed using an Invitrogen™ XCell SureLock® Mini cell with reagents from Invitrogen™ as summarized in Table 2.2.

	Invitrogen™ SDS-PAGE Conditions
Voltage	200 V Constant
Temperature	Ambient
Run Buffer (Cathode)	50 mM MOPS 50 mM TRIS Base 0.1% SDS 1 mM EDTA pH 7.7
Run Buffer (Anode)	50 mM MOPS 50 mM TRIS Base 0.1% SDS 1 mM EDTA pH 7.7
Sample Buffer	106 mM Tris HCl 141 mM Tris Base 2.0% LDS 10% Glycerol 0.51 mM EDTA 0.022 mM SERVA Blue G250 0.175 mM Phenol Red pH 8.5

Table 2.2. Summary of SDS-PAGE electrophoresis conditions and reagents.

Typical electrophoresis times were approximately 50 minutes.

2.5.2. SDS-PAGE of Model Proteins

Bovine zinc carbonic anhydrase (Sigma), yeast zinc alcohol dehydrogenase (Sigma), and Zinc-Copper Superoxide Dismutase (Sigma) lyophilized proteins were dissolved in degassed 20 mM Tris-Cl pH 7.4. 7.5 µg, 5.0 µg, and 2.5 µg of each protein was then combined with 5 µL of Invitrogen™ NuPAGE™ LDS Sample Buffer (4X), and adjusted to a final volume of 20 µL using MilliQ™ water. Samples were then heated to 70 °C for 10 minutes. 10 µL of each sample was then loaded onto duplicate Invitrogen™ 12% Bis-Tris

Novex® NuPAGE™ gels and electrophoresis was performed using an Invitrogen™ XCell SureLock® Mini cell with reagents from Invitrogen™ as summarized in Table 2.2.

2.6. Native Sodium Dodecyl Sulfate Polyacrylamide Gel Electrophoresis

2.6.1. NSDS-PAGE of Select Proteome Fractions from DEAE IEX

Select fractions from DEAE ion exchange chromatography of LLC-PK1 proteome prepared per section 2.3 were concentrated using centrifugal filtration in 0.5 mL Amicon® Ultra 3,000 MWCO tubes. Samples were centrifuged for 30 minutes at 12,000 xg at 4 °C. 15 µL of each of the concentrated proteome fractions was then combined with 5 µL Sample Buffer prepared per formula in Table 2.3. Invitrogen™ 12% Bis-Tris Novex® NuPAGE™ gels were loaded into an Invitrogen™ XCell SureLock® Mini cell and the cathode and anode chambers were filled to volume with MilliQ™ water. Electrophoresis was then performed at 200 V for 30 minutes to remove some of the contaminant zinc, un-polymerized acrylamide, and gel storage buffer. The MilliQ™ water was then decanted and 10 µL of each sample was then loaded onto duplicate Invitrogen™ 12% Bis-Tris Novex® NuPAGE™ gels and electrophoresis was performed using an Invitrogen™ XCell SureLock® Mini cell with reagents and consitions as summarized in Table 2.3.

	NSDS-PAGE Conditions
Voltage	150 V Constant
Temperature	4 °C
Run Buffer (Cathode)	50 mM MOPS 50 mM Tris Base 0.0375% SDS pH 7.7
Run Buffer (Anode)	50 mM MOPS 50 mM Tris Base 0.0375% SDS pH 7.7
Sample Buffer	106 mM Tris HCl 141 mM Tris Base 10% Glycerol 0.22 mM SERVA Blue G250 0.175 mM Phenol Red pH 8.5

Table 2.3. Summary of NSDS-PAGE electrophoresis conditions and reagents.

Typical electrophoresis run times were 90 minutes.

2.6.2. NSDS-PAGE of Model Proteins

Bovine zinc carbonic anhydrase (Sigma), yeast zinc alcohol dehydrogenase (Sigma), and Zinc-Copper Superoxide Dismutase (Sigma) lyophilized proteins were dissolved in degassed 20 mM Tris-Cl pH 7.4. 7.5 µg, 5.0 µg, and 2.5 µg of each protein was then combined with 5 µL of Sample Buffer prepared per formula in Table 2.3, and adjusted to a final volume of 20 µL using MilliQ™ water. 10 µL of each sample was then loaded onto duplicate Invitrogen™ 12% Bis-Tris Novex® NuPAGE™ gels and electrophoresis was performed using an Invitrogen™ XCell SureLock® Mini cell with reagents and conditions summarized in Table 2.3.

2.7. Staining of PAGE gels

2.7.1. Coomassie R-250 Staining of PAGE Gels

PAGE gels were immediately removed from their gel cassettes after electrophoresis was complete and washed in 100 mL of MilliQ™ water on a Red Rocker™ shaker for 15 minutes. The water was then decanted, and 30 mL of either Coomassie R-250 stain, or Invitrogen Simply Blue SafeStain was added and gels were allowed to react with stain solution while shaking for 3 hours. The staining solution was then decanted, and gels were de-stained to remove background staining by washing in 150 mL of water while shaking until the desired sensitivity was achieved. Images were then taken using a HP 6980 visible light scanner.

2.7.2. TSQ Staining of PAGE Gels

PAGE gels containing protein samples were immediately removed from their gel cassettes after electrophoresis was complete and washed in 100 mL of MilliQ™ water on an orbital shaker for 15 minutes. A background image was first taken using an UVP™ EpiChem II® gel documentation system equipped with a 365 nm trans-illuminator and 470 nm peak emission filter. Images were taken using 5 second exposure times. Gels were then placed in a 50 mL solution of 20 uM TSQ (AnaSpec) and placed on an orbital shaker for 30 minutes. A subsequent image was then taken on the gel documentation system using the aforementioned parameters. The gel was then destained to remove excess TSQ by placing the gel in 50 mL of MilliQ™ water, and placing the gel in solution on an orbital shaker for 30 minutes. A subsequent image was then taken using the

aforementioned parameters. PAGE gels were then dried by passive drying described in section 2.8.2., and subsequently analyzed using LA-ICP-MS as described in section 2.10.1.

2.7.3. TPEN Staining of PAGE Gels

PAGE gels containing protein samples were immediately removed from their gel cassettes after electrophoresis was complete and washed in 100 mL of MilliQ™ water on an orbital shaker for 15 minutes. A background image was first taken using an UVP™ EpiChem II® gel documentation system equipped with a 365 nm trans-illuminator and 470 nm peak emission filter. Images were taken using 5 second exposure times. Gels were then placed in a 50 mL solution of 20 uM TSQ (AnaSpec) and placed on an orbital shaker for 30 minutes. A subsequent image was then taken on the gel documentation system using the aforementioned parameters. The gel was then placed in a 50 mL solution of 100 mM TPEN and placed on an orbital shaker for 30 minutes. A subsequent image was then taken using the aforementioned parameters. PAGE gels were then dried by passive drying described in section 2.8.2., and subsequently analyzed using LA-ICP-MS as described in section 2.10.1.

2.8. Drying PAGE Gels

2.8.1. Vacuum Drying

Gels prepared for vacuum drying were removed from the gel cassette immediately after electrophoresis was complete and subsequently washed in 100 mL of milliQ™ water on a Red Rocker™ shaker for 15 minutes. Gels were then placed onto a Whatman® filter paper backing, placed on a vacuum drying unit, where vacuum was supplied by a rotary pump, connected to a moisture trap incubated on dry ice, and vacuum dried while being heated for 2-3 hours. Dried gels were then placed under weight to flatten for 24-48 hours.

2.8.2. Passive Drying

PAGE gels were immediately removed from gel cassettes after electrophoresis was complete and washed in 100 mL of MilliQ™ water on a Red Rocker™ shaker for 15 minutes. Gels were then placed in 30 mL of Invitrogen™ Gel-Dry™ solution for 10 minutes. Invitrogen™ cellophane was then placed in the Gel-Dry™ solution for one minute to wet the material. One piece of wetted Invitrogen™ cellophane was then placed on an Invitrogen™ DryEase® Mini-Gel Drying Base. The PAGE gel was then removed from the Gel-Dry™ solution and placed on top of the piece of cellophane on the DryEase® Mini-Gel Drying Base on top of ½ of the DryEase® Mini-Gel Drying Frame. A second piece of wetted cellophane was then placed on top of the gel, air bubbles were removed, and the second ½ of the DryEase® Mini-Gel Drying Frame was then placed on top of the laminated gel. The frame was then secured with 4 Gel-Dry™

clamps at the edges of the frame and the gel was then dried at room temperature for 24-48 hours. Dried gels were removed from the frames and flattened under weights for 24-48 hours

2.8.3. Modified Passive Drying

Modified gel drying was performed in the same manner as passive gel drying described in section 2.6.6 with the following exceptions. A piece of Saran wrap was placed in-between the second layer of cellophane and the gel. This enabled the second layer of cellophane to be easily removed after drying to expose one face of the PAGE gel. In turn, this allowed for the gel to be directly ablated using LA-ICP-MS. In addition, gels were dried in a humidity controlled HEPA filtered hood to minimize cracking of the gels due to drying too quickly in the low humidity environment. Humidity was controlled at 55 % using a household humidifier.

2.9. Inductively Coupled Plasma Mass Spectrometry

ICP-MS analysis was performed using a Micromass Platform ICP-MS. Data were quantified using zinc standards (Inorganic Ventures) of 100, 50, 10, and 1 ppb zinc and Masslynx® (Waters) software. Samples were prepared by acid digestion in 70 % Optima Nitric Acid (Fischer) and diluted to a final concentration of 5 % Nitric Acid with MilliQ™ water prior to analysis.

2.10. Laser Ablation Inductively Coupled Plasma Mass Spectrometry

Laser ablation inductively coupled plasma mass spectrometry (LA-ICP-MS) was performed using a Cetac LSX-213 laser ablation unit and a Micromass Platform ICP-MS. A NIST glass sample containing various trace metals was ablated, and the ICP-MS was tuned to maximize ^{59}Co response during ablation. All other LA and ICP-MS parameters were adjusted during method development to achieve the goals of each experiment.

2.10.1. Ablation of Polyacrylamide Gels

LA-ICP-MS analysis of PAGE gels was performed by fixing the duplicate, unstained, dried PAGE gel sample to the LA sample stage using 3M double sided tape. The sample was then ablated using the typical parameters in Table 2.4. Laser scan rates, laser energy, and isotopes monitored were varied to achieve the goals of the experiment and were a part of the method development process.

Laser Ablation Parameters	
Energy (%)	50
Spot Size (µm)	200
Scan Rate (µm/sec)	100
Scan Spacing (µm)	250
Helium Flow Rate (L/min)	1.0
Laser Frequency (Hz)	20
ICP-MS Parameters	
Typical Isotopes Monitored	^{13}C, ^{63}Cu, ^{64}Zn, ^{66}Zn, ^{70}Zn, ^{112}Cd, ^{113}Cd, ^{114}Cd
Cool Gas Flow (L/min)	13.5
Intermediate Gas Flow (L/min)	0.84
Mode	Peak Hopping
Total Run-time (hours)	5 - 24

Table 2.4. Summary of LA-ICP-MS parameters for PAGE gel analysis

2.10.2. Qualitative Analysis of ^{202}Hg in Zebra Fish Embryos by LA-ICP-MS

Zebra fish embryos were provided by Dr. Michael Carvan's lab at the School of Freshwater Sciences. A summary of the preparation is a follows: Zebra fish eggs were exposed to 0 uM methyl mercury and 0.1 uM methyl mercury and subsequently fertilized. The embryos were then fixed to glass microscope slides at various time points post fertilization and dried using a 70 % ethanol solution. LA-ICP-MS analysis of dried Zebra fish embryos fixed to glass microscope slides was performed by placing microscope slides in the ablation chamber and centering ablation on individual Zebra fish embryos. Laser scan rates and laser energies were varied to achieve the goals of the experiment and were a part of the method development. Optimized LA-ICP-MS parameters are presented in Table 2.5.

Laser Ablation Parameters	
Energy (%)	100
Spot Size (µm)	10
Scan Rate (µm/sec)	20
Scan Spacing (µm)	10
Helium Flow Rate (L/min)	1.0
Laser Frequency (Hz)	20
ICP-MS Parameters	
Typical Isotopes Monitored	^{13}C, ^{64}Zn, ^{202}Hg
Cool Gas Flow (L/min)	13.5
Intermediate Gas Flow (L/min)	0.84
Mode	Peak Hopping
Total Run-time (hours)	3 - 4

Table 2.5. Summary of LA-ICP-MS parameters for analysis of Zebra fish embryos.

2.10.3. Quantitative Analysis of ^{70}Zn and ^{113}Cd in PAGE gels

Dried polyacrylamide gels from electrophoresis experiments were fixed to the laser ablation sample stage as described in section 2.9.1. ^{70}Zn (96 %, Cambridge Isotope Labs) and ^{113}Cd (90%, Cambridge Isotope Labs) were prepared in NSDS sample buffer in Table 2.3, at concentrations of 2.5 ppm, 1.25 ppm, 625 ppb, 313 ppb, 156 ppb, 75 ppb, 39 ppb, 20 ppb, and 10 ppb. 0.5 uL of each standard was then carefully transferred onto the dried polyacrylamide gel near the edge where no sample was expected to be present. The standards were then allowed to dry for one hour prior to analysis by LA-ICP-MS. The response for each standard was subsequently averaged, plotted, and fitted to a linear regression. Quantitative 2D PAGE gel images were generated by applying the linear regression equation to the data.

3. Results

3.1. Development of LA-ICP-MS for Ablation of PAGE Gels

3.1.1. LA-ICP-MS of PAGE Gel Varying Scan Rate and Laser Energy

In order to effectively perform LA-ICP-MS analysis of a dried PAGE gel, the parameters of the laser ablation unit needed to be adjusted such that the PAGE gel material was ablated through the entirety of the depth profile, without ablating the material that the gel was dried onto, thus avoiding the ablation, and subsequent analysis of the material that the gel was dried onto. To study the effect of scan rate versus laser energy for ablation, an Invitrogen 12% Bis-Tris gel was dried as described in section 2.8.1. A Sharpie permanent marker was used to draw an “X” onto the surface of the clear dried

gel in order to assist in the visualization of ablation. The Laser Ablation unit parameters were then varied to achieve ablation of the gel material, without ablating the filter paper backing (Figure 3.1.)

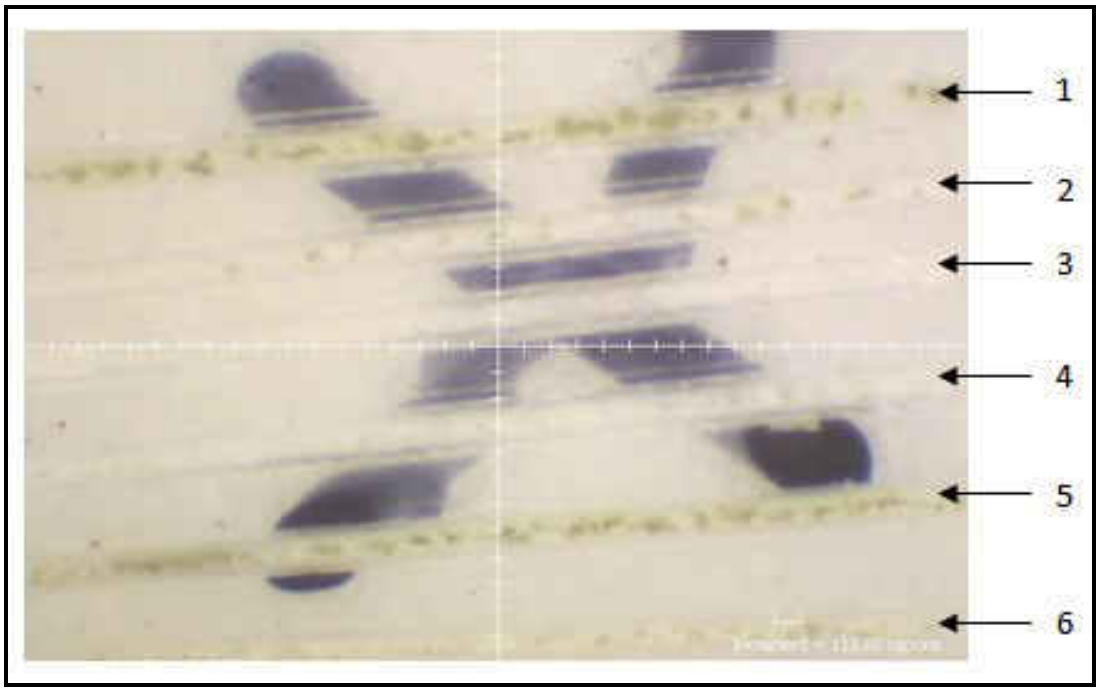

Figure 3.1. LA of PAGE gel vacuum dried onto filter paper. **1**) Laser Energy: 50%, Scan Rate: 50 µm/sec. **2)** Laser Energy: 50%, Scan Rate: 80µm/sec. **3)** Laser Energy: 50%, Scan Rate: 100µm/sec. **4)** Laser Energy: 10%, Scan Rate: 20µm/sec. **5)** Laser Energy: 20%, Scan Rate: 30µm/sec. **6)** Laser Energy: 30%, Scan Rate: 50µm/sec.

Ablation through the gel and burning of the filter paper was observed in scans 1, 2, 5, and 6 while ablation of the gel material without burning of the filter paper was observed in scans 3 and 4. The resultant equation *(3.1)* was then determined to be suitable for the laser ablation unit parameters with respect to the ablation of dried PAGE gels and utilized in subsequent experiments:

$$E = \frac{1}{2}\, Scan\ Rate$$

(3.1)

Where E is the laser energy, and the Scan Rate is the rate at which the laser moves across the sample in µm/second. For each differently sized area of ablation, the amount of time for analysis versus resolution was considered. The mass analyzer of the ICP-MS operated in peak hopping mode monitored each isotope for 0.1 seconds before moving to a subsequent mass. Therefore, using a slower scan rate, with lower energy provided a higher resolution data plot, however, analysis times were increased.

3.1.2. LA-ICP-MS Analysis of Zn-Cd-Proteome Spot

To determine the feasibility of using LA-ICP-MS to detect zinc and cadmium in the context of a protein embedded in a gel matrix, a LLC-PK_1 cell proteome sample prepared as described in section 2.3 and containing 0.9 nano-moles of zinc and 5.7 nano-moles of cadmium was spotted onto an Invitrogen™ 12% Bis-Tris gel dried as described in section 2.8.1 and allowed to dry. A natural distribution of zinc and cadmium isotopes (^{64}Zn, ^{66}Zn, ^{67}Zn, ^{68}Zn, ^{70}Zn, ^{110}Cd, ^{111}Cd, ^{112}Cd, ^{113}Cd, ^{114}Cd, and ^{116}Cd) was contained in the zinc-cadmium proteome spot. Samples were subsequently analyzed using LA-ICP-MS as described in section 2.10.1 (Figure 3.2.).

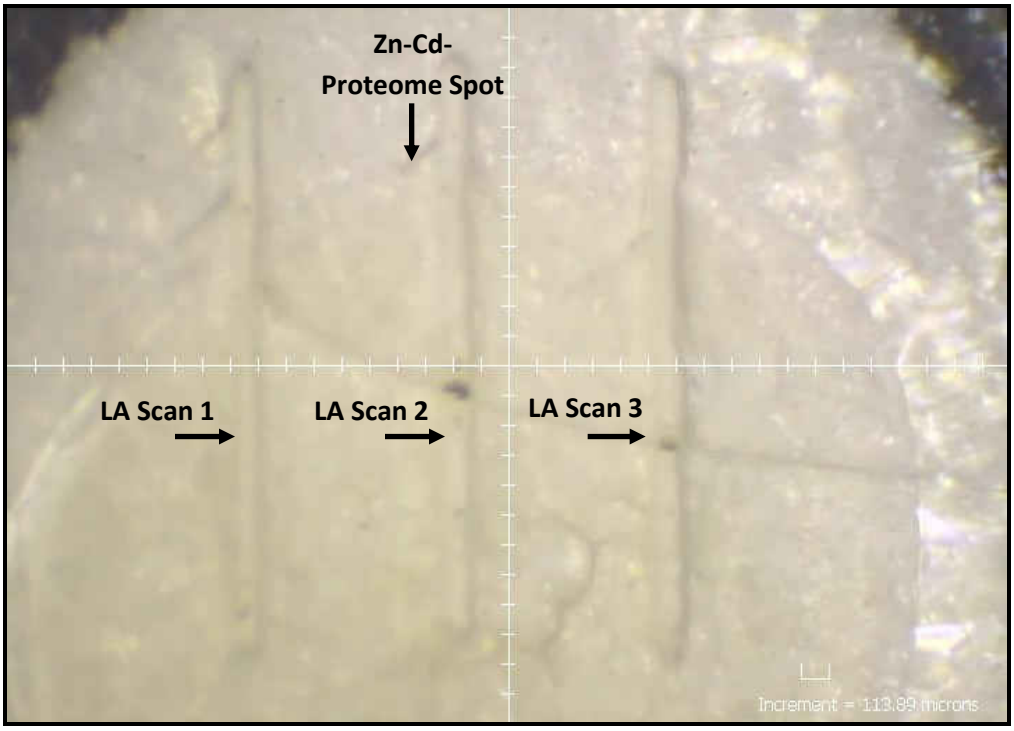

Figure 3.2. Microscope image of LA-ICP-MS of Zn-Cd-proteome spot containing 0.9 nano-moles of Zn and 5.7 nano-moles of Cd, spotted onto vacuum dried PAGE gel.

The LA-ICP-MS results summarized in Table 3.1. indicated a strong correlation between the total response for each isotope of zinc and cadmium with respect to their natural isotopic distribution. This confirmed the specificity of the LA-ICP-MS method as the resultant responses from LA-ICP-MS analysis were due to the zinc and cadmium content each sample, and not caused by material present in the matrices of the sample. In addition, preliminary sensitivity was established, as zinc and cadmium were able to be detected using LA-ICP-MS in the concentration range that is typically used when performing PAGE experiments using fractionated proteome samples.

Zn, Cd Isotope (% abundance)	Integrated Response	% of Total Integrated Response	% Error $\frac{(\%\ of\ Total\ Integrated\ Response - \%abundance)}{\%abundance}$
Zn 70 (0.60%)	1777	1.01%	68%
Zn 67 (4.10%)	7430	4.24%	3.4%
Zn 68 (18.8%)	14900	8.51%	54%
Zn 66 (27.9%)	55500	31.69%	14%
Zn 64 (48.6%)	95533	54.55%	12%
Cd 116 (7.49%)	242333	8.13%	8.5%
Cd 113 (12.2%)	381333	12.79%	4.8%
Cd 110 (12.5%)	334667	11.23%	10%
Cd 111 (12.8%)	384333	12.90%	0.8%
Cd 112 (24.1%)	735667	24.68%	2.4%
Cd 114 (28.7%)	902000	30.27%	5.5%

Table 3.1. Comparison of integrated zinc and cadmium isotope responses from LA-ICP-MS of zinc and cadmium proteome spot in Figure 3.2.versus the natural abundance percentage of isotopes.

3.1.3. In Vitro Reaction of LLC-PK$_1$ Proteome With Invitrogen™ Simply Blue SafeStain®

To determine if a PAGE gel containing LLC-PK$_1$ zinc proteome stained with Invitrogen™ Simply Blue SafeStain® (Coomassie R-250) could be utilized for LA-ICP-MS analysis, a LLC-PK$_1$ proteome sample with 7.0 nano-moles of zinc was reacted *In Vitro* with Invitrogen™ Simply Blue SafeStain®, pH 2.3, for one hour at room temperature (Figure 3.3.). A control sample was also prepared by reacting a LLC-PK$_1$ proteome sample containing 7.7 nano-moles of zinc with 20 mM TRIS-Cl + 5 mM β-ME buffer.

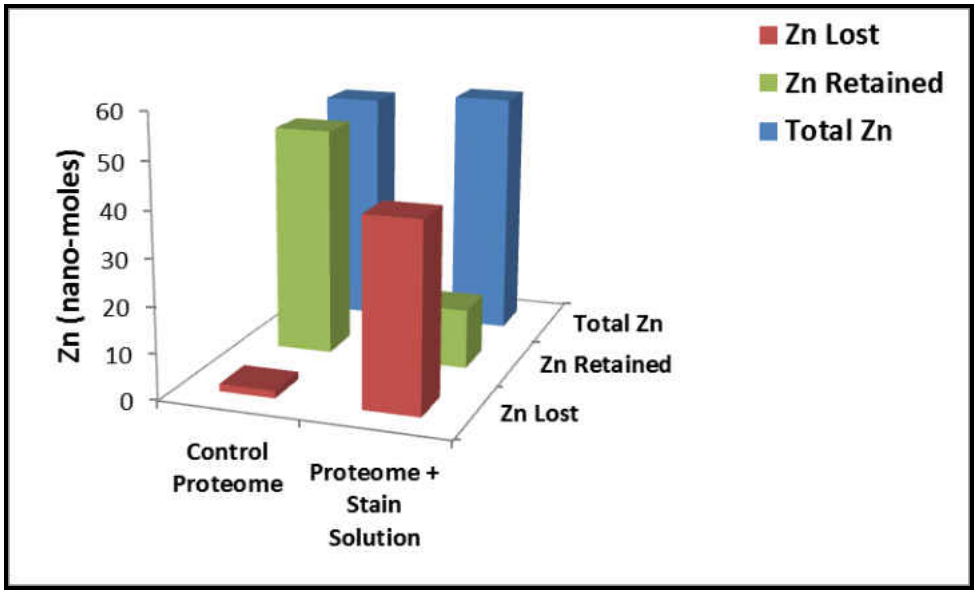

Figure 3.3. Reaction of LLC-PK_1 proteome with 20 mM TRIS-Cl + 5 mM β-ME buffer (Control Proteome) and Invitrogen™ Simply Blue SafeStain® solution used for staining PAGE gels (Proteome + Stain Solution).

A 72.3 percent loss of zinc from the proteome reacted with Invitrogen™ Simply Blue SafeStain® was observed versus the control sample, which was most likely due to the low pH of the stain used to permanently fix proteins into the gel matrix. The results indicated that PAGE gels containing zinc proteome and zinc protein samples needed to be run in duplicate, with one gel being utilized for staining, and the other dried without staining for analysis by LA-ICP-MS.

3.1.4. LA-ICP-MS of Carbonic Anhydrase Run on BN-PAGE Gel

To determine the feasibility of detecting zinc in zinc proteins on dried PAGE gels using LA-ICP-MS, a model zinc protein, Carbonic Anhydrase from bovine erythrocytes (Sigma), was serial diluted, with resultant amounts of zinc loaded onto each lane of the PAGE gel being 1.27, 1.18, 1.01, 0.85, 0.68, 0.51, 0.34, and 0.17 nano-moles for lanes 9, 8, 7, 6, 5, 4, 3, and 2 respectively, and electrophoresed using BN-PAGE in duplicate. One gel was stained to image the protein using Coomassie R-250 stain as described in section 2.7.1, and the other gel was dried as described in section 2.8.1. and analyzed for zinc content using LA-ICP-MS as described in section 2.10.1. A direct correlation between Coomassie R-250 staining of protein bands and amount of zinc loaded was observed (Figure 3.4.). In addition, carbonic anhydrase appeared to migrate through the gel in a series of protein multimer aggregates, with the primary aggregate calculated to be a carbonic anhydrase hexamer of approximately 180 kDa. Other aggregate bands consisted of a heptamer (approximately 150 kDa), a trimer (approximately 90 kDa), and the monomer (approximately 30 kDa).

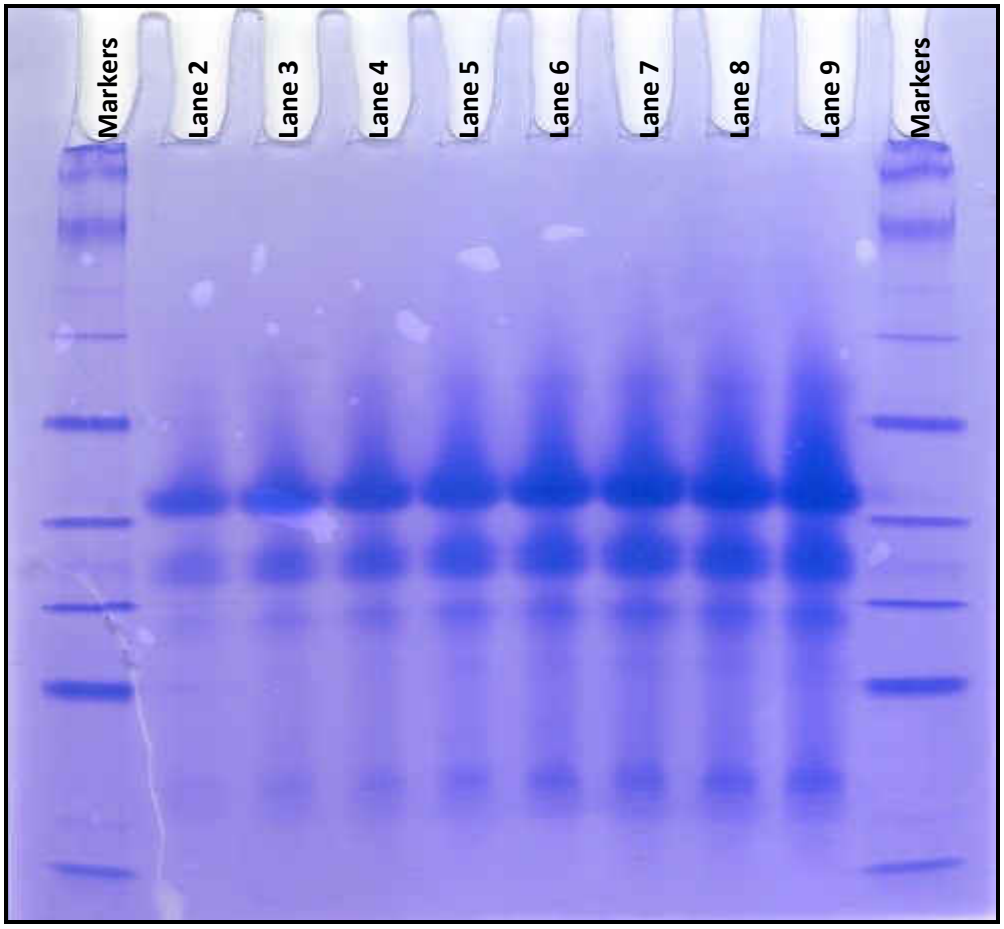

Figure 3.4. Coomassie stained BN-PAGE gel of markers on lanes 1 and 10 and Carbonic Anhydrase on lanes 2-9.

LA-ICP-MS analysis of the dried BN-PAGE gel also showed a direct correlation between ^{66}Zn response, protein concentration per Coomassie R-250 staining, and amount of zinc loaded per gel lane (Figure 3.5.). In addition, each of the protein aggregate bands contained a measurable amount of zinc. A majority of the ^{66}Zn response observed correlated to the hexamer aggregate of carbonic anhydrase.

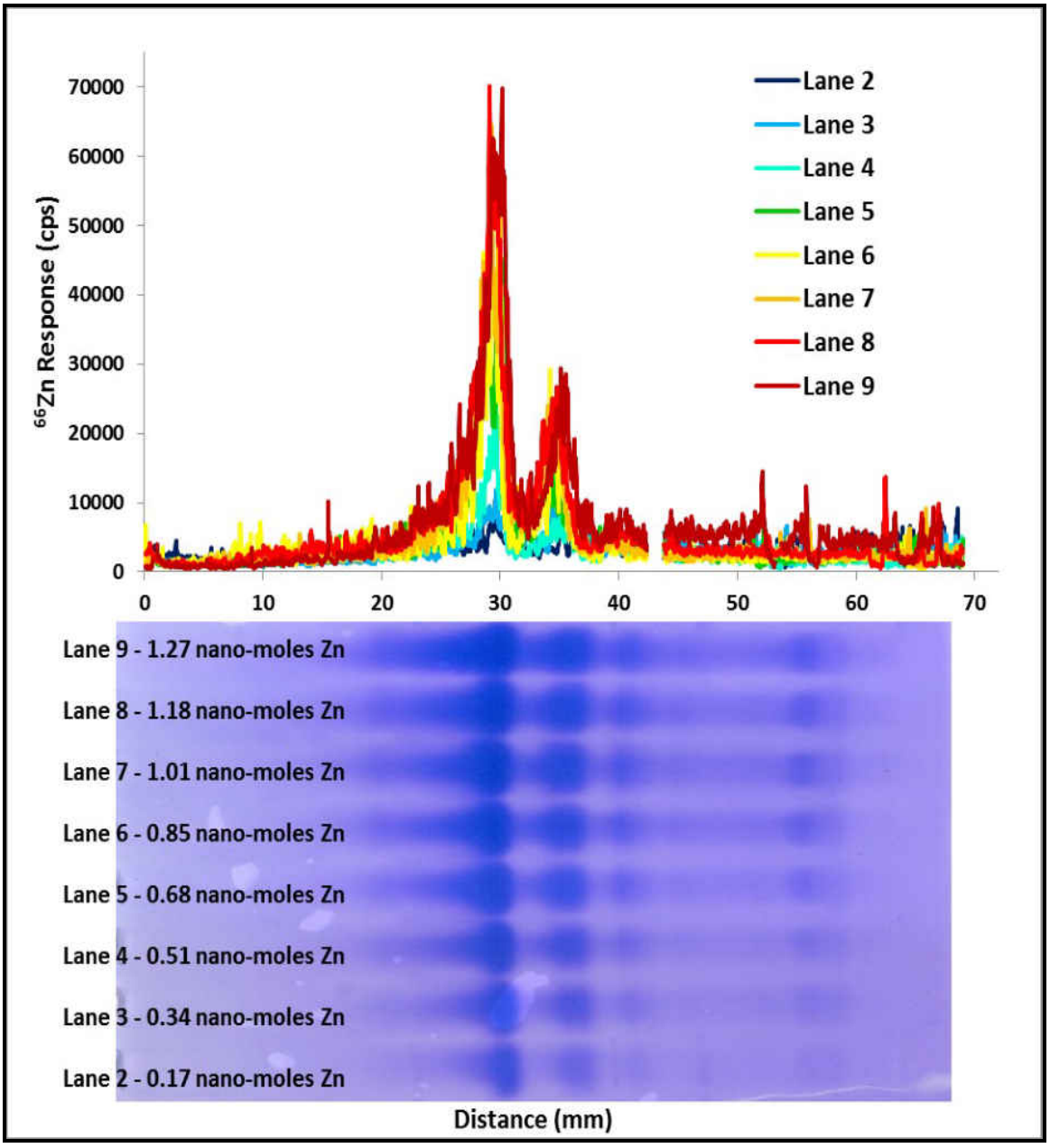

Figure 3.5. LA-ICP-MS analysis of carbonic anhydrase on an unstained, dried BN-PAGE gel. Coomassie R-250 stained BN-PAGE image superimposed for reference of protein band location versus ^{66}Zn response profile.

Replicate LA-ICP-MS analyses of each lane showed that the observed response was consistent for each BN-PAGE gel lane, with the exception of several response spikes which were not reproducible, nor correlated with a stained protein band (Figure 3.6.).

These uncorrelated responses could be due to microscopic cracks that occur on the gel during drying, causing the laser to momentarily ablate the backing material of the dried gel, or contaminant zinc present in the gel matrix from manufacturing processes and handling.

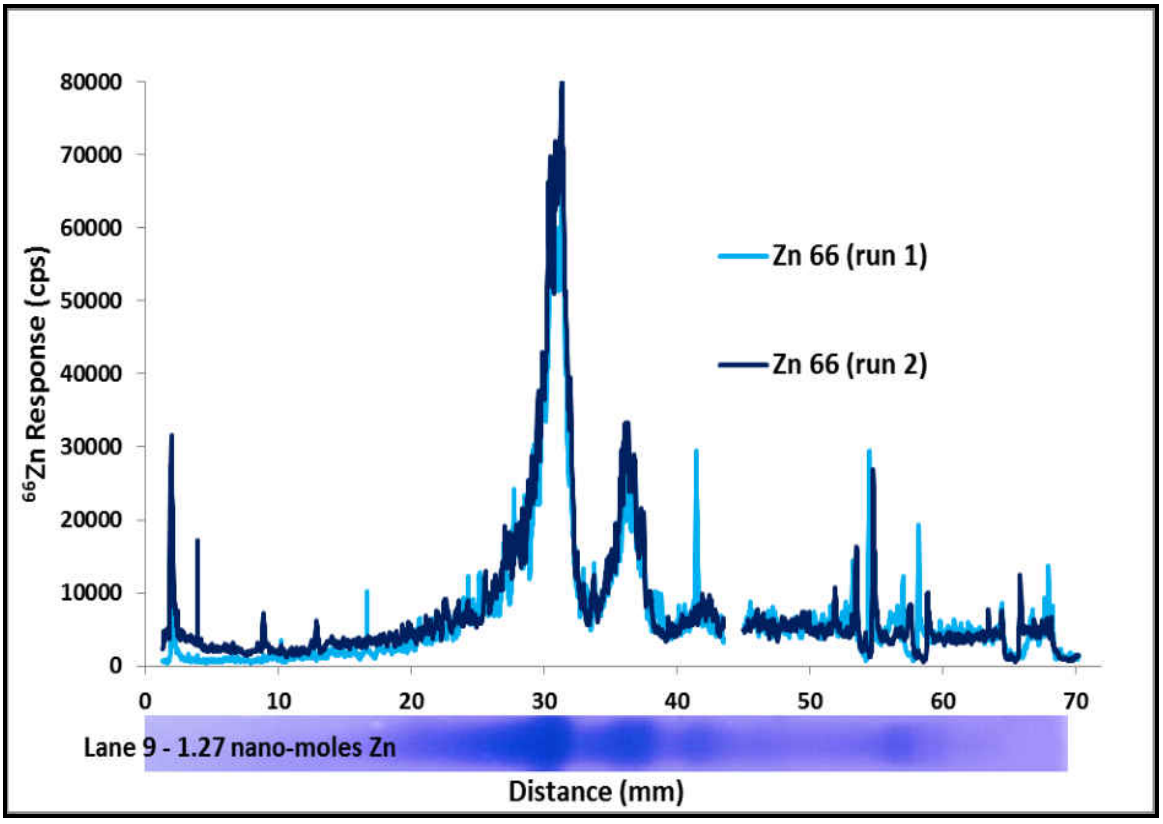

Figure 3.6. Replicate LA-ICP-MS scans of Carbonic Anhydrase on lane 9 of BN-PAGE gel. Coomassie R-250 stained BN-PAGE image of lane 9 superimposed for reference of protein band location versus ^{66}Zn response.

When the response for the entire gel lane was integrated, plotted versus amount of zinc loaded onto each gel lane, and fitted to a linear regression, a 89.3 % correlation was observed (Figure 3.7.) demonstrating the linearity and sensitivity of the LA-ICP-MS method for measuring zinc in the protein bands on the gel.

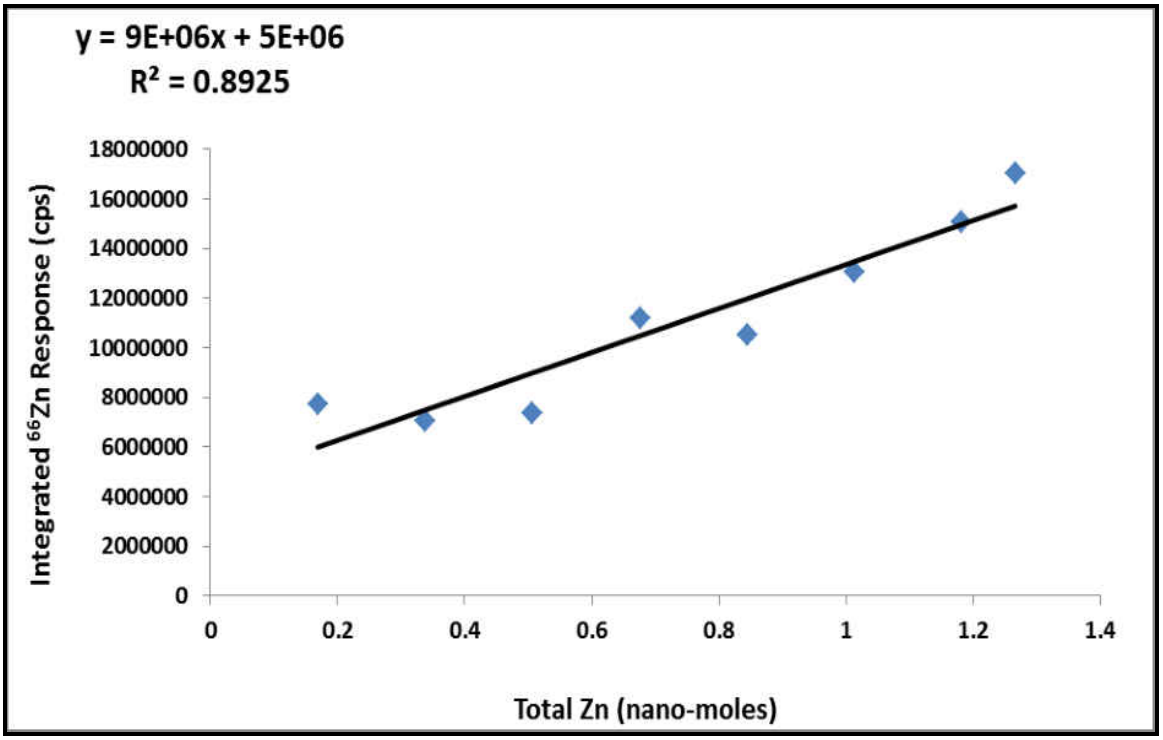

Figure 3.7. Integrated ^{66}Zn response from LA-ICP-MS analysis of each Lane 2-9 in Figure 3.5. with linear regression analysis.

LA-ICP-MS analysis was then performed across the carbonic anhydrase hexamer protein band of approximately 180 kDa (Figure 3.8.). The two observed drops in ^{66}Zn signal intensity were due to the two previous ablations down the gel lanes.

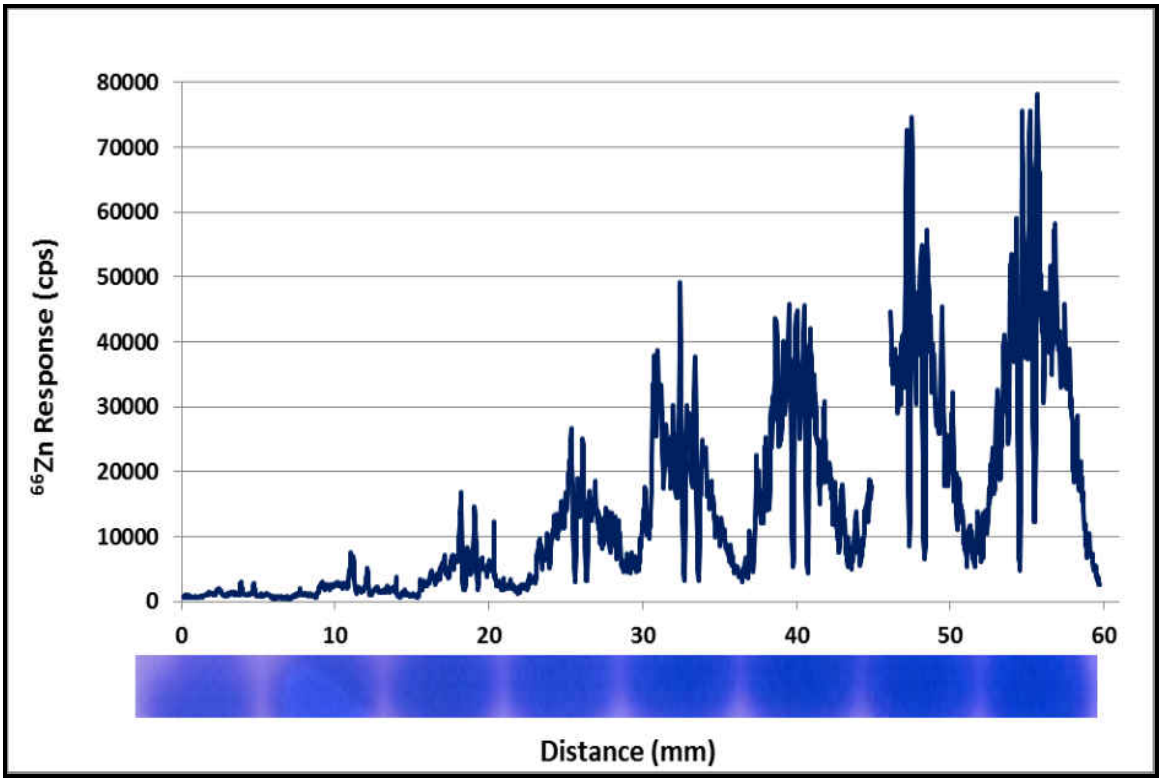

Figure 3.8. Horizontal LA-ICP-MS scan at 31 mm on BN-PAGE gel of primary Carbonic Anhydrase protein band from Figure 3.4. ^{66}Zn response depression spikes from previously ablated material when performing vertical LA scans. Coomassie R-250 stained BN-PAGE image of BN-PAGE gel at 31 mm superimposed for reference of protein band location versus ^{66}Zn response.

The integrated responses for each carbonic anhydrase hexamer band were then integrated, plotted versus total zinc loaded per each lane of the gel, and a linear regression analysis was performed (Figure 3.9.).

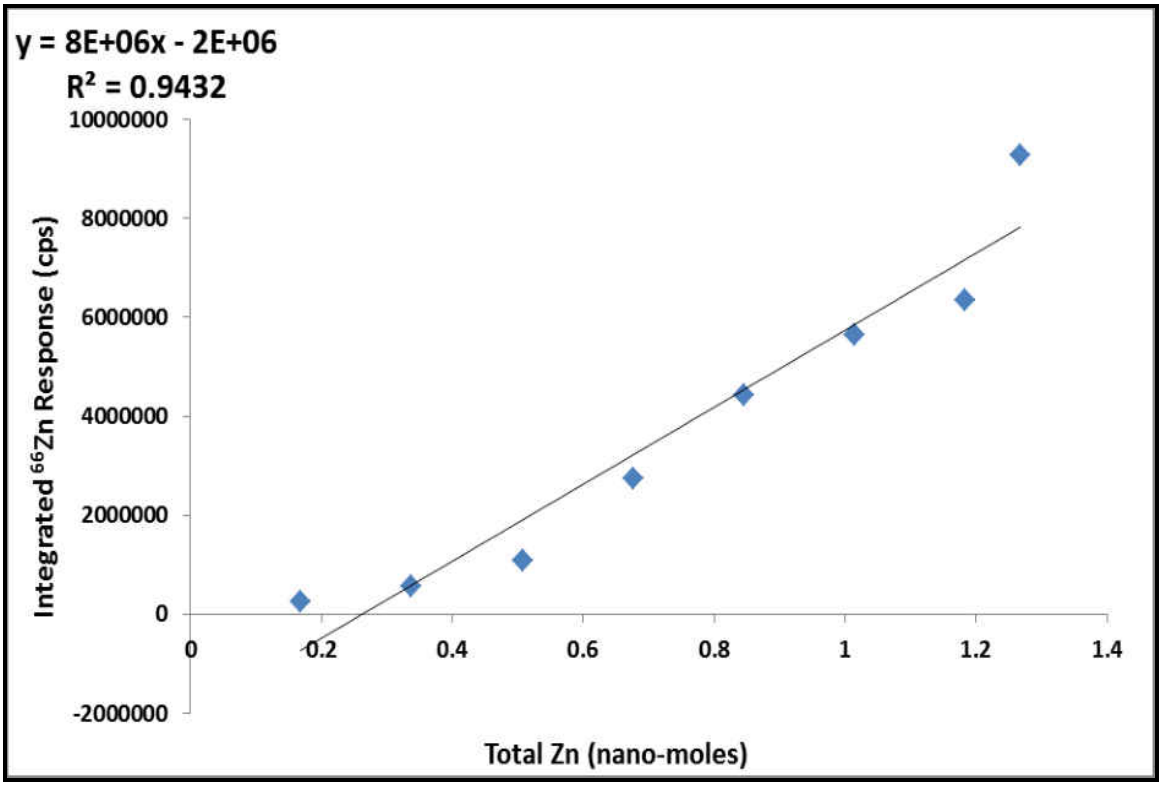

Figure 3.9. Integrated ^{66}Zn response from LA-ICP-MS analysis of horizontal lane scan of primary Carbonic Anhydrase protein bands at 31 mm in Figure 3.8. with linear regression analysis.

The linear regression analysis of the carbonic anhydrase hexamers showed a 94.3 percent correlation between integrated response and amount of zinc loaded onto each gel lane. The correlation Y intercept was substantially different from zero due to the background zinc being measured. This increase in correlation, when compared to the correlation observed when integrating the response from the entire gel lane, is most likely due to the measurement of the background gel response of the entire gel lane, which can vary due to cracks or contamination in the gel. These results further supported the linearity and sensitivity of the LA-ICP-MS method for detecting zinc in protein bands.

3.1.5. LA-ICP-MS of Proteome Run on BN-PAGE Gel

Proteome obtained from LLC-PK_1 cells was fractionated using DEAE ion exchange chromatography as described in section 2.3, and subsequent analysis of 280 nm absorbance using UV-Vis, and zinc content using AAS were performed as described in section 2.2. In addition, each fraction was reacted with 20 uM TSQ for 30 minutes, and the resultant fluorescent emission from 400-600 nm was integrated as described in section 2.3.1 and results were plotted (Figure 3.10.)

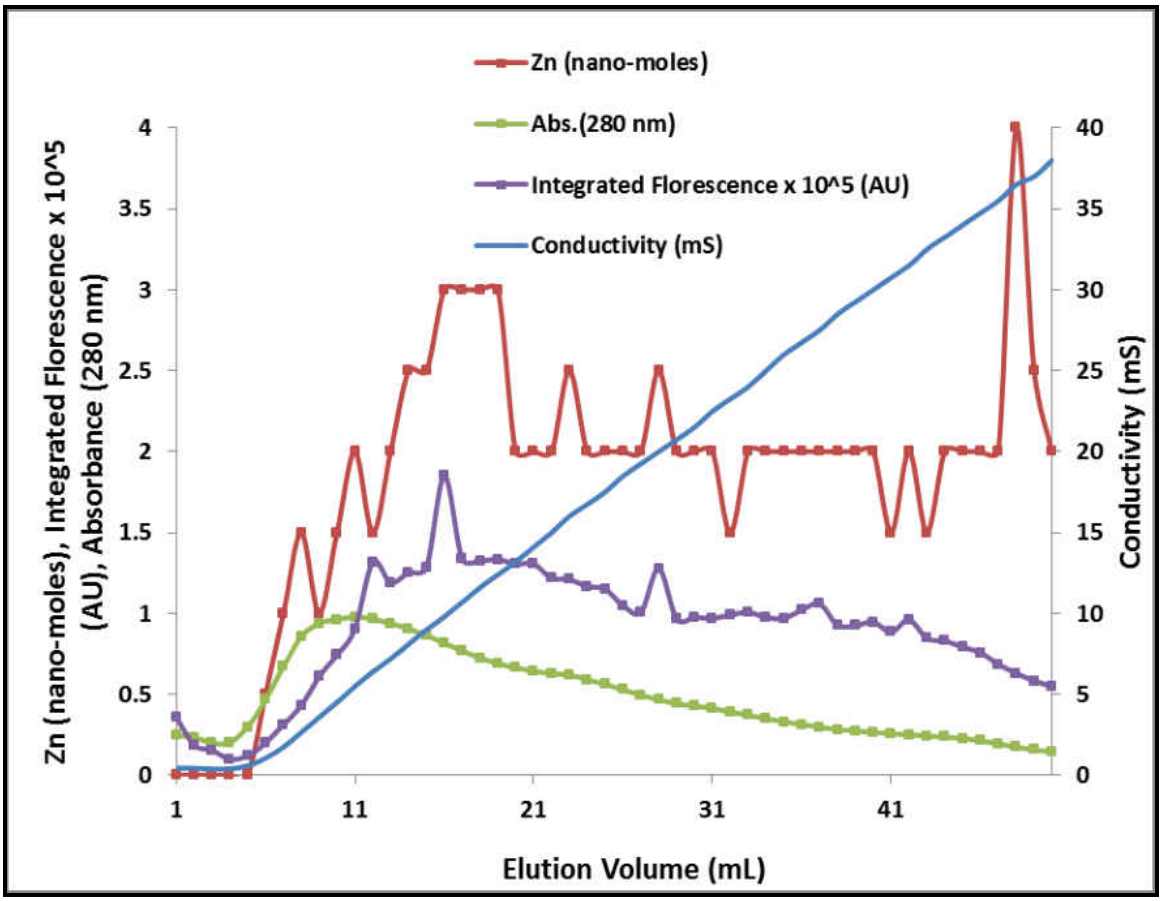

Figure 3.10. Chromatogram of DEAE IEX of LLC-PK_1 proteome.

Nearly all of the fractionated proteome samples contained 280 nm absorbance, zinc, and TSQ activity. Fractions containing high amounts of 280 nm absorbance, zinc, and TSQ activity (Fractions 12, 14, 16, 18, 20, 22, 24, 26, and 28) were then concentrated using centrifugal filtration and separated using BN-PAGE as described in section 2.4.1, with one gel being stained using Coomassie R-250 stain for imaging of protein bands as described in section 2.7.1 (Figure 3.11.), and the other gel dried for LA-ICP-MS analysis as described in section 2.8.1. Table 3.2 summarizes the total amount of zinc, loaded amount of zinc on BN-PAGE gel, 280 nm absorbance, integrated fluorescence, and conductivity of each fraction utilized for BN-PAGE.

Fraction / Lane	Total Zinc / Zinc Loaded BN-PAGE (nano-moles)	280 nm Abs. (AU)	Integrated Fluorescence (AU)	Conductivity (mS)
12 / 2	0.75 / 0.0375	0.97	1.32×10^5	6.4
14 / 3	1.25 / 0.0625	1.25	1.23×10^5	8.1
16 / 4	1.50 / 0.075	0.82	1.85×10^5	9.8
18 / 5	1.50 / 0.075	0.73	1.33×10^5	11.6
20 / 6	1.00 / 0.050	0.66	1.31×10^5	13.2
22 / 7	1.00 / 0.050	0.63	1.23×10^5	15.0
24 / 8	1.00 / 0.050	0.59	1.17×10^5	16.8
26 / 9	1.00 / 0.050	0.53	1.05×10^5	18.5
28 / 10	1.25 / 0.050	0.47	1.23×10^5	20.0

Table 3.2. Zinc content, 280 nm Abs., Integrated fluorescence, and conductivity of select fractionated LLC-PK_1 proteome samples.

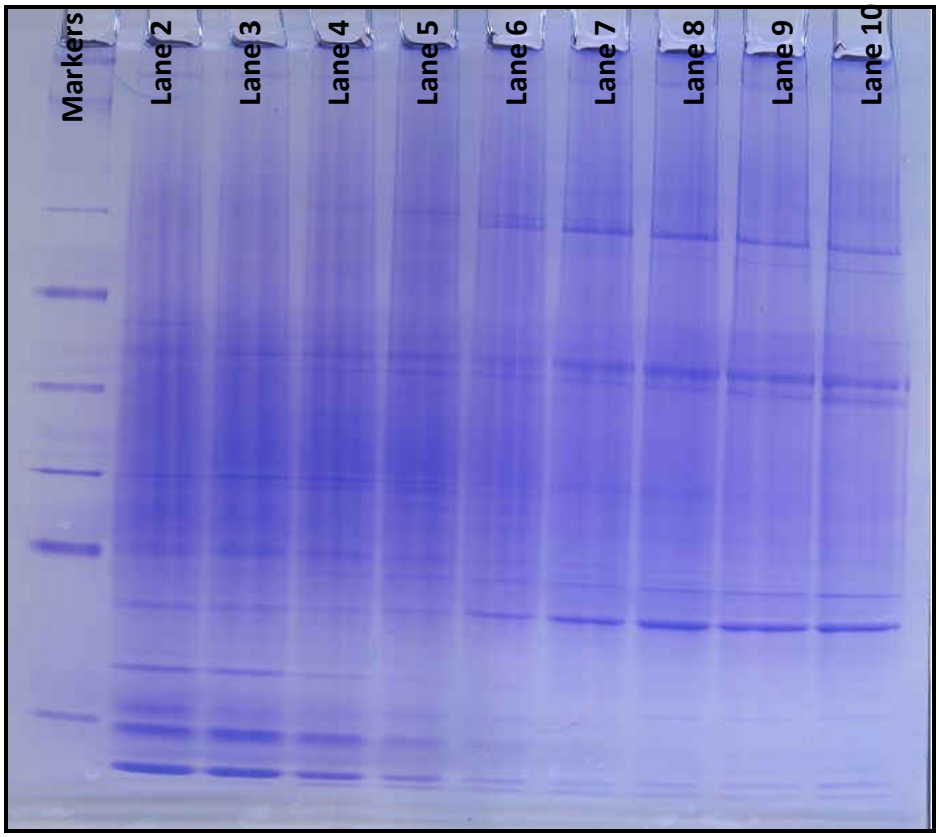

Figure 3.11. Coomassie R-250 stained BN-PAGE gel of markers and select cytosolic proteome fractions from DEAE IEX chromatography in Figure 3.10 summarized in Table 3.2.

The Coomassie stained BN-PAGE gel displayed poorly resolved protein bands that appeared as streaks down the gel lane, with very few punctate, well resolved, protein bands. Subsequent LA-ICP-MS analysis of the unstained, dried BN-PAGE gel lanes (Figure 3.12. and Figure 3.13.) showed large areas of zinc content in the gel lanes, however, poorly resolved response peaks. Having many unresolved protein bands and a low amount of zinc loaded per sample that could potentially be distributed among many of the unresolved protein bands, resulted in no specific designation of zinc content to a particular protein band.

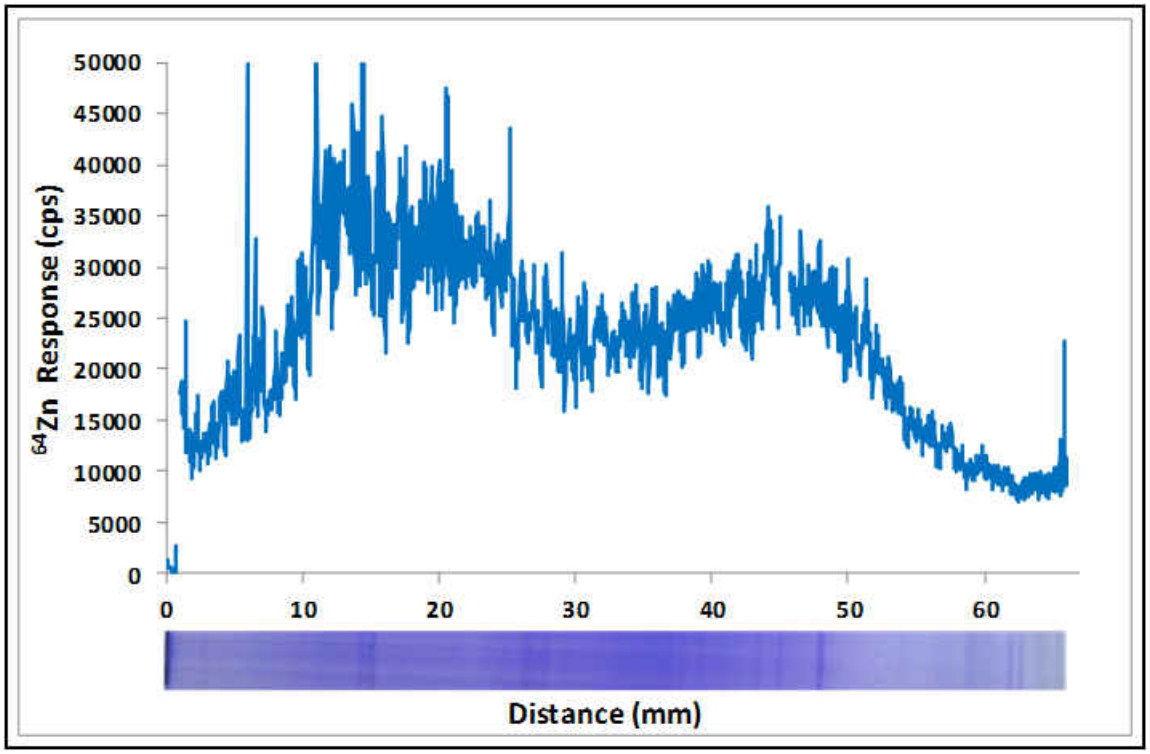

Figure 3.12. LA-ICP-MS ^{64}Zn analysis of lane 6 from BN-PAGE gel in Figure 3.11. Coomassie R-250 stained gel lane superimposed for reference.

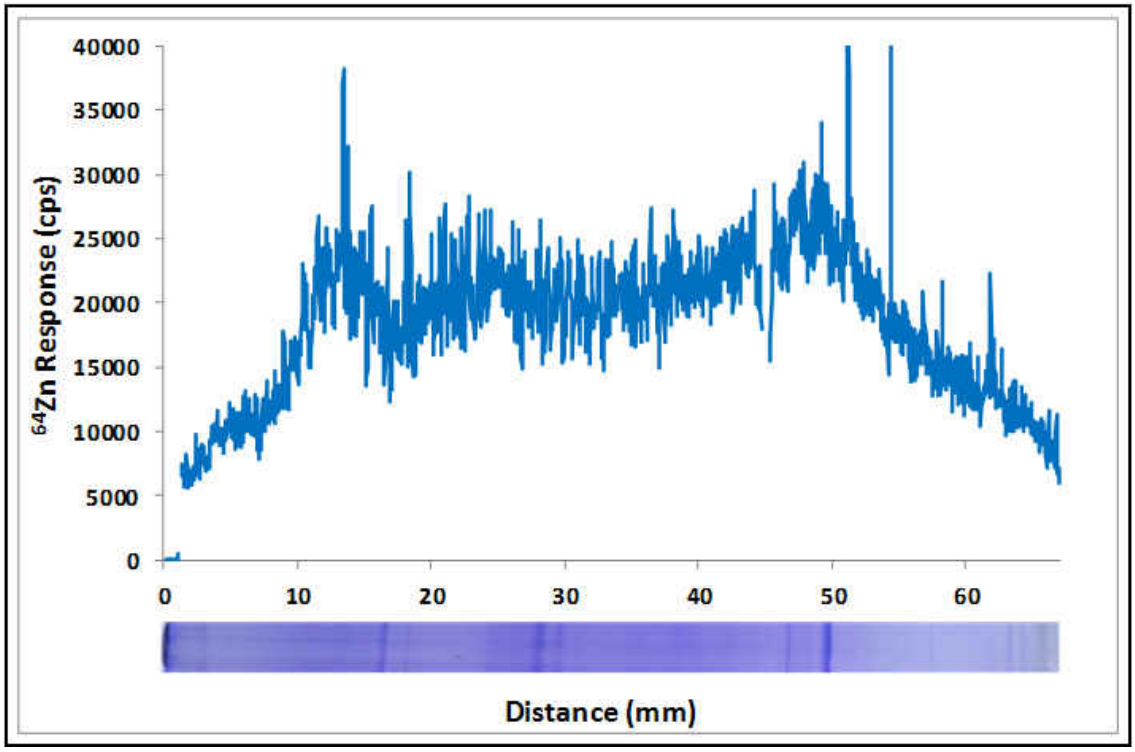

Figure 3.13. LA-ICP-MS ^{64}Zn analysis of lane 10 from BN-PAGE gel in Figure 3.11. Coomassie R-250 stained gel lane superimposed for reference.

These results indicated that BN-PAGE is not a suitable PAGE method for the separation of complex fractionated proteome samples due to the lack of resolution.

3.1.6. LA-ICP-MS of Proteome Run on SDS-PAGE Gel

The same LLC-PK$_1$ cytosolic proteome fractions from Figure 3.10. and Table 3.2. were separated using a denaturing SDS-PAGE method per section 2.5.1. on duplicate gels. One gel was stained using Invitrogen™ Simply Blue SafeStain™ staining for protein band visualization as described in section 2.7.1. (Figure 3.14.), and the other dried as described in section 2.8.1. The dried gel was analyzed using LA-ICP-MS according to section 2.10.1., to determine if SDS-PAGE could better resolve the proteins present in

the proteome fractions, and allow for the designation measured zinc responses from LA-ICP-MS to specific protein bands.

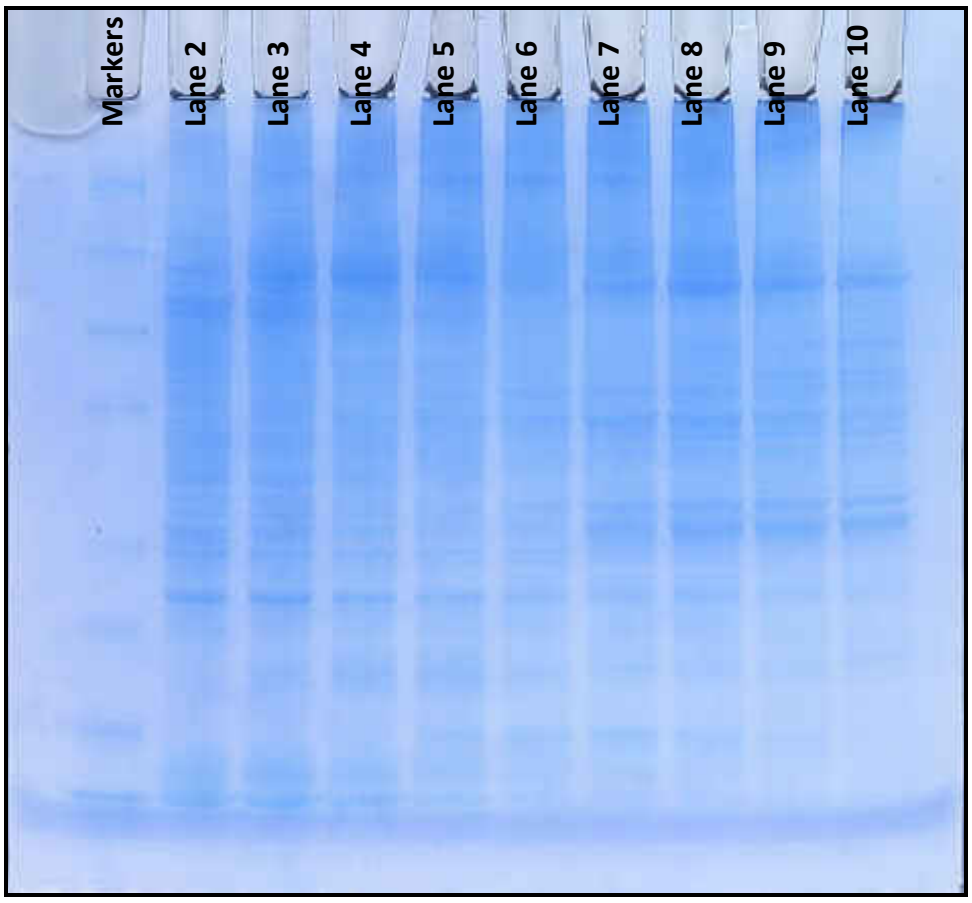

Figure 3.14. Coommassie stained SDS-PAGE gel of markers and select cytosolic proteome fractions from DEAE IEX chromatography in Figure 3.10. and fractionated proteome samples summarized in Table 3.2.

In the stained SDS-PAGE gel image (Figure 3.14.) punctate, resolved, protein bands are observed. However, they appear to overlap in many cases due to the number of unique proteins present in the fractionated proteome samples. Subsequent LA-ICP-MS analysis (Figure 3.15. and Figure 3.16.) showed the displacement of a large amount of zinc from the proteins in the sample which migrated with the dye front of the gel, however, some

zinc was still bound to proteins on the gel, and could be assigned to specific protein bands. Several signal spikes appeared across the gel lane which did not correlate to any particular protein band, which could have been due to microscopic cracks in the gel from drying, or contaminant zinc in the gel matrix, which made the designation of trace level zinc response to specific protein bands questionable. By comparison (Figure 3.17. and Figure 3.18.) the zinc responses from LA-ICP-MS analysis were much easier to assign to specific proteins by using SDS PAGE for separation versus BN-PAGE. This observation demonstrated that although SDS-PAGE is referred to as a denaturing PAGE method, some proteins do not become fully denatured under the conditions described in Table 2.2., and that the adjustment of the method conditions could improve zinc retention in fractionated proteome samples.

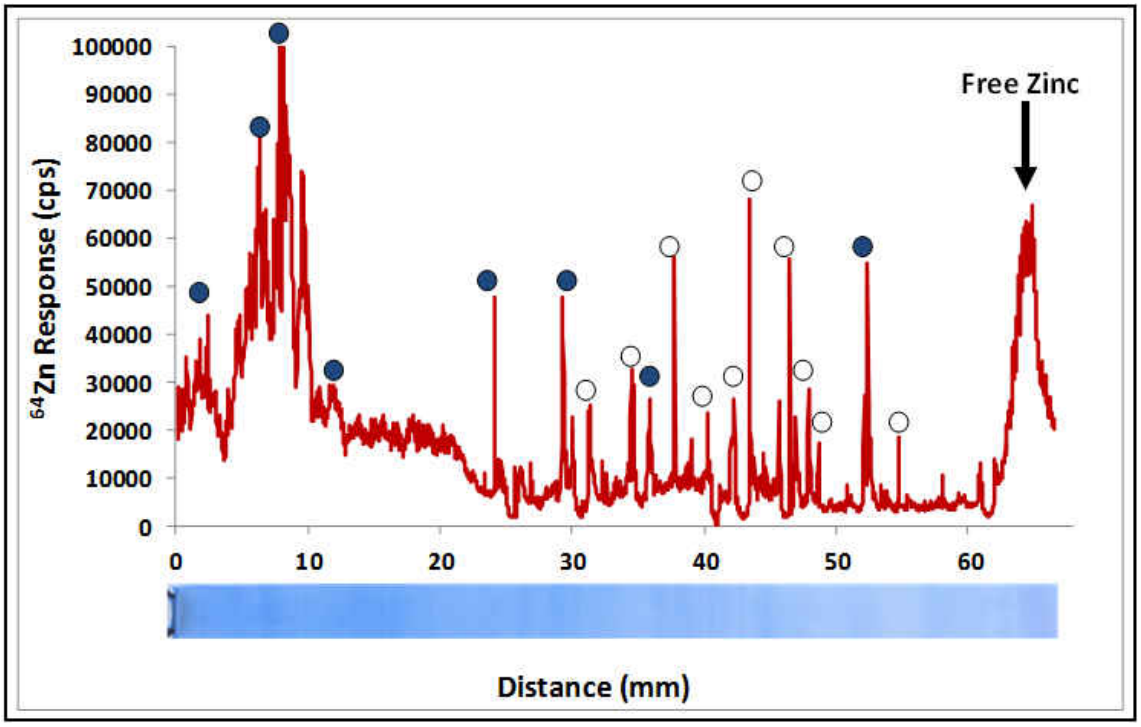

Figure 3.15. LA-ICP-MS ^{64}Zn analysis of lane 6 from SDS-PAGE gel in Figure 3.14. Invitrogen™ Simply Blue SafeStain® stained image of gel lane superimposed for reference. ● Highlights zinc peaks which correspond to protein bands, ○ highlights zinc peaks which do not correspond to protein bands.

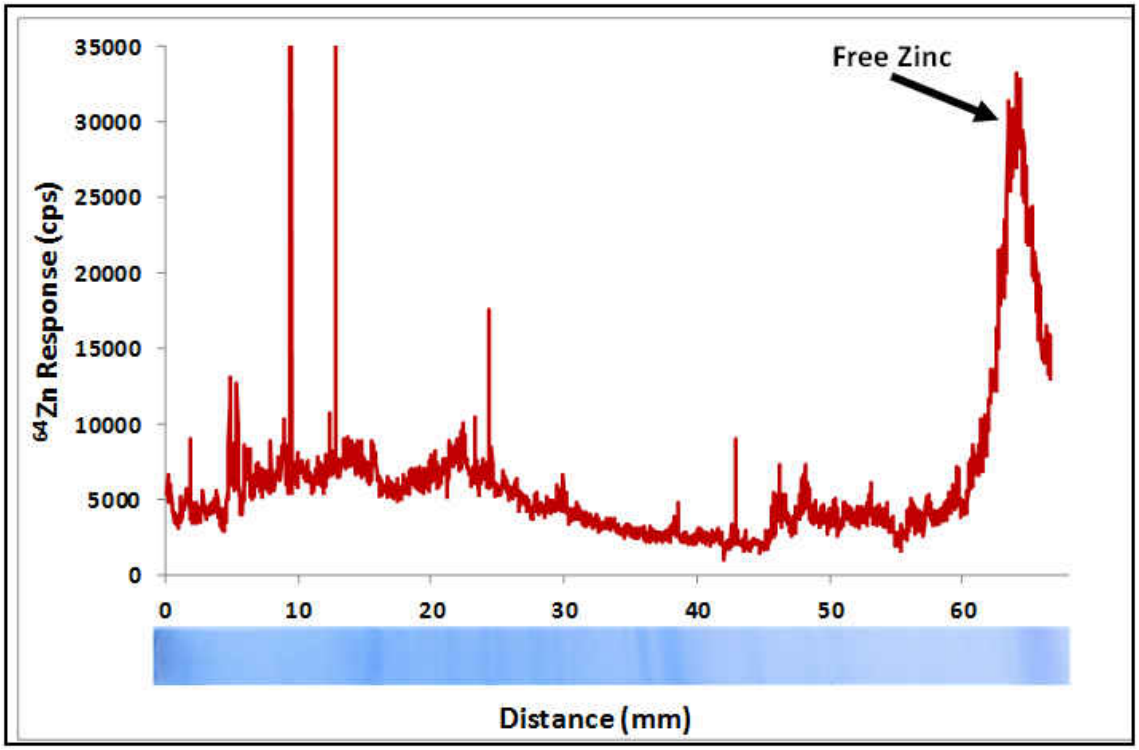

Figure 3.16. LA-ICP-MS ^{64}Zn analysis of lane 10 from SDS-PAGE gel in Figure 3.14. Invitrogen™ Simply Blue SafeStain® stained image of gel lane superimposed for reference.

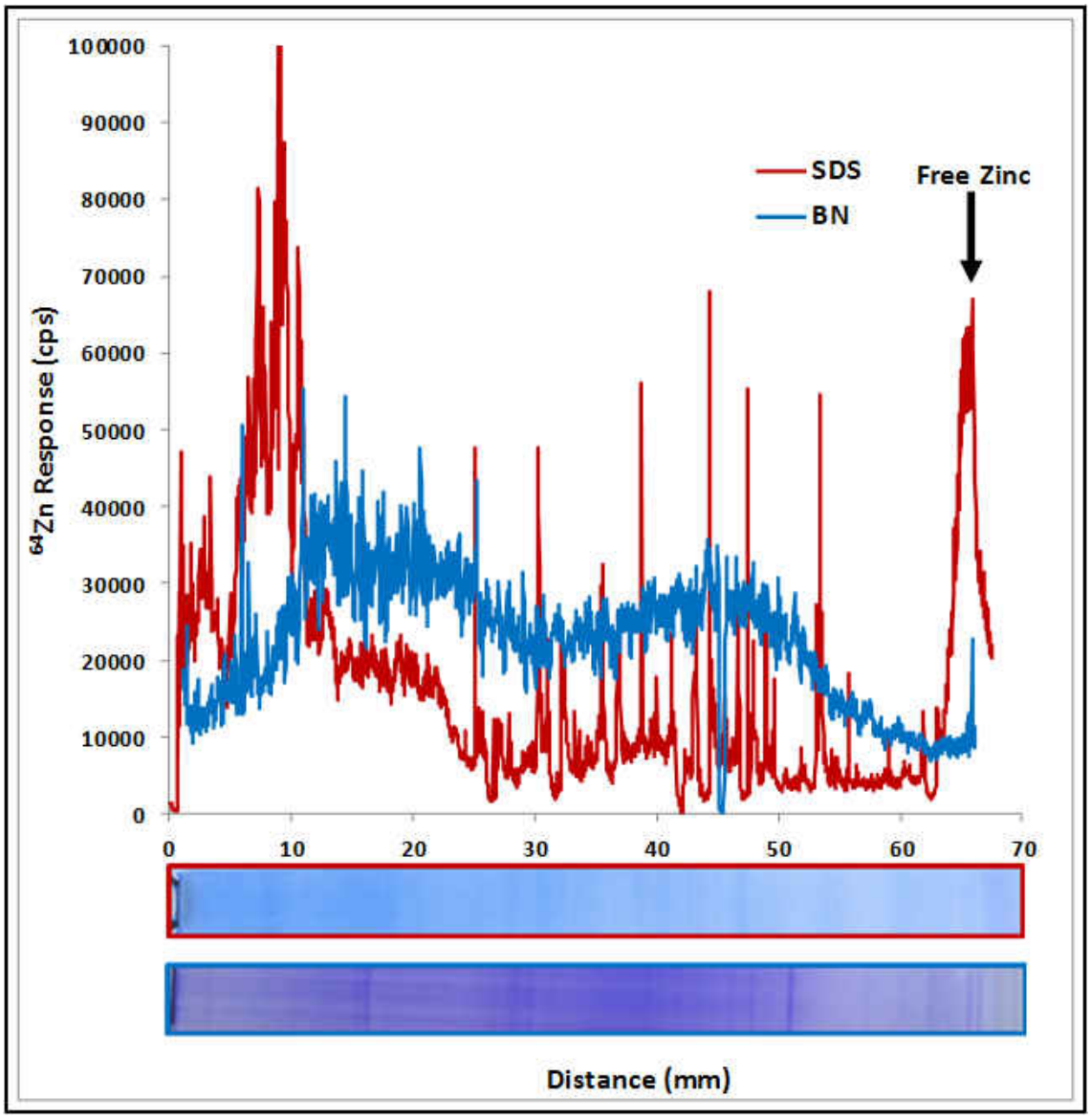

Figure 3.17. LA-ICP-MS ^{64}Zn analysis comparison of lane 6 from SDS-PAGE gel and BN-PAGE gel in Figure 3.14. and Figure 3.12. respectively.

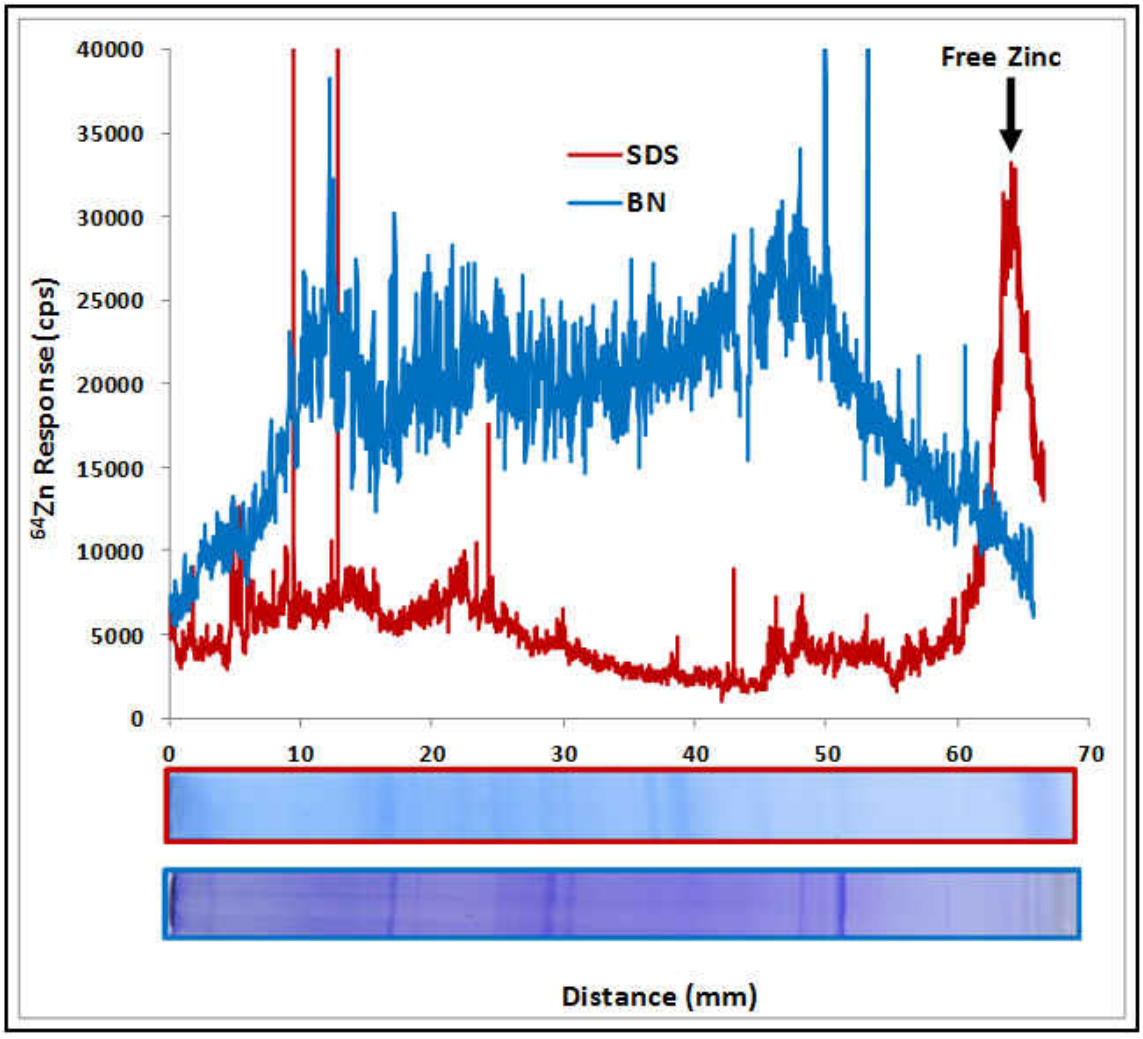

Figure 3.18. LA-ICP-MS ^{64}Zn analysis comparison of lane 10 from SDS-PAGE gel and BN-PAGE gel in Figure 3.15. and Figure 3.13. respectively.

3.1.7. 2D LA-ICP-MS of 2D PAGE Gel

In order to determine if micro cracks or zinc contamination were the cause of signal spikes when performing LA-ICP-MS analysis of PAGE gels to determine zinc content in protein bands, a two dimensional analysis and image of zinc content in a vacuum dried 2D-PAGE gel (Isoelectric focusing, which separates proteins based on their isoelectric point, by SDS-PAGE, Invitrogen™) containing a DEAE IEX fractionated LLC-PK$_1$ proteome

sample (provided by Drew Nowakowski) was analyzed for ^{64}Zn content using LA-ICP-MS (Figure 3.20). In Figure 3.19, several punctate protein spots are imaged using silver staining on the duplicate 2D PAGE gel. When comparing the stained protein pattern in the silver stained gel image, to the ^{64}Zn pattern in the LA-ICP-MS image, no correlation can be made between any of the stained protein spots and regions of observed ^{64}Zn content. Rather, both micro cracks and contaminant zinc were imaged on the gel matrix. The pattern of zinc content in the 2D PAGE gel LA-ICP-MS image mirrored the supporting sample stage frame of the vacuum gel drying unit. These results suggested that there was labile, contaminant zinc present in the gel, which migrated in solution toward the last part of the gel to dry, which was directly above the frame of the vacuum gel drying unit. This adventitious source of zinc dominated the observed distribution of zinc.

Figure 3.19. Image of silver stained fractionated LLC-PK_1 proteome on 2D PAGE gel.

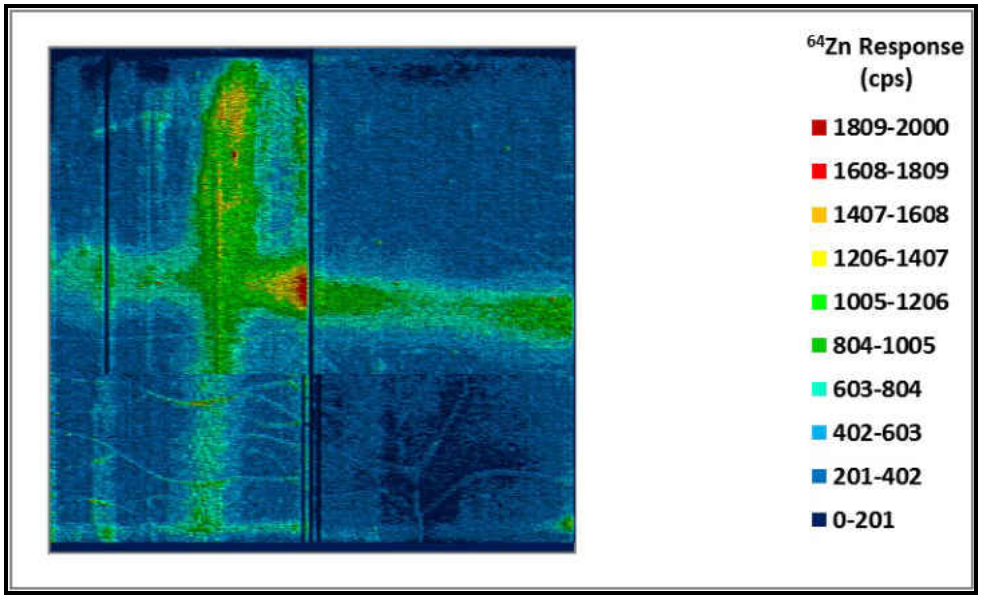

Figure 3.20. 2D false color map of LA-ICP-MS ^{64}Zn analysis of LLC-PK_1 fractionated proteome on 2D PAGE gel.

3.2. Analysis of Transition Metal Contamination in Commercial PAGE Meterials

3.2.1. ICP-MS Analysis of Acid Digested Invitrogen PAGE Materials

To quantify the amount of contaminant zinc present in materials utilized to perform PAGE analysis of proteome samples, materials utilized in Invitrogen™ SDS-PAGE methods were analyzed using ICP-MS for contaminant zinc. ^{64}Zn and ^{66}Zn isotopes were analyzed. Results are summarized in Table 3.3. with the polyacrylamide gel containing a majority of the zinc contamination (1,030 ppb in gel). This large amount of zinc present in the polyacrylamide gel correlated with previously determined poor detection limits for the analysis of zinc in proteins separated on PAGE gels which were in the low ppm range.

Material	Zinc Content
Run Buffer	Below limit of detection
Cellophane	35 ng/g (ppb)
Sample Buffer	Below limit of detection
Gel Storage Solution	0.95 μM
Gel Dry Solution	Below limit of detection
12% Bis-Tris Acrylamide Gel	1,030 ng/g (ppb)

Table 3.3. Quantification of zinc contamination in commercially available PAGE materials.

The results in Table 3.3. show that the primary source of zinc contamination in PAGE materials was the polyacrylamide gel, which contained 1,030 ppb of contaminant zinc. This large amount of contaminant, labile zinc, accounts for the pattern of zinc observed in Figure 3.20. and makes zinc proteins increasingly difficult to detect above the background signal in the PAGE gel matrix.

3.2.2. ICP-MS Analysis of PAGE Materials Before and After Electrophoresis

To determine the lability of contaminant zinc present in the polyacrylamide gel, and its fate upon electrophoresis, ICP-MS analysis of PAGE materials was conducted before and after performing PAGE as described in Table 2.2. ^{64}Zn and ^{66}Zn isotopes were analyzed. Results are summarized in Table 3.4.

Material	**Zinc Content**
Run Buffer (pre-run)	Below limit of detection
Run Buffer, Anode (post-run) 600 mL	7.49 µ-moles
Run Buffer, Cathode (post-run) 200 mL	0.66 µ-moles
12% Bis-Tris Acrylamide Gel (pre-electrophoresis)	1,260 ng/g
12% Bis-Tris Acrylamide Gel (post-electrophoresis)	171 ng/g

Table 3.4. Quantification of Zn contamination in commercially available PAGE materials before and after performing electrophoresis.

The results in Table 3.4 indicate that the contaminant zinc in the polyacrylamide gel was quite labile. When electrophoresis was performed, the contaminant zinc moved into the electrophoresis buffers with 7.49 micro-moles of the zinc having migrated into the cathode buffer, and 0.66 micro-moles of the zinc having migrated into the anode buffer. These results indicated that a large amount of the contaminant zinc could be removed from the gel matrix by performing electrophoresis prior to loading proteome samples onto the gel, therefore eliminating a substantial amount of background zinc, making the designation of zinc to protein bands more clear.

3.2.3. Quantitative LA-ICP-MS of PAGE Gels

To determine if the amount of zinc and cadmium measured on a PAGE gel by LA-ICP-MS was quantifiable, and to determine limits of detection for the visualization zinc and cadmium on a PAGE gel, a serial dilution of natural abundance of zinc and cadmium isotope standards were spotted onto dried PAGE gels (Figure 3.21) and subsequently analyzed by LA-ICP-MS. Standards were prepared by spiking NSDS sample buffer with 2.5 ppm (17.8 pico-moles of zinc and 11.1 pico-moles of cadmium), 1.25 ppm, 652 ppb, 313 ppb, 156 ppb, 75 ppb, 39 ppb, 20 ppb, and 10 ppb (77.0 femto moles of zinc and 44.3 femto-moles of cadmium) levels of zinc and cadmium. 0.5 µL of each standard was then spotted onto an Invitrogen™ NuPAGE® 12% Bis-Tris gel dried per section 2.8.3 and allowed to dry for one hour prior to LA-ICP-MS analysis. ^{64}Zn, ^{66}Zn, ^{70}Zn, and ^{112}Cd isotopes were analyzed.

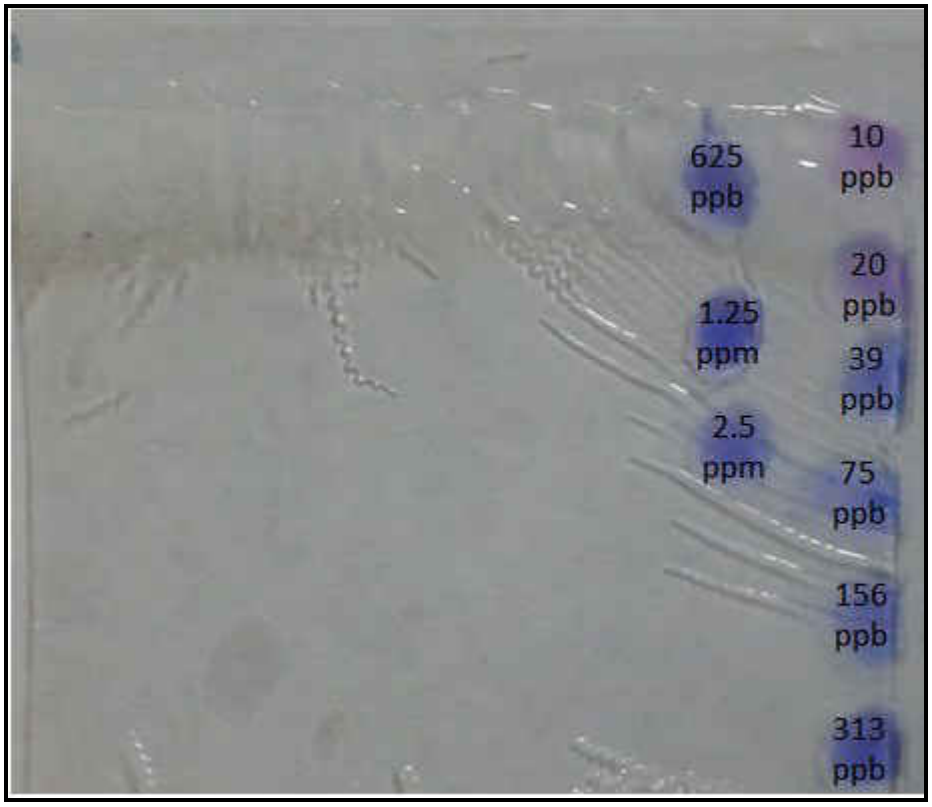

Figure 3.21. Image of dried 12% BisTris PAGE gel with natural isotope abundance Zn and Cd standards spotted onto gel. 2.5 ppm standard spot contains 17.8 pico-moles of zinc and 11.1 pico-moles of cadmium. 10 ppb spot contains 77.0 femto moles of zinc and 44.3 femto-moles of cadmium.

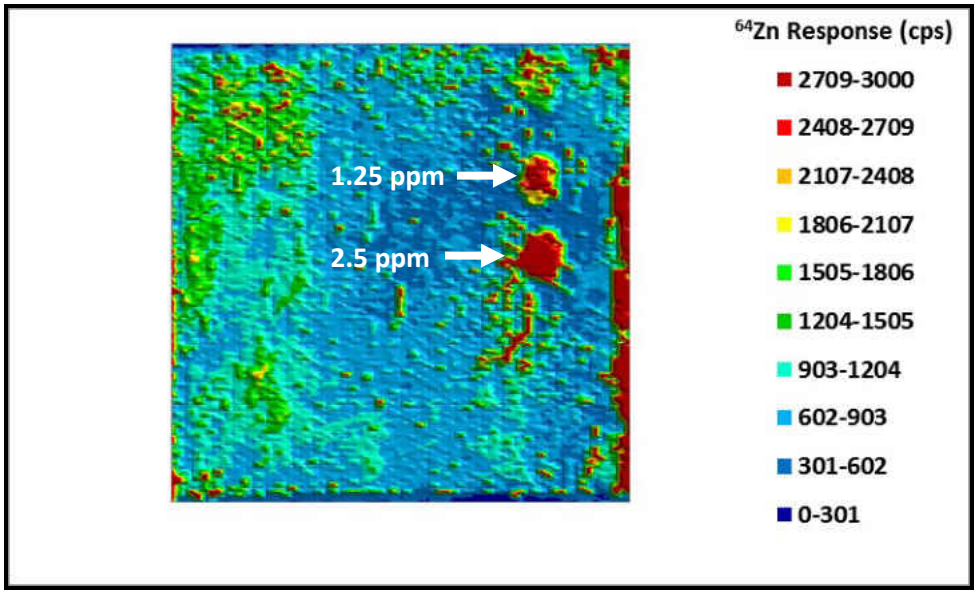

Figure 3.22. LA-ICP-MS analysis of ^{64}Zn in Figure 3.21.

Due to the large amount of contaminant zinc on the PAGE gel (Figure 3.22. and Figure 3.23), the lowest concentration of zinc standard that could be readily visualized was 1.25 ppm. This accounted for the ambiguity in literature regarding the determination of trace amounts of zinc that were expected to be present in a proteome sample in the presence of a gel matrix[4]. However, in Figure 3.24, the amount of contaminant ^{70}Zn present was negligible, due to the low natural abundance percentage of ^{70}Zn (0.68 %). In addition, the lack of cadmium contamination in the gel matrix allowed for the detection of cadmium on the PAGE gel at 75 ppb. These results confirmed that the limitation of detecting metals in a PAGE gel by LA-ICP-MS was not due to the LA-ICP-MS method. Rather, it was limited by the purity of available PAGE gel materials with respect to metal content.

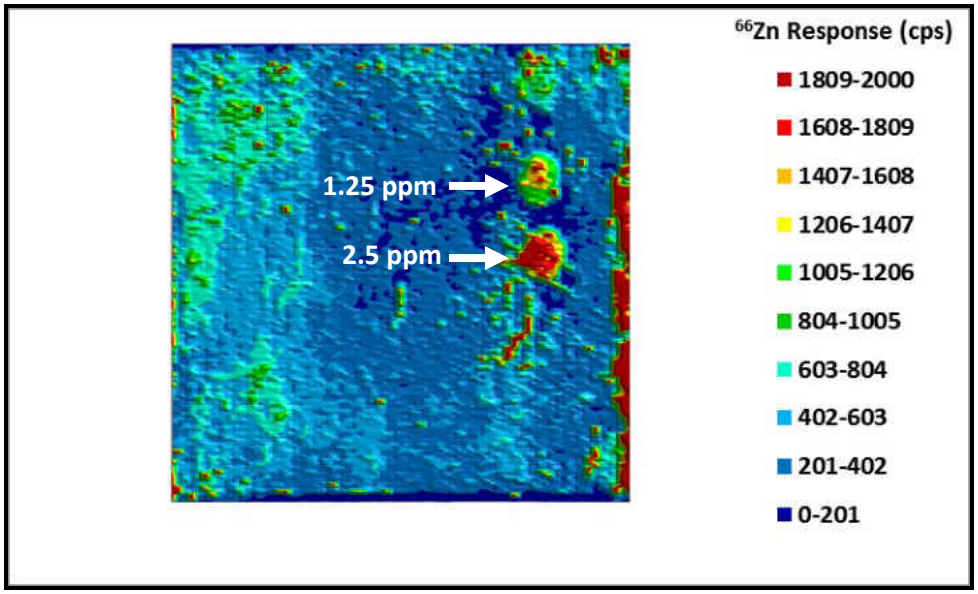

Figure 3.23. LA-ICP-MS analysis of ^{66}Zn in Figure 3.21.

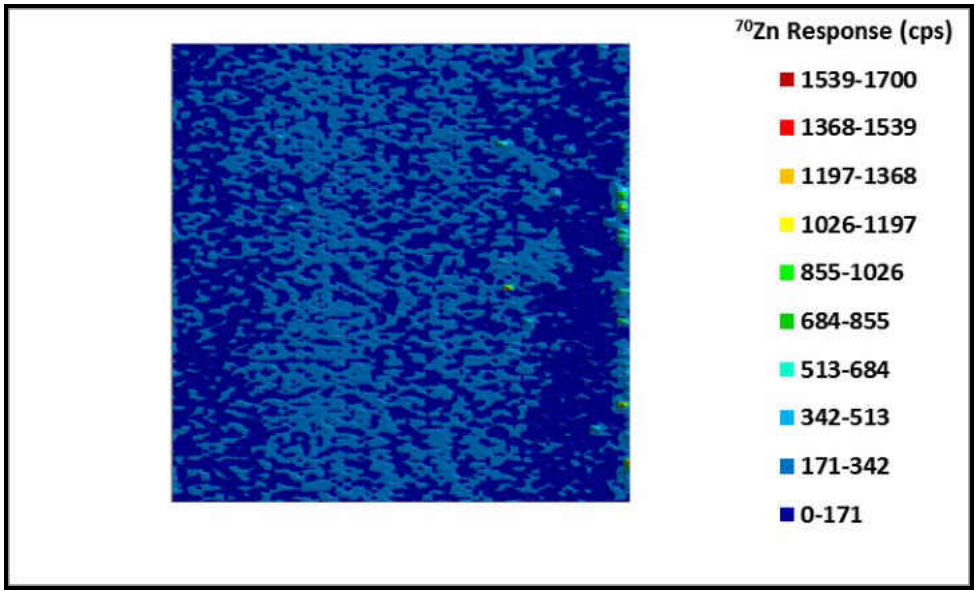

Figure 3.24. LA-ICP-MS analysis of ^{70}Zn in Figure 3.21.

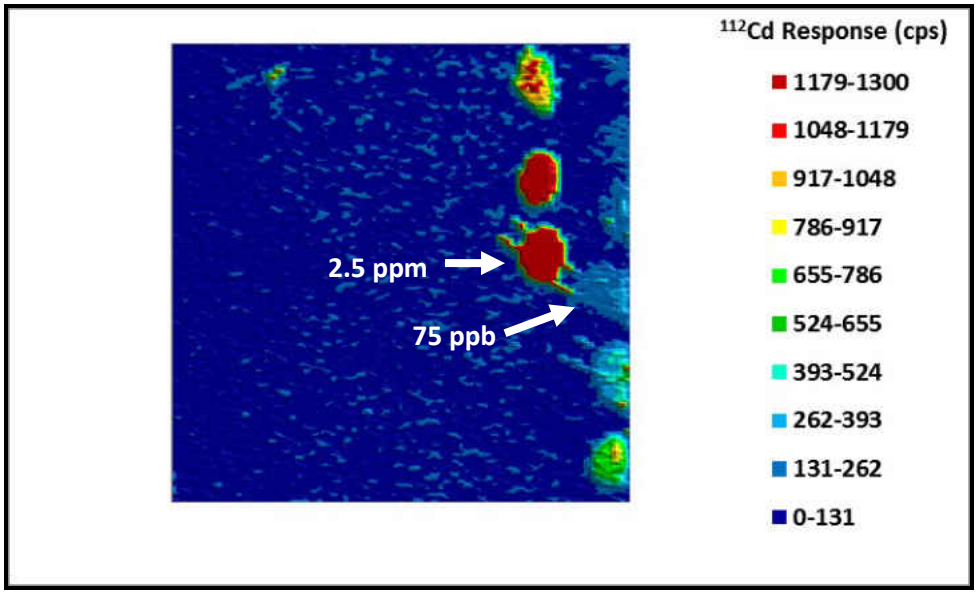

Figure 3.25. LA-ICP-MS analysis of ^{112}Cd in Figure 3.21.

3.2.4. LA-ICP-MS of Western Blot Nitrocellulose for Background Zn and Cd

To determine if using a Western Blot of a PAGE gel would provide better detection limits for zinc, a piece of nitrocellulose from an Invitrogen™ Western Blot kit was spotted with natural abundance zinc and cadmium standards as previously described in section 3.23 (Figure 3.26.), and subsequently analyzed using LA-ICP-MS as described in section 2.10.1 with the exception that the laser energy was lowered to 5 %. ^{64}Zn, ^{66}Zn, ^{70}Zn, and ^{112}Cd isotopes were analyzed. The results from the subsequent LA-ICP-MS analysis (Figure 3.27 and Figure 3.28) show that there was a substantial amount of zinc contamination in the nitrocellulose. The contaminant zinc in the false color images generated from 2D LA-ICP-MS analysis in Figures 3.27 and 3.28 corresponded to at least 1.25 ppm – 2.5 ppm, such that no standard spots were able to be readily visualized for ^{64}Zn or ^{66}Zn. This contaminant zinc most likely originated from the metal electrode used in Western Blots

which is stored in solution with the nitrocellulose in an Invitrogen™ Western Blot kit. In addition, cadmium was only able to be detected at a level of 313 ppb, compared to 75 ppb in Figure 3.25. This loss of sensitivity was due to the dispersion of the standard spots to a larger area upon placement onto the nitrocellulose compared to a dried PAGE gel, where the spots do not disperse upon placement onto the surface. This demonstrated that performing a Western Blot was not a suitable alternative for direct LA-ICP-MS analysis of a fractionated proteome sample from a PAGE gel.

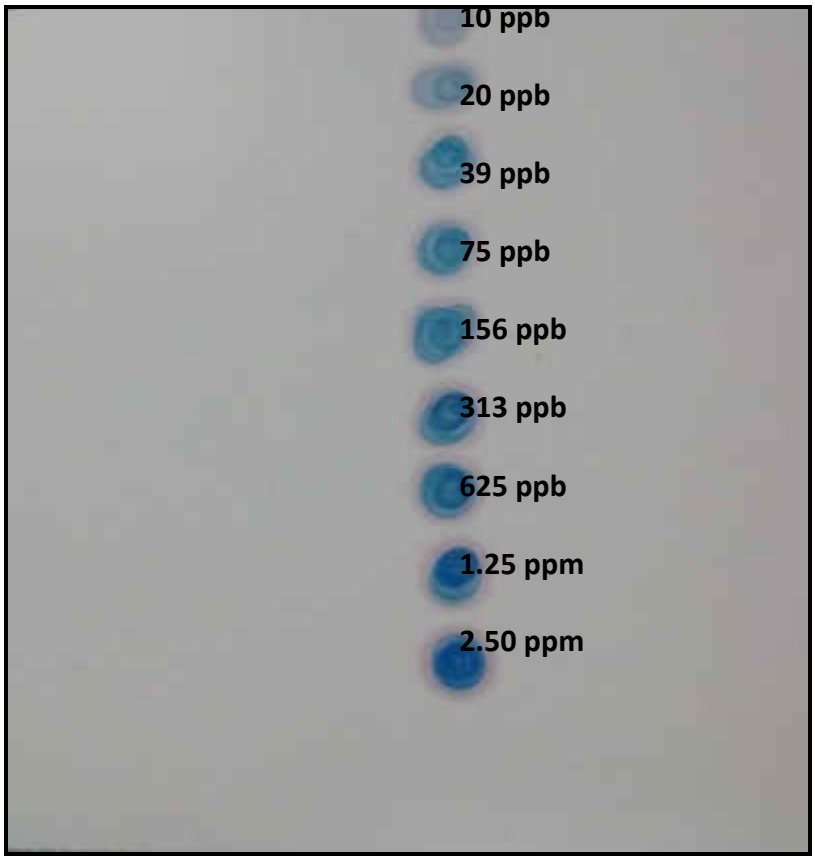

Figure 3.26. Image of Invitrogen™ Western Blot nitrocellulose material spotted with 0.5 µL of natural abundance distribution zinc-cadmium isotope standards. 2.5 ppm standard spot contains 17.8 pico-moles of zinc and 11.1 pico-moles of cadmium. 10 ppb spot contains 77.0 femto moles of zinc and 44.3 femto-moles of cadmium.

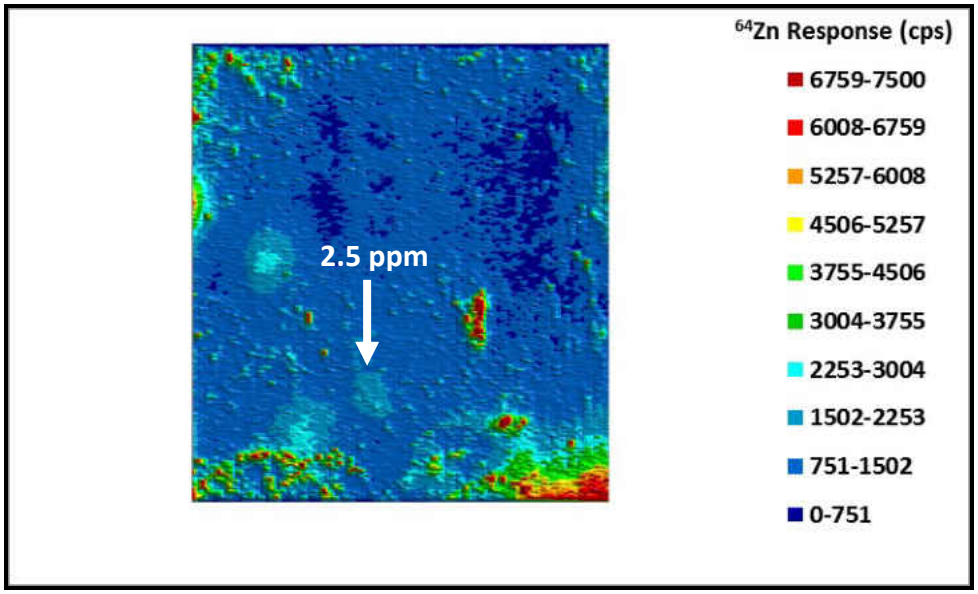

Figure 3.27. LA-ICP-MS analysis of ^{64}Zn in Figure 3.26.

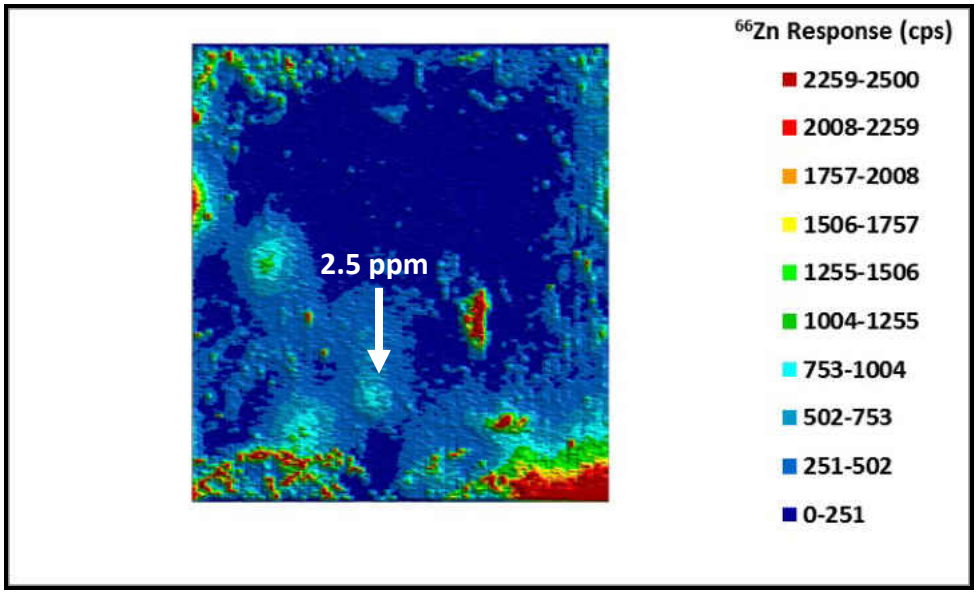

Figure 3.28. LA-ICP-MS analysis of ^{66}Zn in Figure 3.26.

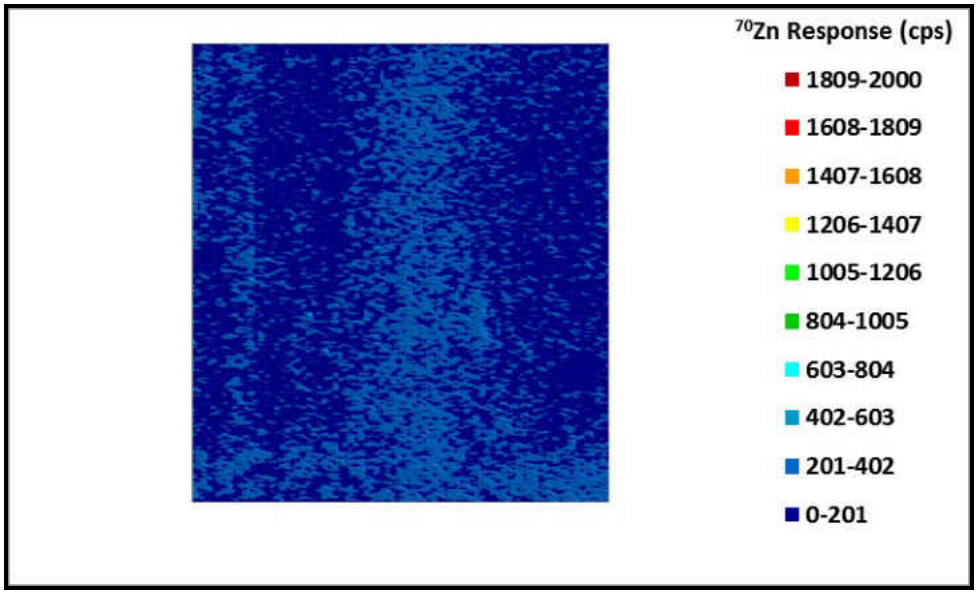

Figure 3.29. LA-ICP-MS analysis of ^{70}Zn in Figure 3.26.

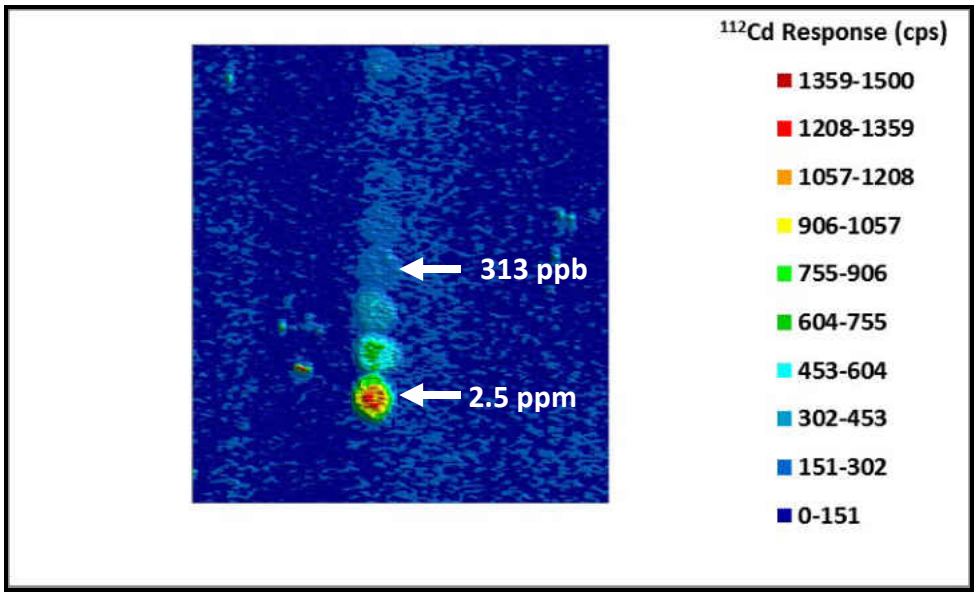

Figure 3.30. LA-ICP-MS analysis of ^{112}Cd in Figure 3.26.

3.2.5. Quantitative LA-ICP-MS of PAGE Gel Using ^{70}Zn and ^{113}Cd

ICP-MS analysis measures each isotope of a particular element individually. For example, a zinc standard contains all isotopes of zinc, ^{64}Zn, ^{66}Zn, ^{67}Zn ^{68}Zn, and ^{70}Zn, at their natural distribution percentages, 48.6 %, 27.9 %, 4.10 %, 18.8 %, and 0.60 %, respectively. Unless a summation of all responses is performed, a measurement of a single isotope of an element with multiple isotopes is at most only measuring the isotope percentage amount of the element. For example, if ^{64}Zn is measured in a sample that contains a natural distribution of zinc isotopes, only 48.6 % of the zinc can actually be measured. The same principle applies to cadmium, which has multiple isotopes. To determine if using as single ^{70}Zn isotope would improve detection limits of zinc in a PAGE gel matrix, and to determine if using a single isotope of cadmium (^{113}Cd) would improve detection limits of cadmium in a PAGE gel matrix, a serial dilution of ^{70}Zn and ^{113}Cd standard (prepared as described in section 2.8.3) was spotted onto a dried PAGE gel prepared as described in section 2.10.3. (Figure 3.31), and subsequently analyzed using LA-ICP-MS. Figure 3.31 shows the spotted standards on the dried polyacrylamide gel, labeled with their respective concentrations of zinc and cadmium, which contain phenol red to allow spots to be visualized. A large amount of contaminant zinc was detected in the gel matrix as shown in Figure 3.32, which is imaged as a high background and numerous punctate spikes in zinc response. By using a ^{70}Zn isotope, the background was eliminated, and zinc could be detected (detection limit being defined as a signal that was 3 times the noise or background) at a level of 39

ppb on the gel (Figure 3.33) compared to a natural distribution of zinc isotopes where the detection limit for ^{64}Zn was determined to be 1.25 ppm (Figure 3.22). This determined detection limit of 39 ppb was suitable for the analysis of trace levels of zinc present in proteins from a proteome. The ^{70}Zn standards could be visualized on the false color image at a level of 1.22 ppb, however, the signal response of 250 cps was only slightly above the background signal response of 150 cps. Next, the average response for each zinc standard spot was calculated, and a linear regression analysis of the data was performed. The resultant correlation was determined to be 97.1 % (Figure 3.34). An improved detection limit for cadmium was observed (Figure 3.35) when a single isotope of cadmium was used, where cadmium could now be detected at a level of 2.4 ppb compared to a natural distribution of cadmium isotopes where the detection limit for ^{112}Cd was determined to be 75 ppb (Figure 3.25). The cadmium was able to be detected at a lower limit than zinc due to a higher signal response for cadmium at the same concentration as zinc. The ^{113}Cd standards could be visualized on the false color image at a level of 1.22 ppb, however, the signal response of 450 cps was only slightly above the background signal response of 350 cps. Next, the average response for each cadmium standard spot was calculated, and a linear regression analysis of the data was performed. The resultant correlation was determined to be 94.8 % (Figure 3.36). The lack of background interference allowed for the detection and subsequent quantification of ^{70}Zn and ^{113}Cd at trace levels.

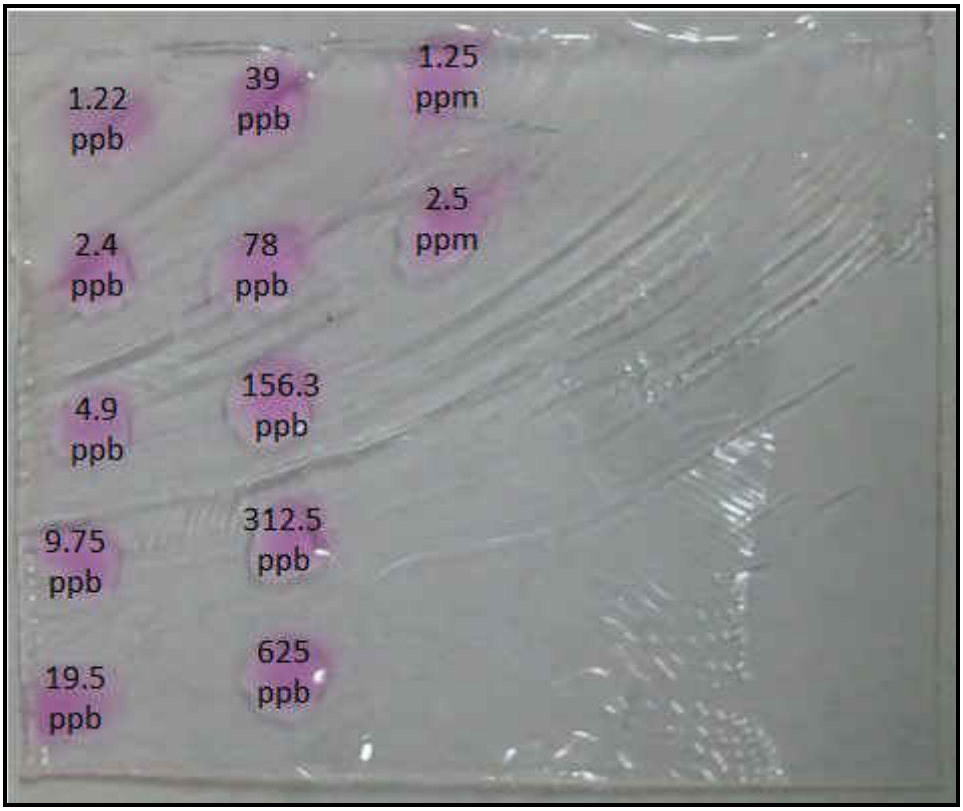

Figure 3.31. Image of 12% Invitrogen™ Bis-Tris gel spotted with 0.5 µL of each ^{70}Zn and ^{113}Cd standard. 2.5 ppm standard spot contains 17.8 pico-moles of ^{70}Zn and 11.1 pico-moles of ^{113}Cd. 1.22 ppb spot contains 8.7 femto moles of ^{70}Zn and 5.4 femto-moles of ^{113}Cd.

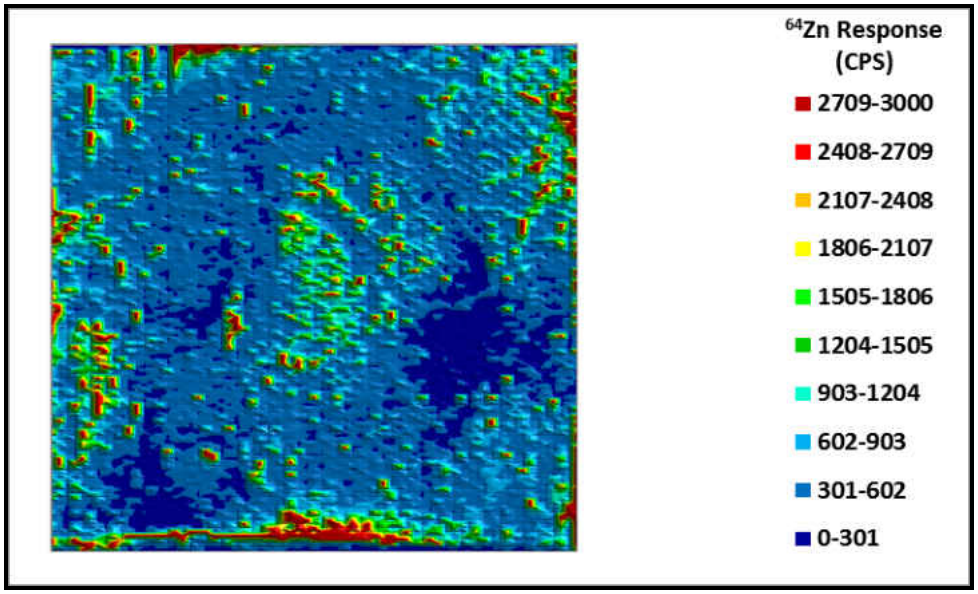

Figure 3.32. LA-ICP-MS analysis of ^{64}Zn in Figure 3.31.

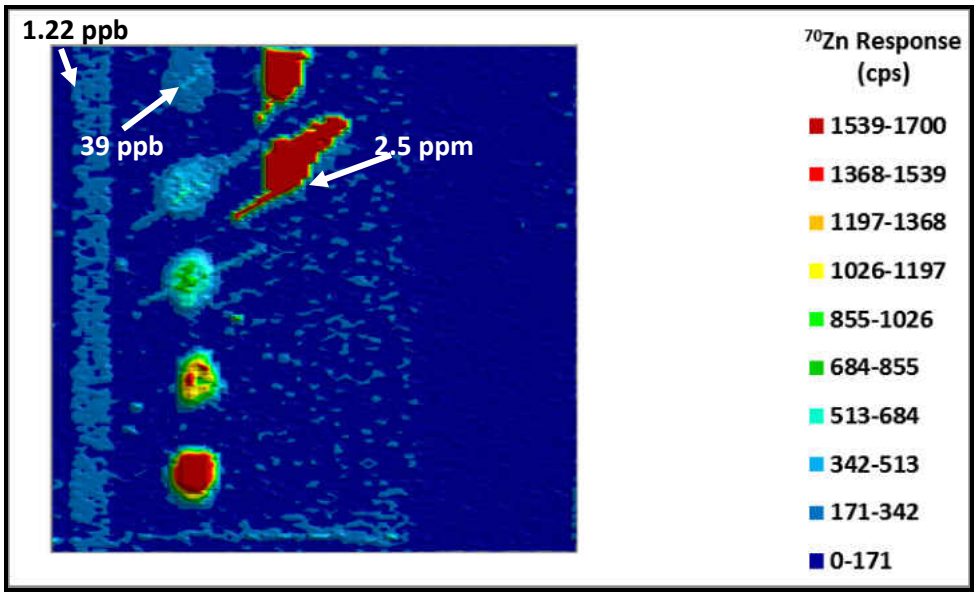

Figure 3.33. LA-ICP-MS analysis of ^{70}Zn standards in Figure 3.31.

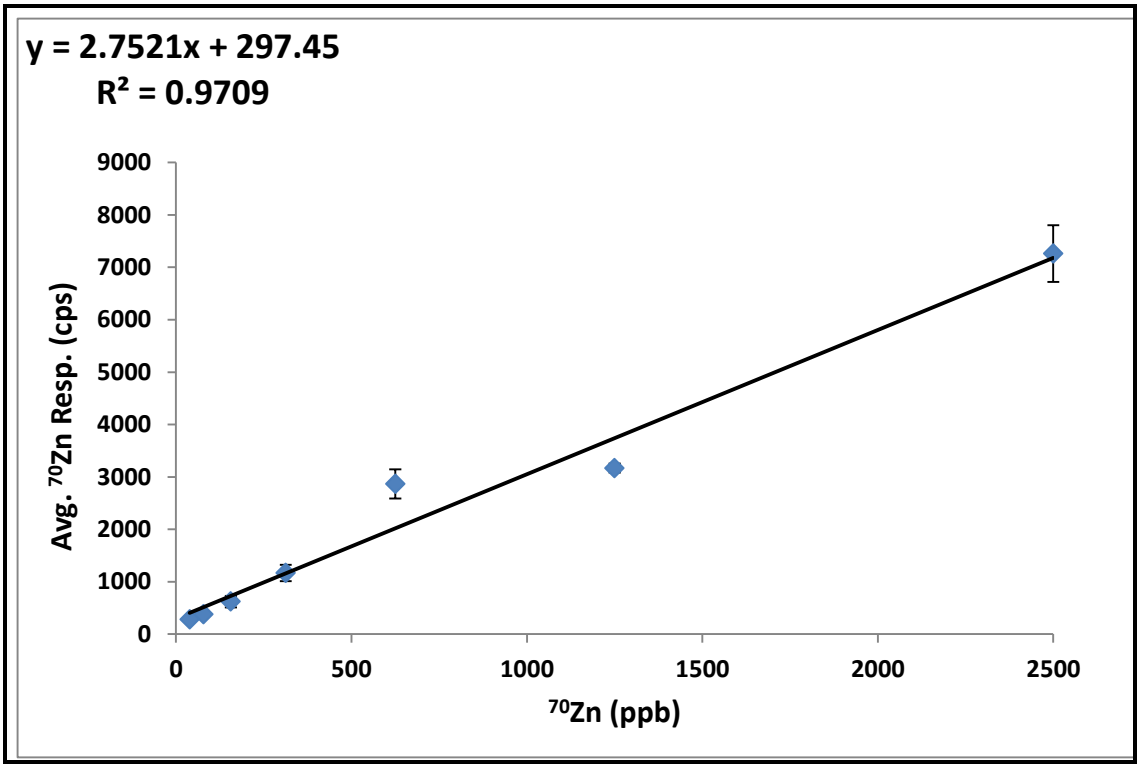

Figure 3.34. Linear regression analysis of average ^{70}Zn responses from standards in Figure 3.33.

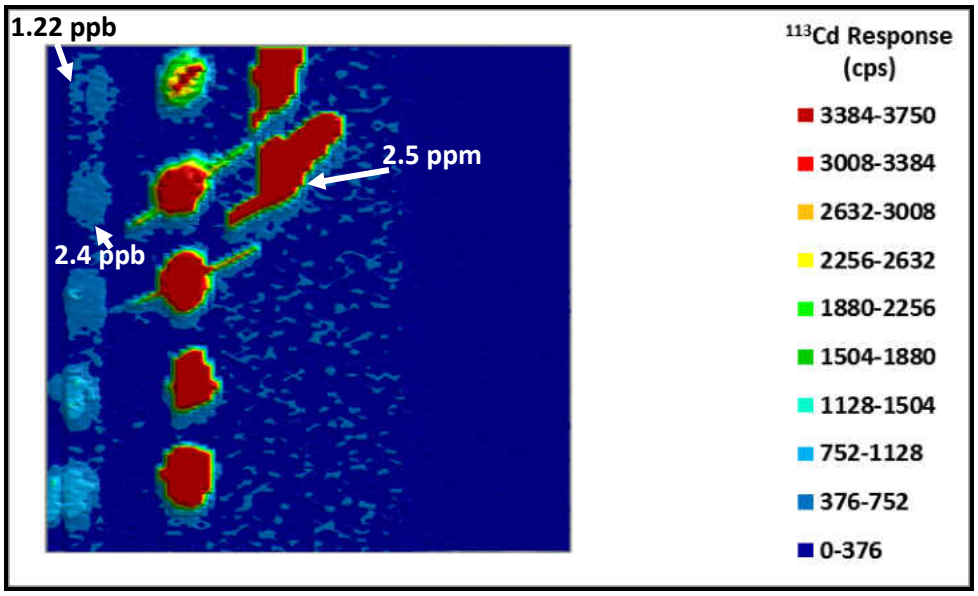

Figure 3.35. LA-ICP-MS analysis of ^{113}Cd standards in Figure 3.31.

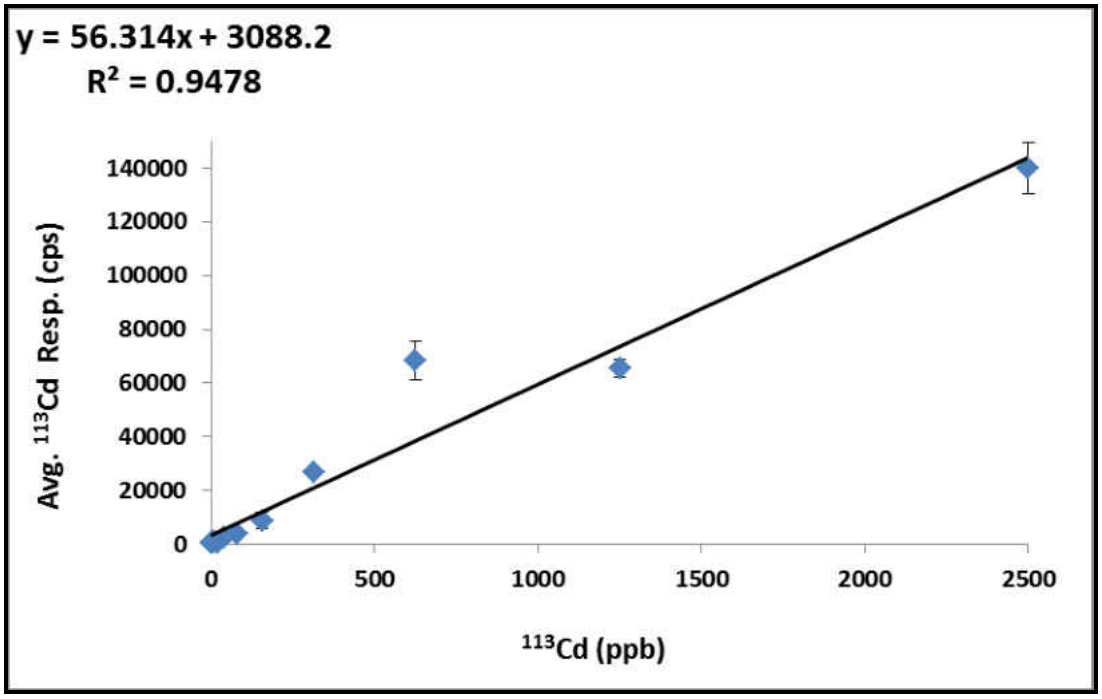

Figure 3.36. Linear regression analysis of average ^{113}Cd responses from standards in Figure 3.35.

3.3. Development of Native Sodium Dodecyl Sulfate Polyacrylamide Gel Electrophoresis

3.3.1. SDS-PAGE of Proteome With and Without Sample Heating Step (A Collaboration with Drew Nowakowski)

SDS-PAGE is an electrophoresis method that separates proteins with high resolution on a polyacrylamide gel. Sodium Dodecyl Sulfate (SDS) is an anionic detergent, which both denatures proteins, and coats them with negative charge to cause the proteins to migrate through the polyacrylamide gel under an applied electrochemical potential. Commercially available SDS-PAGE methods from Invitrogen™ utilize several denaturing

steps which have questionable relevance in their importance to the method's high resolution. In brief, these questionable denaturing steps include heating samples to 70 °C prior to electrophoresis, utilizing a metal chelator (1 mM EDTA) in both the sample and run buffers, and using a high concentration of detergent (2.0 % LDS) in the sample buffer. To determine if heating a PAGE protein sample to 70 °C per the Invitrogen™ SDS-PAGE specifications was necessary to achieve adequate resolution, proteome samples summarized in Table 3.2. were run per the Invitrogen™ SDS-PAGE conditions with one exception. One gel was run with heating the samples to 70 °C before performing SDS-PAGE, and the other gel was run without heating the samples to 70 °C before performing SDS-PAGE. Figure 3.37 shows that heating does not provide substantial improvement in resolving protein bands when performing SDS-PAGE. By not heating the protein samples, denaturation conditions are moderated, favoring the retention of zinc by proteins during electrophoresis.

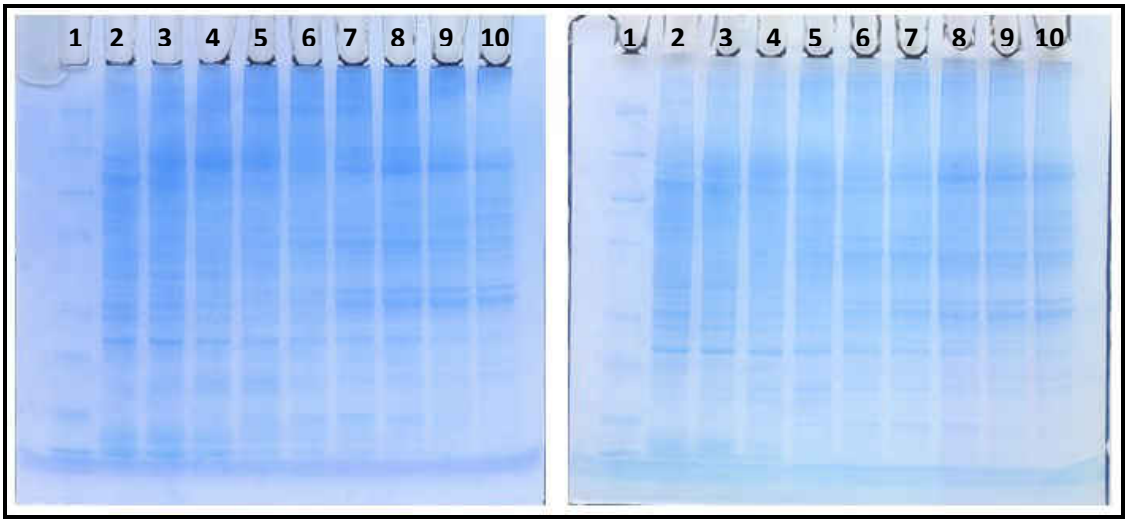

Figure 3.37. Invitrogen™ Simply Blue SafeStain® stained SDS-PAGE gels. SDS-PAGE gel (left) was run without heating samples to 70° C for 10 minutes prior to loading onto gel. SDS-PAGE gel (right) was run after heating samples to 70° C for 10 minutes prior to loading onto gel.

3.3.2. In Vitro Reaction of Proteome with Invitrogen™ 1X MOPS SDS Run Buffer

To determine the effect of the electrophoresis run buffer on the retention of zinc in zinc proteins, zinc proteome from LLC-PK_1 cells prepared per 2.1.1. was reacted with excess 1X MOPS run buffer from Invitrogen™ at room temperature for 1 hour. Figure 3.38 shows a 65.7 percent loss of zinc from proteome when reacted with the SDS sun buffer compared to the control. This loss of zinc from the proteome was likely due to the high concentrations of SDS (0.1 %) and EDTA (1.0 mM) in the run buffer. Since SDS is a denaturing detergent, and EDTA is a strong chelator, the combination of protein denaturation and metal chelation accounted for the large loss of zinc from proteins in the proteome sample.

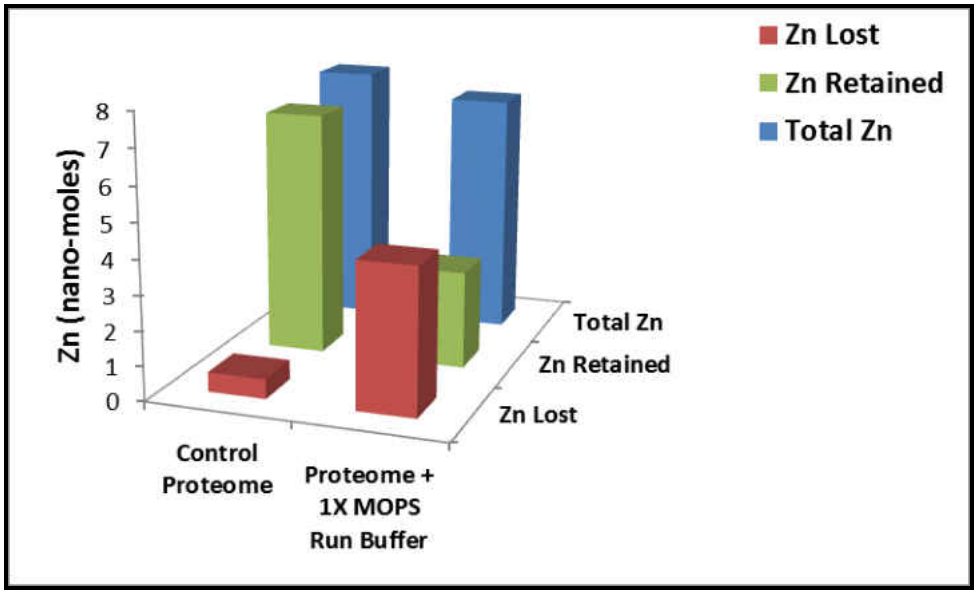

Figure 3.38. Reaction of LLC-PK_1 proteome with 20 mM TRIS-Cl + 5 mM β-ME buffer (control) and Invitrogen MOPS 1X SDS run beffer solution used for SDS-PAGE method (Proteome + 1X MOPS Run Buffer).

3.3.3. NSDS-PAGE of Superoxide Dismutase, Carbonic Anhydrase, and Alcohol Dehydrogenase (A Collaboration with Drew Nowakowski)

After the observation that some zinc proteins retained their complement of zinc to some extent after performing denaturing SDS-PAGE as shown in section 3.1.6, and that the sample heating step had no effect on the SDS-PAGE separation of proteins as shown in section 3.3.1, further investigation into other SDS-PAGE conditions was performed. It was hypothesized that adjusting the method parameters further may improve the retention of zinc in protein samples after electrophoresis while maintaining the high resolution capabilities of the method. After an examination of the current commercial SDS-PAGE method conditions, several different parameters were selected for

modification. First, it was determined that the 1 mM EDTA present in the sample and run buffers needed to be removed, as EDTA is a strong metal chelator. As shown in experiments performed by Drew Nowakowski, removing EDTA entirely from the sample and run buffers had no effect on the resolution between protein bands from fractionated LLC-PK_1 proteome samples. Second, it was hypothesized that the LDS may be able to be removed from the sample buffer, as LDS is a detergent that can denature proteins. Experiments performed by Drew Nowakowski have shown that removing LDS from the sample buffer had no effect on the resolution between protein bands. Third, it was hypothesized that lowering the SDS concentration in the run buffer could reduce protein denaturation during electrophoresis, while maintaining the resolution of the method. Experiments performed by Drew Nowakowski have shown that the SDS concentration could be lowered from 0.1 % to 0.0375 % while still maintaining adequate resolution between protein bands. In addition, the voltage of the method was lowered from 200 V constant to 150 V constant to reduce the amount of heat generated during electrophoresis, and to lower the applied electrochemical potential in an attempt to further reduce metal loss. Lastly, electrophoresis was performed at 4 °C to reduce the degradation of proteins. The newly developed PAGE method with the previously described modifications to SDS-PAGE is referred to as native SDS-PAGE (NSDS-PAGE). To evaluate if NSDS-PAGE would reduce denaturation of proteins during electrophoresis while maintaining high resolution, PAGE analysis of model zinc proteins superoxide dismutase, alcohol dehydrogenase, and carbonic anhydrase was performed using SDS-PAGE, NSDS-PAGE, and BN-PAGE conditions summarized in Table 3.5. Model

protein samples were prepared as described in sections 2.4.2, 2.5.2, and 2.6.2. Gels were run in duplicate with one gel stained with Coomassie blue as described in section 2.7.1, and the other dried as described in section 2.8.1, followed by subsequent LA-ICP-MS analysis as described in section 2.10.1. Figure 3.39 shows a comparison of the Coomassie stained gel images. The SDS-PAGE gel provided adequate separation of SOD, ADH, and CA. However, a majority of the SOD, a zinc copper protein that is a dimer in its native conformation, became denatured, and separated into its monomeric subunits when compared to the NSDS-PAGE and BN-PAGE separated SOD. In addition, fragmentation of CA appeared to occur. Several low molecular weight bands appeared on the SDS-PAGE gel that were not present on the NSDS-PAGE or BN-PAGE gels. ADH was the only model protein which did not display any visual degradation on the SDS-PAGE gel. The ADH separation pattern on the SDS-PAGE gel is comparable to the ADH separation pattern on the NSDS-PAGE gel, where ADH separated in its native dimer conformation. The NSDS-PAGE gel provided adequate resolution between SOD, ADH, and CA. If the lanes containing SOD, CA, and ADH were to be superimposed, the protein bands would not overlap, allowing each individual protein band to be visualized. The BN-PAGE gel did not provide adequate resolution between SOD, ADH, and CA. If the lanes containing SOD, CA, and ADH were to be superimposed, the protein bands would overlap, which showed that in the case of a simple protein mixture consisting of only three proteins, BN-PAGE already failed to provide the separation necessary to visualize each protein.

PAGE Methods and Conditions			
	SDS-PAGE (Invitrogen™)	**BN-PAGE (Invitrogen™)**	**NSDS-PAGE (Petering, Nowakowski, Wobig)**
Voltage	200 V Constant	150 V Constant	150 V Constant
Temperature	Ambient	Ambient	4 °C
Run Buffer (Cathode)	50 mM MOPS 50 mM TRIS Base 0.1% SDS 1 mM EDTA pH 7.7	50 mM BisTris 50 mM Tricine 0.002% Coomassie G-250 pH 6.8	50 mM MOPS 50 mM Tris Base 0.0375% SDS pH 7.7
Run Buffer (Anode)	50 mM MOPS 50 mM TRIS Base 0.1% SDS 1 mM EDTA pH 7.7	50 mM BisTris 50 mM Tricine pH 6.8	50 mM MOPS 50 mM Tris Base 0.0375% SDS pH 7.7
Sample Buffer	106 mM Tris HCl 141 mM Tris Base 2.0% LDS 10% Glycerol 0.51 mM EDTA 0.022 mM SERVA Blue G250 0.175 mM Phenol Red pH 8.5	50 mM BisTris 6 N HCl 50 mM NaCl 10% w/v Glycerol 0.001% Ponceau S pH 7.2	106 mM Tris HCl 141 mM Tris Base 10% Glycerol 0.22 mM SERVA Blue G250 0.175 mM Phenol Red pH 8.5

Table 3.5. Comparison of conditions and reagents used in BN-PAGE, SDS-PAGE, and NSDS-PAGE.

3.3.4. LA-ICP-MS of SDS-PAGE, NSDS-PAGE, and BN-PAGE of SOD

To compare the amount of zinc and copper retained in SOD after performing SDS-PAGE, BN-PAGE, and NSDS-PAGE, LA-ICP-MS analysis of ^{64}Zn and ^{63}Cu of the 7.5 µg lanes of SOD was performed. In Figure 3.40. LA-ICP-MS analysis of ^{64}Zn content in SOD was compared between SDS-PAGE, NSDS-PAGE, and BN-PAGE. No ^{64}Zn above the baseline

was observed from the SDS-PAGE gel, while ^{64}Zn was clearly measured on the NSDS-PAGE and BN-PAGE gels, which directly correlated with the SOD stained bands on the Coomassie stained gels. In addition, in Figure 3.41 ^{63}Cu associated with SOD was also observed in all three PAGE methods, however, on the SDS-PAGE gel, ^{63}Cu was only observed in association with the non-denatured dimer SOD protein band on the gel, and the peak response was only approximately 800 cps versus 2,000 – 2,500 cps on the NSDS and BN PAGE gels. As summarized in Table 3.6, 95.0 % retention of zinc and 83.6 % retention of copper were observed in NSDS when compared to BN at 100 %. Also summarized in Table 3.6, 0 % retention of zinc and 27 % retention of copper were observed in SDS when compared to BN at 100 %. As expected, these results confirmed that SDS PAGE caused a majority of the associated copper and zinc to be lost from SOD due to protein denaturation. Some of the lost copper and zinc can be observed at the gel front in Figure 3.40 and Figure 3.41 respectively. In addition, these results confirmed that the separation of SOD using NSDS-PAGE did not cause substantial loss of associated copper and zinc from SOD, which confirmed the minimization of protein denaturation, while providing superior resolution to BN-PAGE.

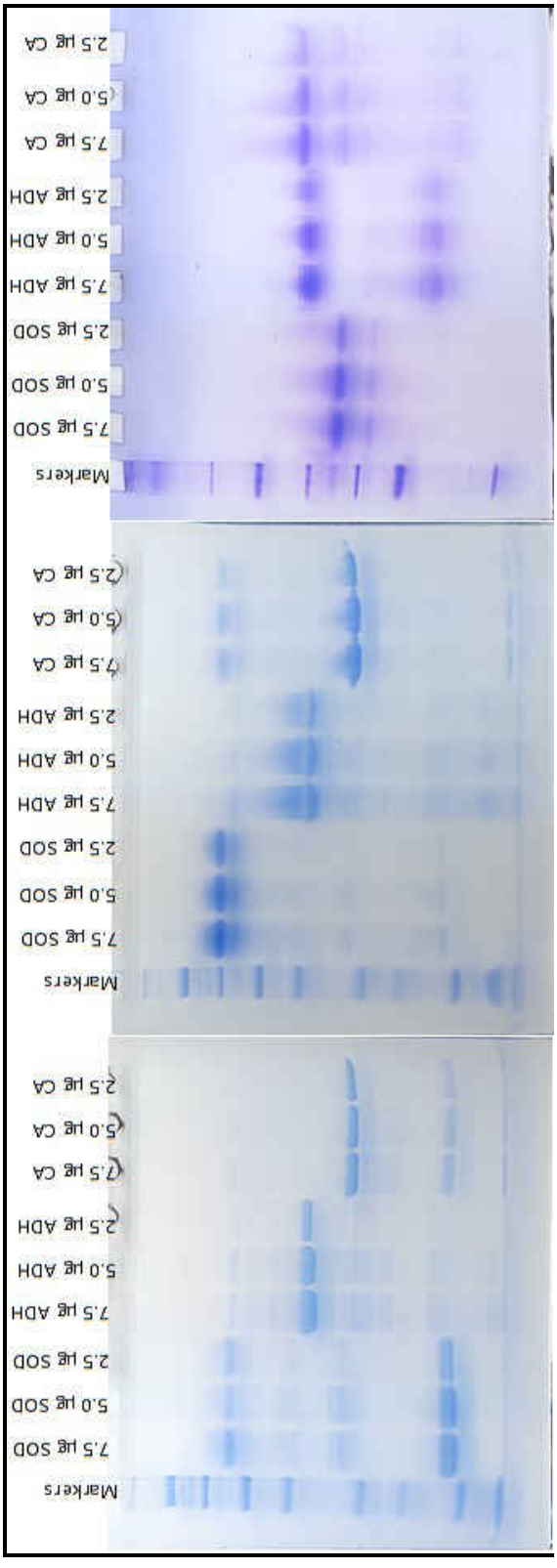

Figure 3.39. Coomassie stained gel image s of SOD, ADH, and CA run using conditions in Table 3.4. (left) SDS-PAGE, (middle) NSDS-PAGE, (right) BN-PAGE.

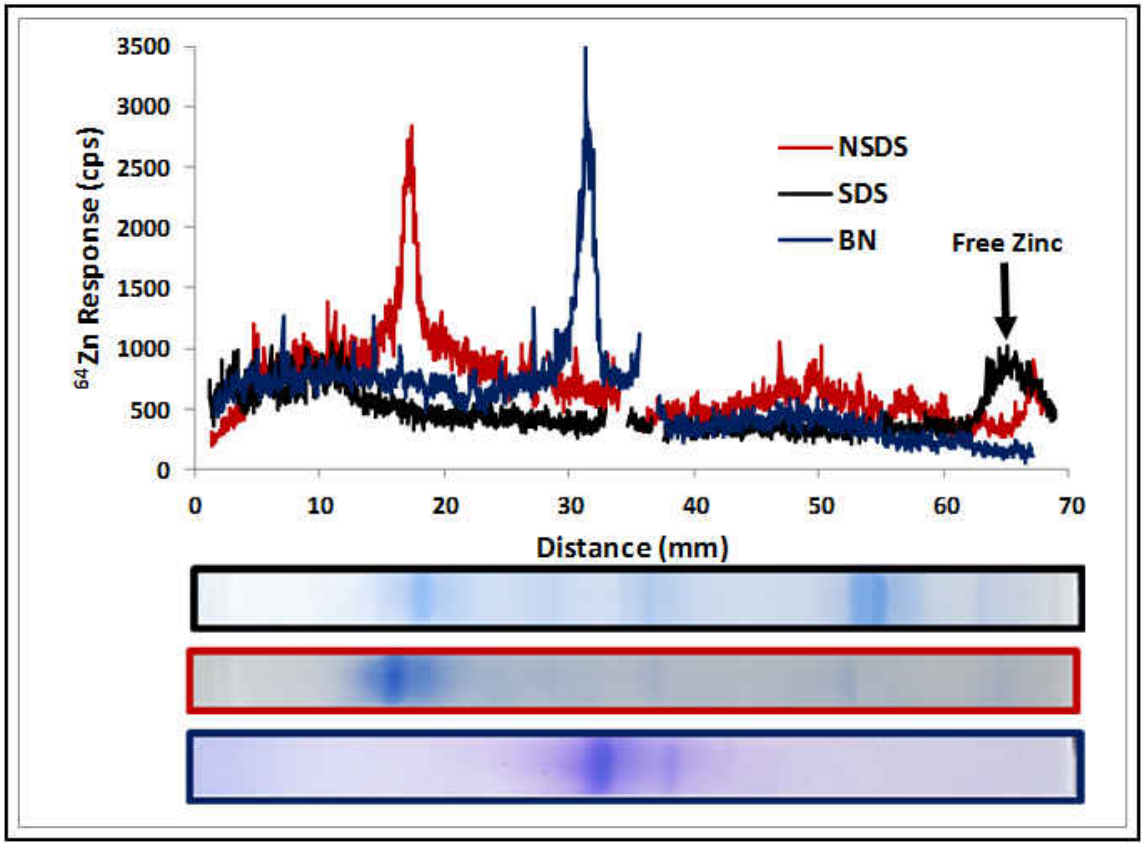

Figure 3.40. LA-ICP-MS analysis of ^{64}Zn in SOD (7.5 µg SOD, 231 pico-moles of Zn) separated by SDS-PAGE, NSDS-PAGE, and BN-PAGE.

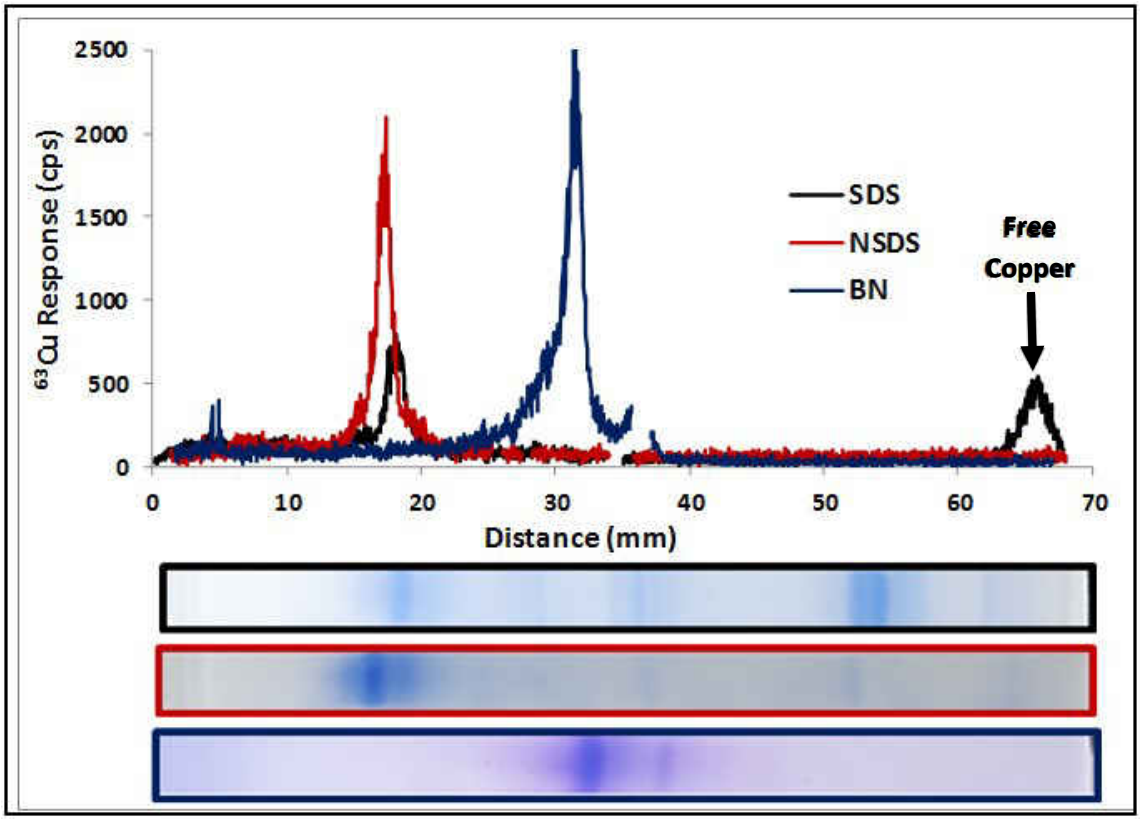

Figure 3.41. LA-ICP-MS analysis of ^{63}Cu in SOD (7.5 µg SOD, 231 pico-moles of Cu) separated by SDS-PAGE, NSDS-PAGE, and BN-PAGE.

Comparison of Integrated SOD Peaks			
	SDS	**BN**	**NSDS**
Integrated Zn (cps)	82319 (baseline)	130019	123479
% Retention Zn	0%	100%	95.0%
Integrated Cu (cps)	20839	77061	63446
% Retention Cu	27.0%	100%	83.6%

Table 3.6. Comparison of integrated LA-ICP-MS responses for ^{63}Cu and ^{64}Zn between SDS-PAGE, BN-PAGE, and NSDS-PAGE of SOD protein band.

3.3.5. Quantitative LA-ICP-MS of ^{70}Zn-Proteome on NSDS-PAGE and SDS-PAGE

To eliminate background zinc, and quantify the amount of zinc associated with protein arrays separated on PAGE gels, LLC-PK_1 proteome was enriched with ^{70}Zn, and fractionated first using DEAE ion exchange chromatography (provided by Drew Nowakowski) and then separated using NSDS-PAGE or SDS-PAGE for comparison as shown in Figure 3.42. Quantitative LA-ICP-MS analysis was performed as described in section 2.10.3 (calibration curves shown in Figure 3.44 and 3.45) of the ^{70}Zn on the SDS gel showed that despite the denaturing conditions of the method, several groups of protein bands were able to retain their associated zinc (encircled in Figure 3.43). By comparison, NSDS-PAGE was able to resolve protein bands nearly as well as SDS-PAGE when Coomassie R-250 stained gel images were compared. The total integrated ^{70}Zn response from each gel showed, by comparison, a 122.2 % increase in the amount of zinc that was retained by proteins on the NSDS-PAGE gel versus the SDS-PAGE gel (Table 3.6). By visual comparison, this value appeared to underestimate the increase in retained zinc on the NSDS-PAGE gel versus the SDS-PAGE gel. This underestimation was most likely due to the integration of the background levels of zinc on the SDS-PAGE gel. Most zinc containing proteins contained zinc in the 22 – 38 ppb range, which would not previously have been able to be quantified due to the large background of contaminant zinc. Unfortunately, due to the complexity of each fractionated sample, no punctate zinc protein bands were observed. The inability to image isolated zinc protein bands due to poor resolution native PAGE methods or lack of sensitivity using LA-ICP-MS,

however, is no longer the limiting factor. The resolving power and native characteristics of the electrophoretic method, and the detection limit of the LA-ICP-MS method have been optimized to be suitable for the isolation and detection of individual zinc proteins.

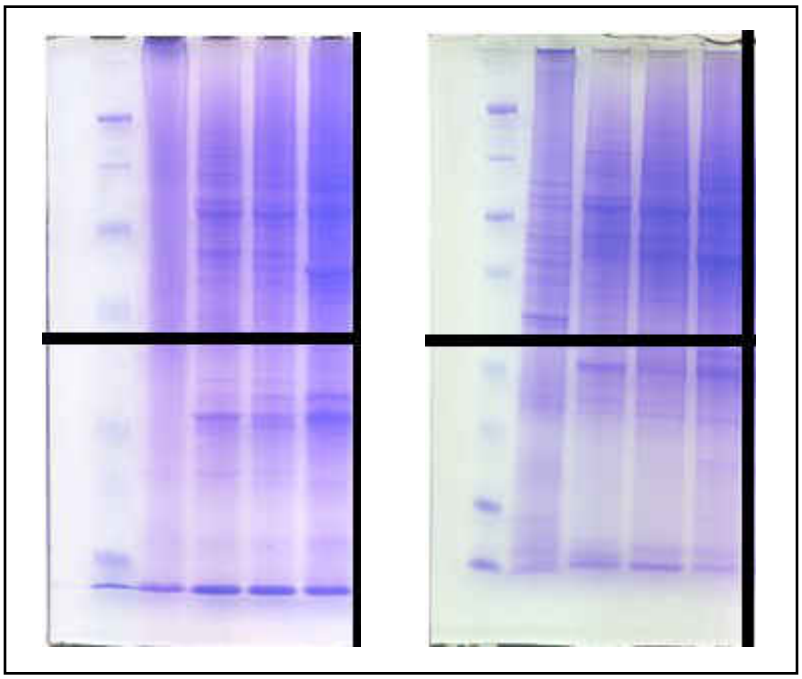

Figure 3.42. Comparison of Coomassie stained gel images of ^{70}Zn enriched proteome separated on NSDS (left) and SDS (right) PAGE gels.

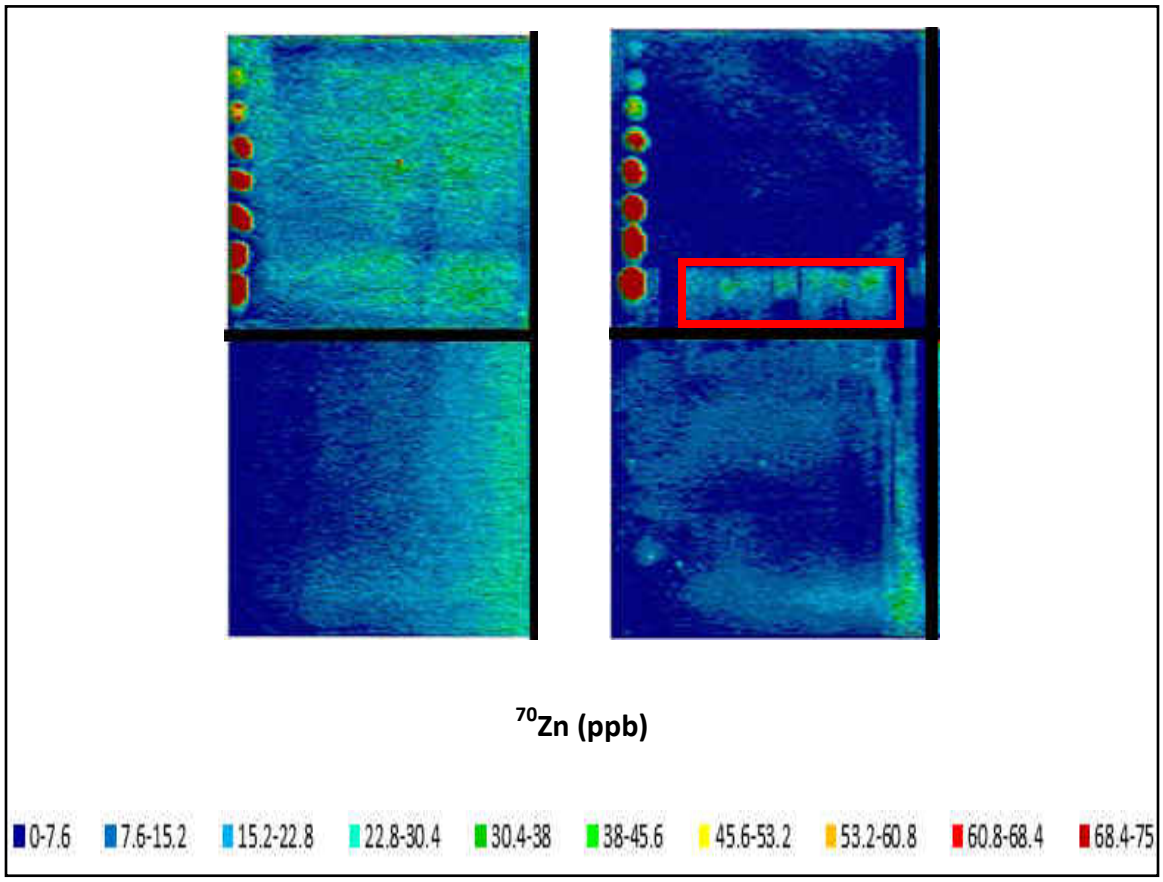

Figure 3.43. Quantitative LA-ICP-MS analysis of ^{70}Zn enriched proteome on NSDS (left) and SDS (right) PAGE gels.

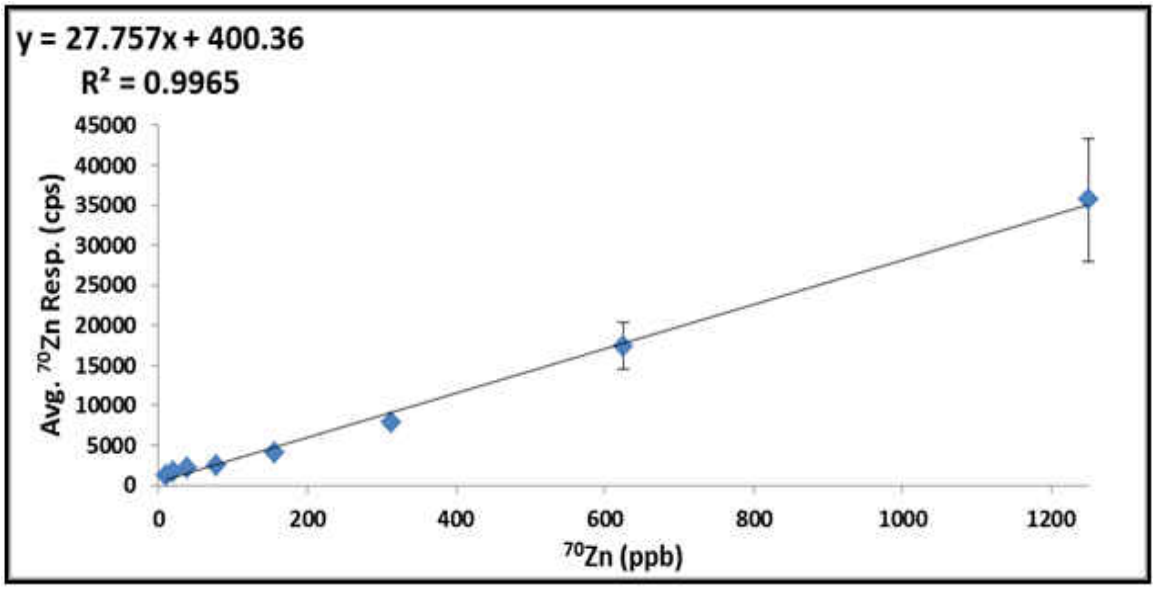

Figure 3.44. Calibration curve of ^{70}Zn standards used for quantitative LA-ICP-MS analysis of NSDS-PAGE gel in Figure 3.43.

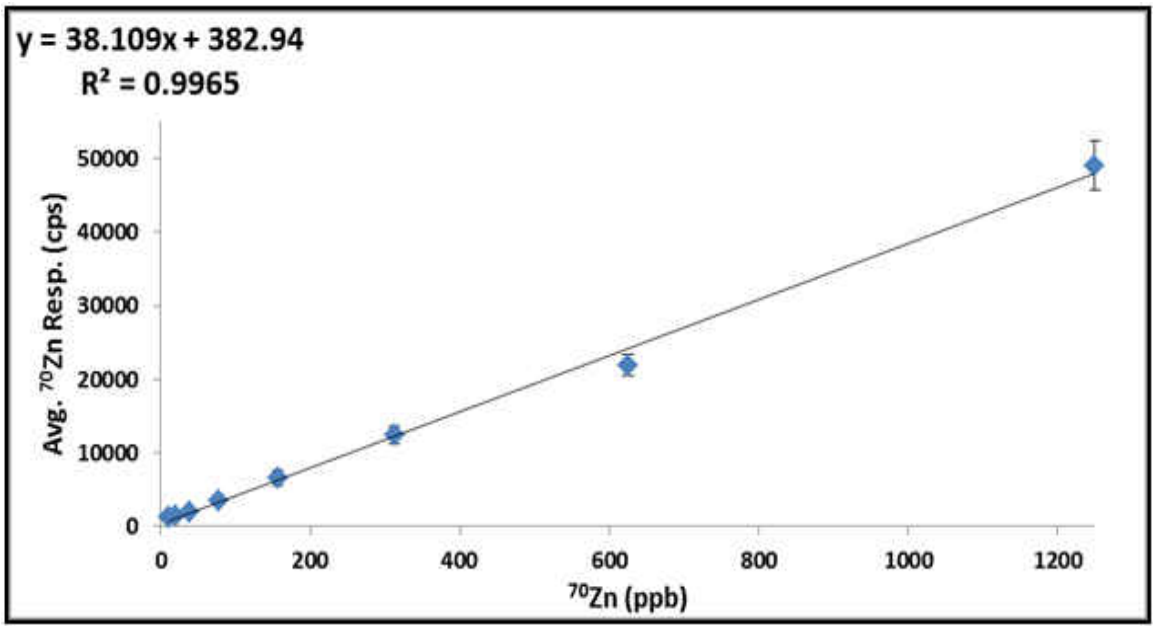

Figure 3.45. Calibration curve of ^{70}Zn standards used for quantitative LA-ICP-MS analysis of SDS-PAGE gel in Figure 3.43.

	SDS-PAGE	NSDS-PAGE
Total ^{70}Zn in Gel (ppb)	6.3×10^{5}	1.4×10^{6}
% Retention Increase vs. SDS-PAGE	----------	122.2

Table 3.7. Total ^{70}Zn present in SDS-PAGE and NSDS-PAGE gels from Figure 3.43.

3.4. Applications of LA-ICP-MS

3.4.1. Identification of TSQ Reactive Zn-Proteins from Proteome using LA-ICP-MS and LC-MS (A Collaboration with Drew Nowakowski)

Previous experiments have shown an enhancement of cellular fluorescence upon reaction with the zinc sensor TSQ [30]. More specifically, previous experiments have shown that this enhancement is due to the reaction of TSQ with zinc from zinc proteins to form TSQ-Zn-Protein ternary adducts [28,29]. NSDS-PAGE separations of proteome, followed by reaction with TSQ, analysis of zinc by LA-ICP-MS, and analysis by LC-MS could identify which zinc proteins react with TSQ. PAGE-LA-ICP-MS was used to identify zinc proteins from the LLC-PK_1 cytosolic proteome, prepared as described in section 2.1.1. The resulting proteome preparation contained 56 mg of protein and 256 nano-moles of zinc. The proteome was separated using DEAE chromatography as described in section 2.3. (Figure 3.46), which provided a large set of fractionated proteome containing zinc. Fractions 6, 11, 16, 21, 26, 31, 36, 41, and 46 containing substantial amounts of zinc and protein were selected for subsequent centrifugal filtration for further purification. These fractions were centrifuged in Amicon 100,000 Da MWCO tubes and the filtrate of proteins less than 100,000 Da were separated using NSDS-PAGE

in duplicate. One gel was stained with Coomassie blue stain as described in section 2.6.2. The other stained with TSQ as described in section 2.7.2, imaged on a fluorescence gel documentation system, and subsequently analyzed for zinc content using LA-ICP-MS as described in section 2.10.1. No background fluorescence measured with an emission filter wavelength of 460 nm – 510 nm of the gel and protein bands was observed. After staining the gel with TSQ, an estimated 25 punctate fluorescent protein bands were observed (Figure 3.47). These bands correlated with Coomassie R-250 stained proteins on the duplicate gel (Figure 3.47). LA-ICP-MS analysis of ^{66}Zn content in Lane 4 (Figure 3.48) identified a single, large zinc response, corresponding to a protein band that stained with Coomassie blue stain and TSQ at approximately 15 mm from the top of the gel. The band was sent to the Medical College of Wisconsin's protein mass spectrometry facility where the band of interest was identified using trypsin digestion, followed by LC-MS and a data base search. This technique employs trypsin to digest proteins into their individual amino acids. The unique relative amounts and ratios of amino acids in the digested sample are then analyzed by high resolution LC-MS. The results are then compared to genomic sequences in a data base, which can be linked to known or hypothetical proteins. The primary component of the protein band was heat shock protein HSP90, among other potential proteins including Transitional endoplasmic reticulum ATPase, Endoplasmin, Actin (cytoplasmic), and Villin-1 (Table 3.8). HSP90 is not classified as a zinc protein is the Protein Data Bank, however, a crystal structure of HSP90 shows numerous histidine amino acid residues in close proximity to each other (Figure 3.49 and Figure 3.50). These histidine residues might coordinate to zinc through

their imidazole ring nitrogens [31]. An example of such binding occurs in zinc carbonic anhydrase, where three imidazole nitrogens from three different histidine amino acid residues in close spatial proximity to each other, coordinate to the catalytic zinc in the active site[32-34]. To verify the binding of zinc to HSP90, future studies include obtaining recombinantly expressed HSP90 from the author of the crystal structure to determine in HSP90 binds zinc stoichiometricaly.

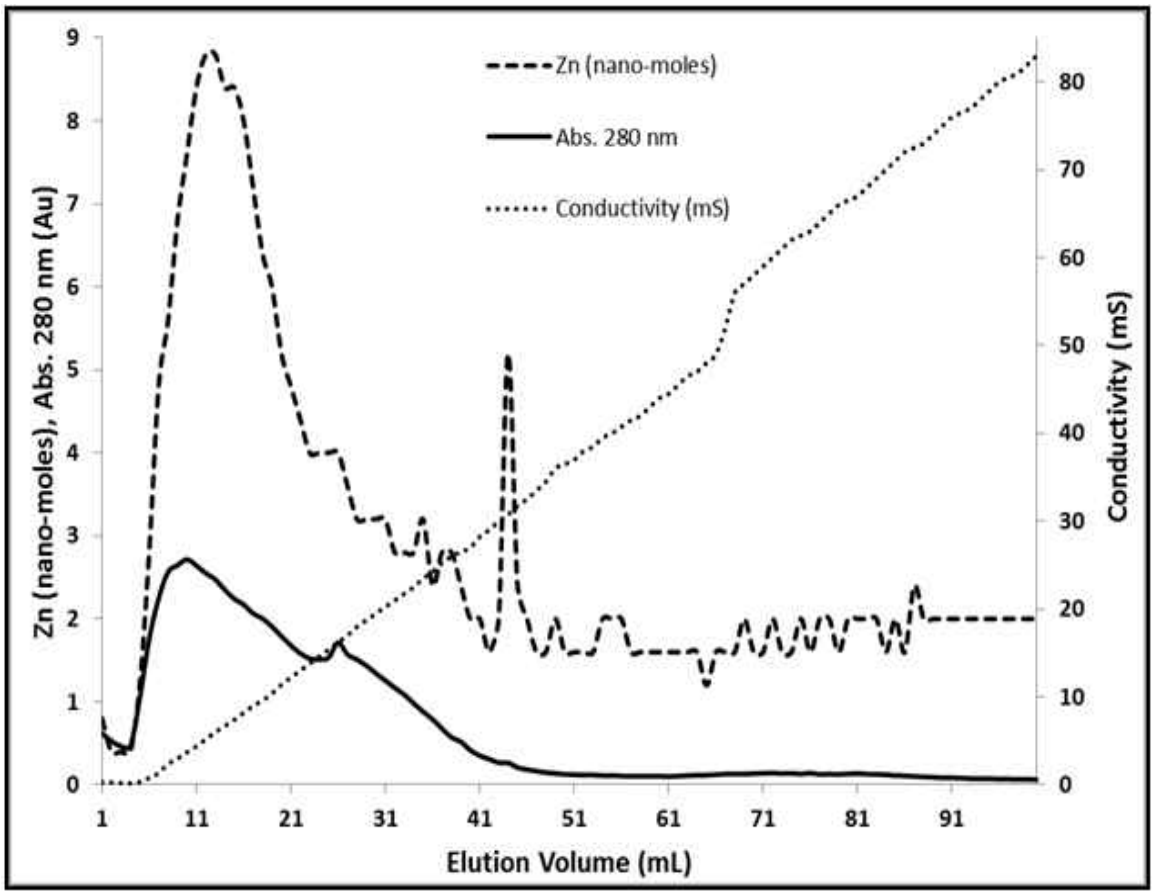

Figure 3.46. DEAE ion exchange chromatogram of LLC-PK_1 cytosolic proteome.

Figure 3.47. Coomassie stained gel image of select proteome fractions from DEAE IEX chromatography in Figure 3.46. (left) Background 470 nm fluorescence (middle). 470 nm fluorescense after staining in 20 µM for 30 minutes followed by destaining in MilliQ water for 30 minutes

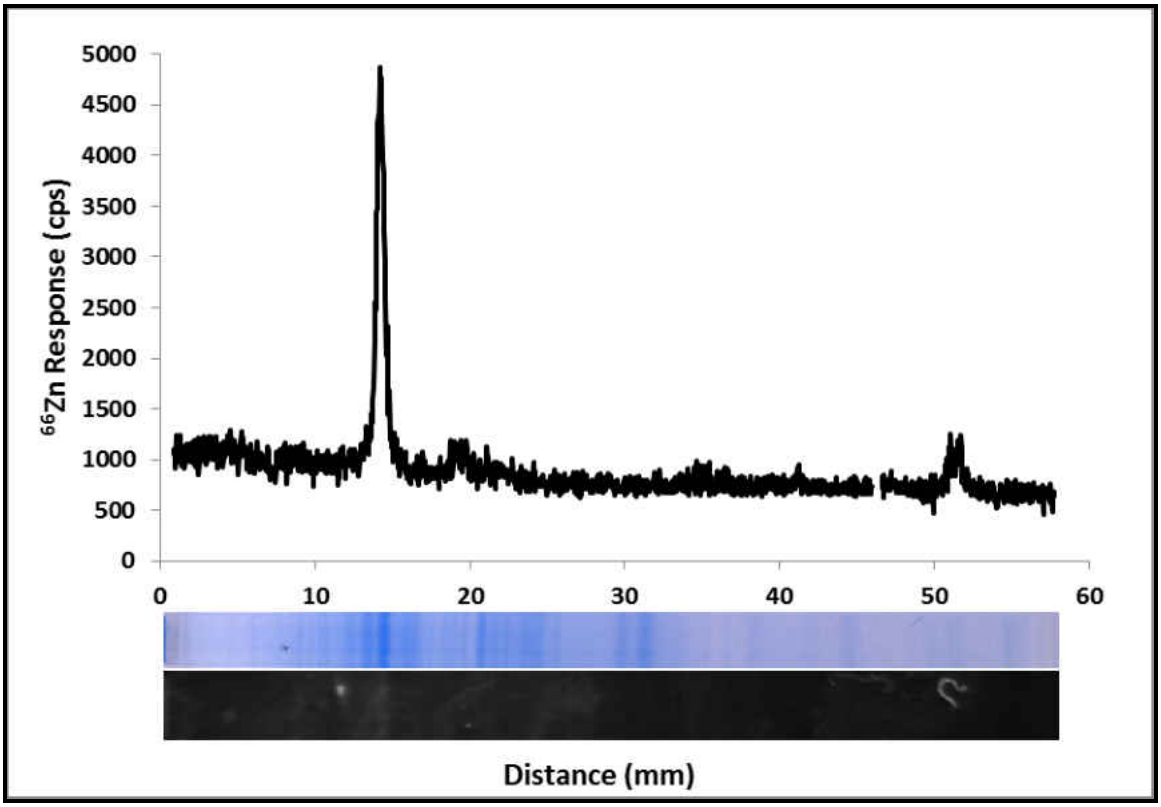

Figure 3.48. LA-ICP-MS analysis of ^{66}Zn in lane 4 from gels in Figure 3.47.

Accession	Description	Score	Coverage	# Proteins	# Unique Peptides	# Peptides	# PSMs	# AAs	MW [kDa]	calc. pI
O02705	Heat shock protein HSP 90-alpha OS=Sus scrofa GN=HSP90AA1 PE=2 SV=3 - [HS90A_PIG]	930.36	45.29	1	31	31	264	733	84.7	5.01
P03974	Transitional endoplasmic reticulum ATPase OS=Sus scrofa GN=VCP PE=1 SV=5 - [TERA_PIG]	264.49	27.17	1	17	17	73	806	89.2	5.26
Q29092	Endoplasmin OS=Sus scrofa GN=HSP90B1 PE=2 SV=3 - [ENPL_PIG]	263.03	23.76	1	16	16	74	804	92.4	4.83
Q6QAQ1	Actin, cytoplasmic 1 OS=Sus scrofa GN=ACTB PE=2 SV=2 - [ACTB_PIG]	195.44	32.27	1	5	9	54	375	41.7	5.48
P68137	Actin, alpha skeletal muscle OS=Sus scrofa GN=ACTA1 PE=3 SV=1 - [ACTS_PIG]	112.29	27.85	1	3	7	32	377	42.0	5.39
Q29261	Villin-1 OS=Sus scrofa GN=VIL1 PE=2 SV=2 - [VILI_PIG]	35.76	7.01	1	5	5	12	827	92.6	5.87
P02550	Tubulin alpha-1A chain OS=Sus scrofa GN=TUBA1A PE=1 SV=1 - [TBA1A_PIG]	33.45	9.98	2	3	3	8	451	50.0	5.03
Q29387	Elongation factor 1-gamma (Fragment) OS=Sus scrofa GN=EEF1G PE=2 SV=2 - [EF1G_PIG]	28.23	6.25	1	3	3	9	432	49.6	6.57
P19620	Annexin A2 OS=Sus scrofa GN=ANXA2 PE=1 SV=4 - [ANXA2_PIG]	16.42	13.57	1	3	3	5	339	38.5	6.93

Table 3.8. LC-MS analysis and protein content identification of TSQ reactive, ^{66}Zn containing protein band at approximately 15 mm from Figure 3.47. "Score" refers to best match, with a higher score corresponding to a batter match.

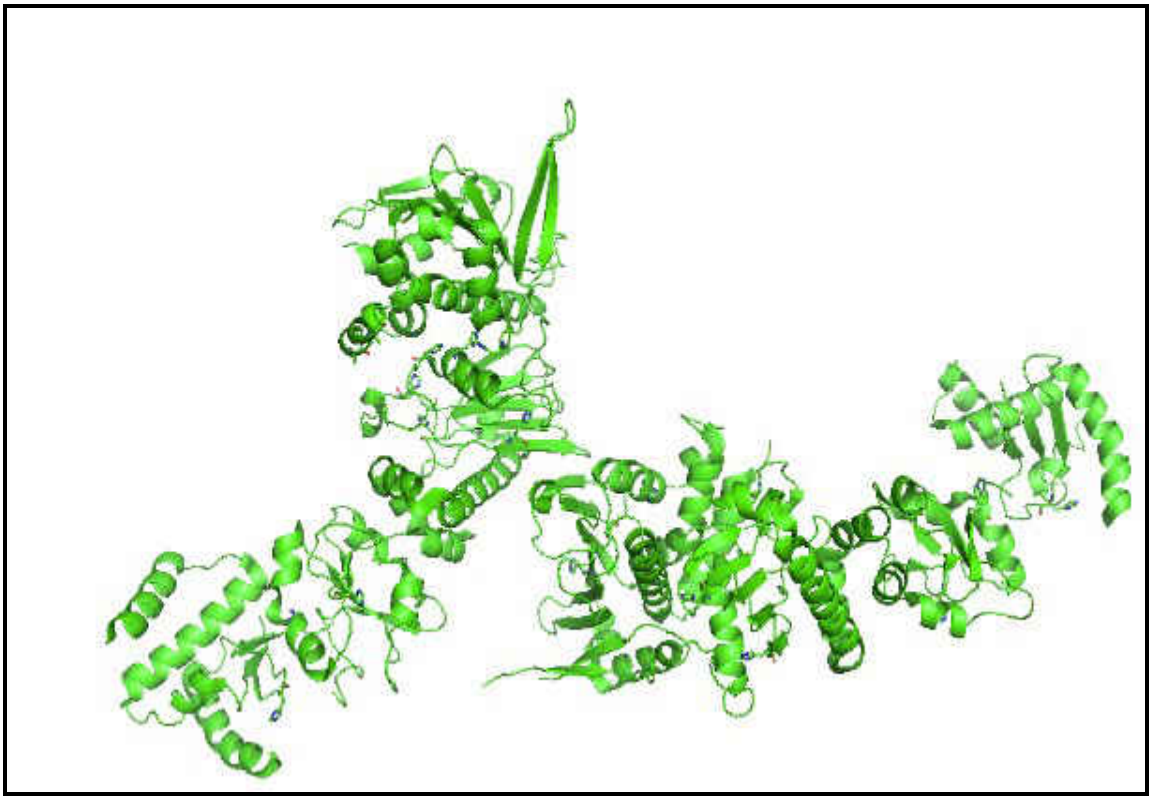

Figure 3.49. X-ray crystal structure of HSP90 [31]

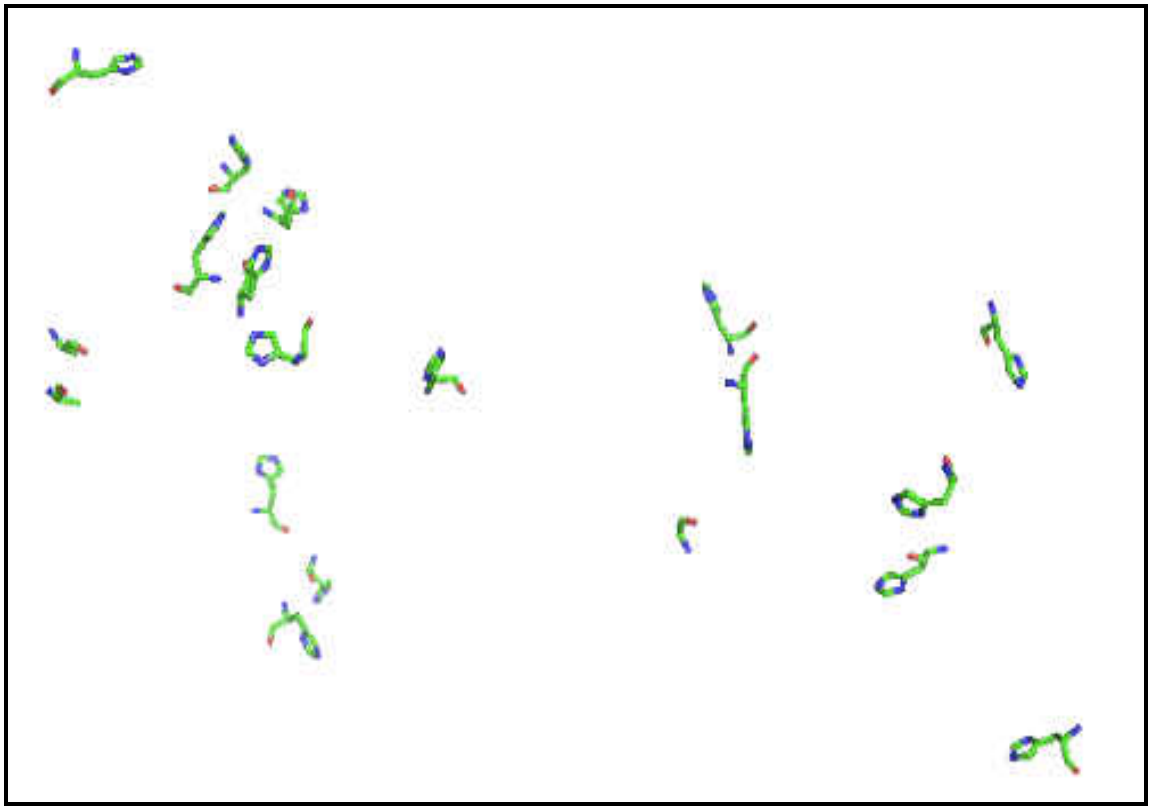

Figure 3.50. X-ray crystal structure of HPS90. Protein backbone is subtracted, and spatial location of His AA residues is shown [31]

3.4.2. Determination of Reaction mechanism of TSQ and TPEN with Zn-proteins (A Collaboration with Drew Nowakowski)

Previous proteomic and cellular microscopy experiments have shown that upon reaction with TSQ, cells and proteins show an enhanced fluorescent emission at 470 nm, which has been demonstrated to be largly due to zinc proteins forming ternary adducts with TSQ[1]. Subsequently, when cells and proteome are reacted with TPEN after TSQ reaction, a majority of the fluorescence is quenched[10]. To determine if the fluorescence is quenched by chelation of zinc from zinc proteins, or by ligand substitution of TSQ-zinc

proteins with TPEN to form TPEN-zinc-proteins NSDS-PAGE gels prepared as described in section 2.6.1 containing fractionated proteome samples (fractions 5, 10, 15 and 20 run on lanes 2, 3, 4, and 5) from DEAE ion exchange chromatography (Figure 3.46) prepared as described in section 2.3 were stained with TSQ as described in section 2.7.2, followed by reaction with TPEN as described in section 2.7.3, and subsequent analysis by LA-ICP-MS as described in section 2.10.1. Possible reaction schematics are shown as Figures 3.51, 3.52, and 3.53. The NSDS PAGE gel contained a large array of proteins as shown by coomassie R-250 blue staining (Figure 3.54). No background fluorescence was observed at 470 nm (Figure 3.54). Upon staining with TSQ, an estimated 25 unique, well resolved, protein bands displayed fluorescence emission within the filter wavelengths of 460 nm – 510 nm (Figure 3.54). Subsequent incubation of the gel with TPEN completely quenched the fluorescense (Figure 3.54). These results confirmed the observation from previous experiments that TSQ bound to zinc forming TSQ-zinc-protein ternary adducts which exhibited a characteristic fluorescent emission of 470 nm, and that subsequent reaction with TPEN quenched the fluorescence[15]. To determine if (a) the observed fluorescense in protein bands from TSQ staining could be correlated to zinc content, (b) if TPEN quenched fluorescence by chelating zinc from zinc-proteins, or (c) if TPEN quenched fluorescense by ligand substitution with TSQ-zinc-protein adducts to form TPEN-zinc-protein adducts, LA-ICP-MS analysis of the electrophoretogram for ^{66}Zn content was performed. In addition, LA-ICP-MS analysis was performed on the NSDS gel that was not stained with TSQ or TPEN as a control. The control NSDS-PAGE gel was placed in water for the same amount of time as the other gels were reacted with TSQ and TPEN

solutions. Qualitatively, the ^{66}Zn profile of lanes 2 and 3, shown in Figures 3.55 and 3.56 were consistent when comparing the control gel to the gel stained with TSQ, and the gel stained with TSQ followed by being stained with TPEN. This supported the reaction scheme shown in Figure 3.51 as zinc was still measured in each gel lane which correlated to protein bands. However, the results could not be quantified since there were no standards measured for comparison, and these experiments were performed prior to the ^{70}Zn proteome experiments. Therefore, many of the observed zinc responses could also be due to contaminant zinc present in the gel matrix. In addition a direct comparison of the analyses' was not possible due to the experiments being performed on different days, where the instrument response could have varied over time. As a result, a conclusion about the amount of zinc present could not be made.

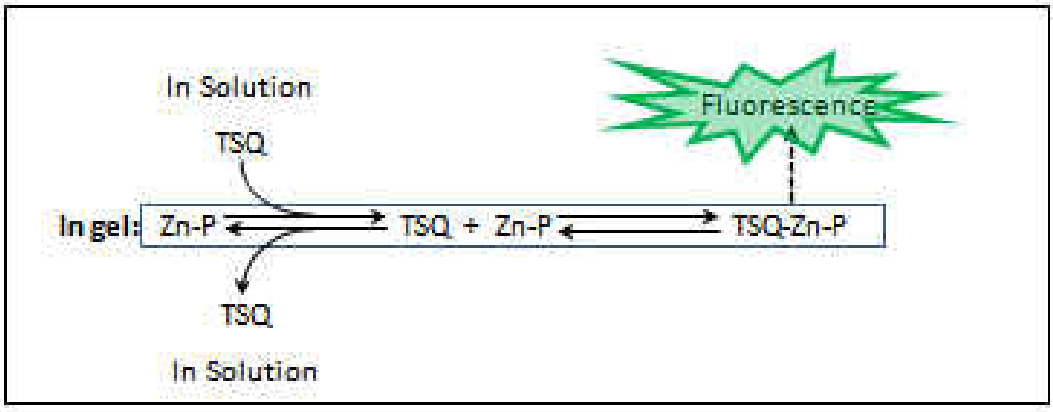

Figure 3.51 Reaction of TSQ with zinc proteins on a PAGE gel forming a ternary adduct

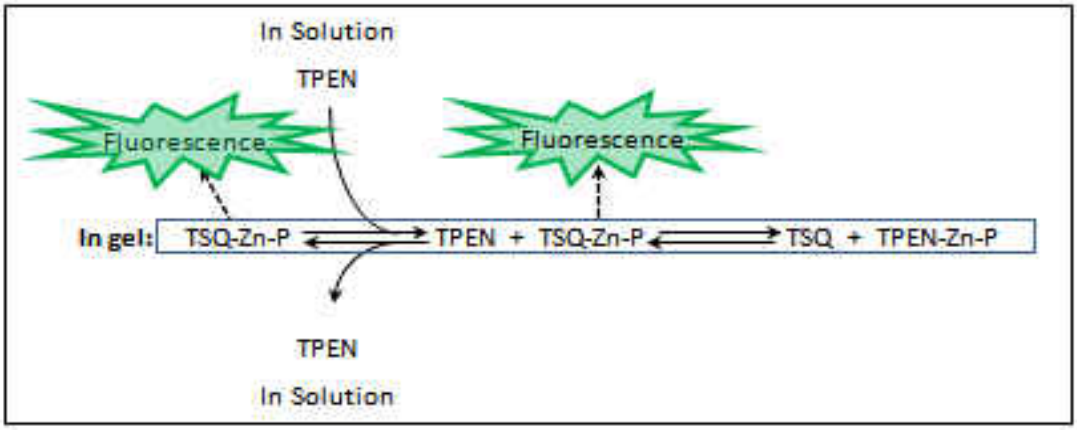

Figure 3.52 Reaction of TSQ with zinc proteins on a PAGE gel forming a ternary adduct, followed by ligand substitution with TPEN, quenching the fluorescent emission.

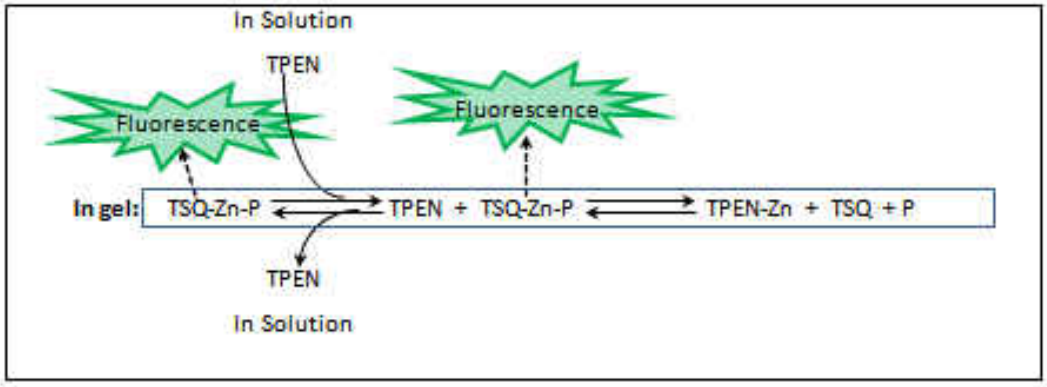

Figure 3.53 Reaction of TSQ with zinc proteins on a PAGE gel forming a ternary adduct, followed by TPEN chelation of zinc from zinc proteins, quenching the fluorescent emission.

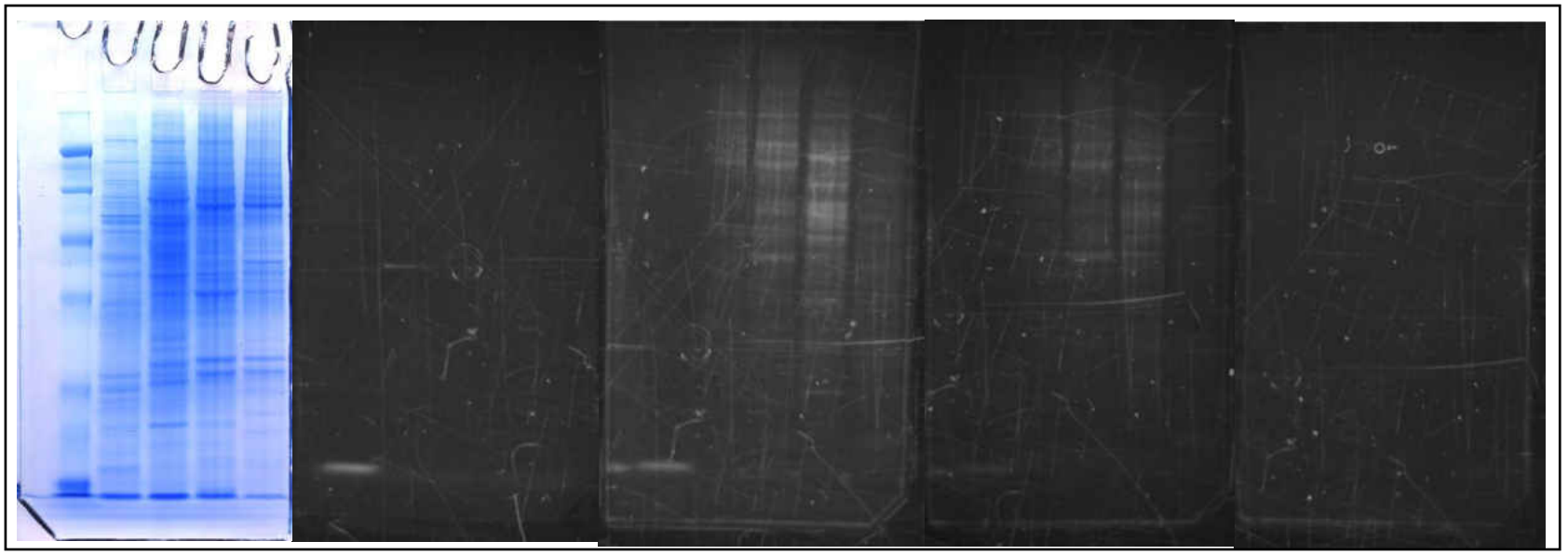

Figure 3.54. Coomassie stained gel image of NSDS-PAGE gel containing select proteome fractions from DEAE IEX chromatography in Figure 3.46. (left) Background 470 nm fluorescence (2nd left). 470 nm fluorescense after staining in 20 µM TSQ (middle). 470 nm fluorescence after destaining in MilliQ water (2nd right). 470 nm fluorescence after staining in 100 µM TPEN.

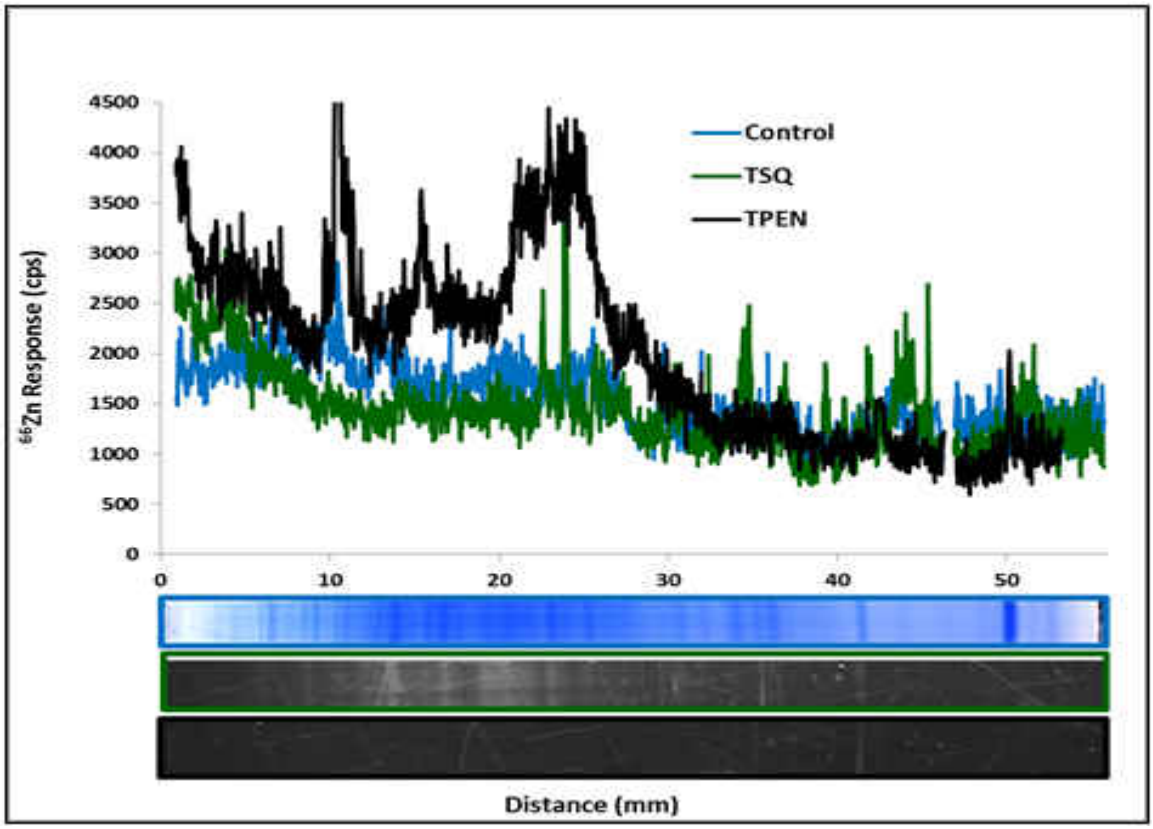

Figure 3.55. Comparison of LA-ICP-MS analysis of ^{66}Zn in lane 2 of control gel, gel stained with TSQ, and gel stained with TSQ followed by TPEN.

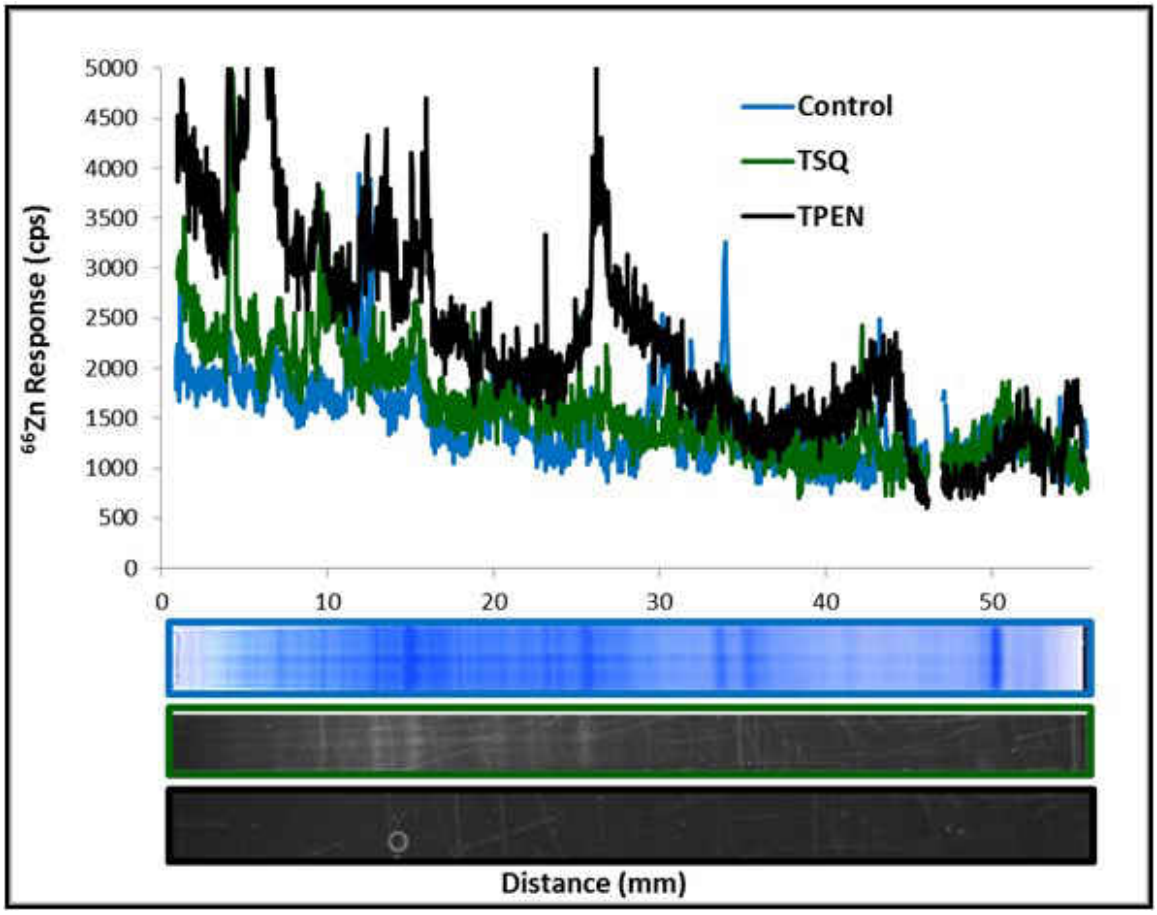

Figure 3.56. Comparison of LA-ICP-MS analysis of ^{66}Zn in lane 3 of control gel, gel stained with TSQ, and gel stained with TSQ followed by TPEN.

3.4.3. Determination of Cadmium Binding Sites in Proteome using NSDS-PAGE and LA-ICP-MS

Cadmium is a divalent transition metal ion which has been shown to have toxic effects on cells [22-25]. Previous experiments performed by Mohammad Ali Namdarghanbari have shown that when zinc proteome from LLC-PK_1 cells is reacted with cadmium, the zinc proteome binds cadmium. Upon binding cadmium, zinc is displaced from the proteome. NSDS separations of zinc proteome and zinc proteome reacted with cadmium, followed by LA-ICP-MS analysis, can provide insight into this reaction at the biomolecular level. As a result, the relative amount of cadmium binding and zinc displacement could be determined for individual proteins. In addition, specific proteins that react with cadmium could be identified.

These experiments were performed with LLC-PK_1 proteome, prepared as described in section 2.1.2., and separated by DEAE ion exchange chromatography (Figure 3.46) as described in section 2.3. Select fractions (Table 3.9) were then divided into two aliquots and one aliquot was reacted with a 1:1 ratio of cadmium as described in section 2.3.2. The fractionated proteome samples were then separated using NSDS-PAGE as described in section 2.6.1. Gels were run in duplicate with one gel stained using Invitrogen™ Simply Blue SafeStain® as described in section 2.7.1, and one gel dried as described in section 2.8.2. The dried gel was subsequently analyzed using LA-ICP-MS for zinc and cadmium content as described in section 2.10.1. As shown in Figure 3.57., no apparent

change in the protein array profile occurs as a result of proteome reaction with cadmium, which suggested that no protein-protein interactions were disrupted. From 2D LA-ICP-MS analysis of ^{66}Zn content on the control gel, several punctate zinc containing protein bands were imaged in Figure 3.58 in each of the lanes 2-5. One example protein in lane 3 is labeled as "Example Protein 1" in Figure 3.58. There appeared to be zinc that dissociated from protein bands and migrated with the electrophoresis dye front as free zinc during electrophoresis which suggested that although NSDS-PAGE is more native than SDS-PAGE, some denaturation still occurred as shown in Figure 3.58 and Figure 3.64. Also, no interferences from the matrix were detected that imaged as cadmium in the control gel in Figure 3.59. 2D LA-ICP-MS analysis of ^{66}Zn on the NSDS-PAGE gel which contained fractionated proteome that had been reacted with cadmium showed the dissociation of zinc measured as free zinc at the gel front was enhanced. A profile view of the ^{66}Zn content in lane 3 on the control (Figure 3.64) and cadmium reacted proteome (Figure 3.63) NSDS-PAGE gels more clearly showed the displacement of zinc. In the control experiment (Figure 3.64) the response from free zinc at the gel front was measured to be 2,500 to 4,500 cps, whereas in the experiment where proteome was reacted with cadmium, the response from free zinc at the gel front was measured to be 3,000 to 5,500 cps. This suggested that a displacement of zinc had occurred from the reaction of cadmium with zinc proteins (Figure 3.59). In addition to the increase of zinc measured at the gel front, the amount of zinc associated with proteins decreased as evident when Figures 3.58 and 3.60 were compared. The example protein labeled as "Example Protein 1" in Figures 3.58, 3.59,

3.60, 3.61, 3.62, and 3.63 shows that initially, the amount of zinc in the protein had a measured response of approximately 2,000 cps. Upon reaction with cadmium, the amount of zinc in “Example Protein 1” had a measured response of approximately 1,000 cps, and the amount of cadmium had a measured response of 2,800 cps. The difference in response of zinc before and after reaction with cadmium in “Example Protein 1” corresponds to a 50 % loss of zinc. This observation displayed the reaction of cadmium with a zinc protein from a proteome, causing a displacement of zinc, at the biomolecular level. Gel lanes 4 and 5 in Figure 3.61 also contained cadmium binding proteins which are well resolved on the PAGE gel, and imaged using LA-ICP-MS, showing multiple occurrences of cadmium binding to zinc proteins. These results confirmed the observations from experiments performed by Mohammad Ali Namdarghanbari, which had shown that the reaction of cadmium with the zinc proteome displaced zinc from proteins. The NSDS-PAGE and LA-ICP-MS experiments show that cadmium reacts with a specific sub-set of proteins in a proteome, including zinc proteins, and not just non-specifically.

Fraction / Lane	Zinc/Cadmium Loaded NSDS-PAGE (nano-moles)	Conductivity (mS)
8 / 2	0.056	2.4
13 / 3	0.088	6.0
18 / 4	0.064	9.6
23 / 5	0.040	13.8

Table 3.9 Fractionated proteome reacted with cadmium

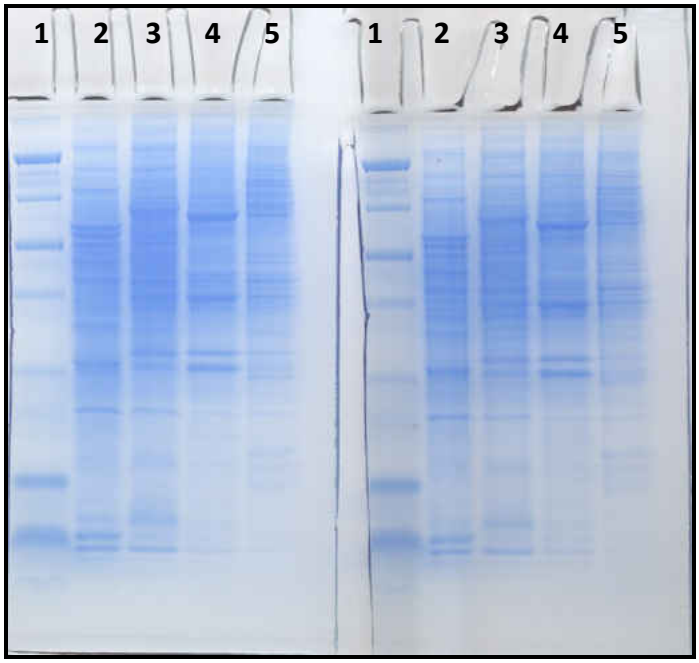

Figure 3.57 Image of control proteome (left) and proteome reacted with cadmium on NSDS-PAGE gel stained with Invitrogen™ Simply Blue SafeStain®

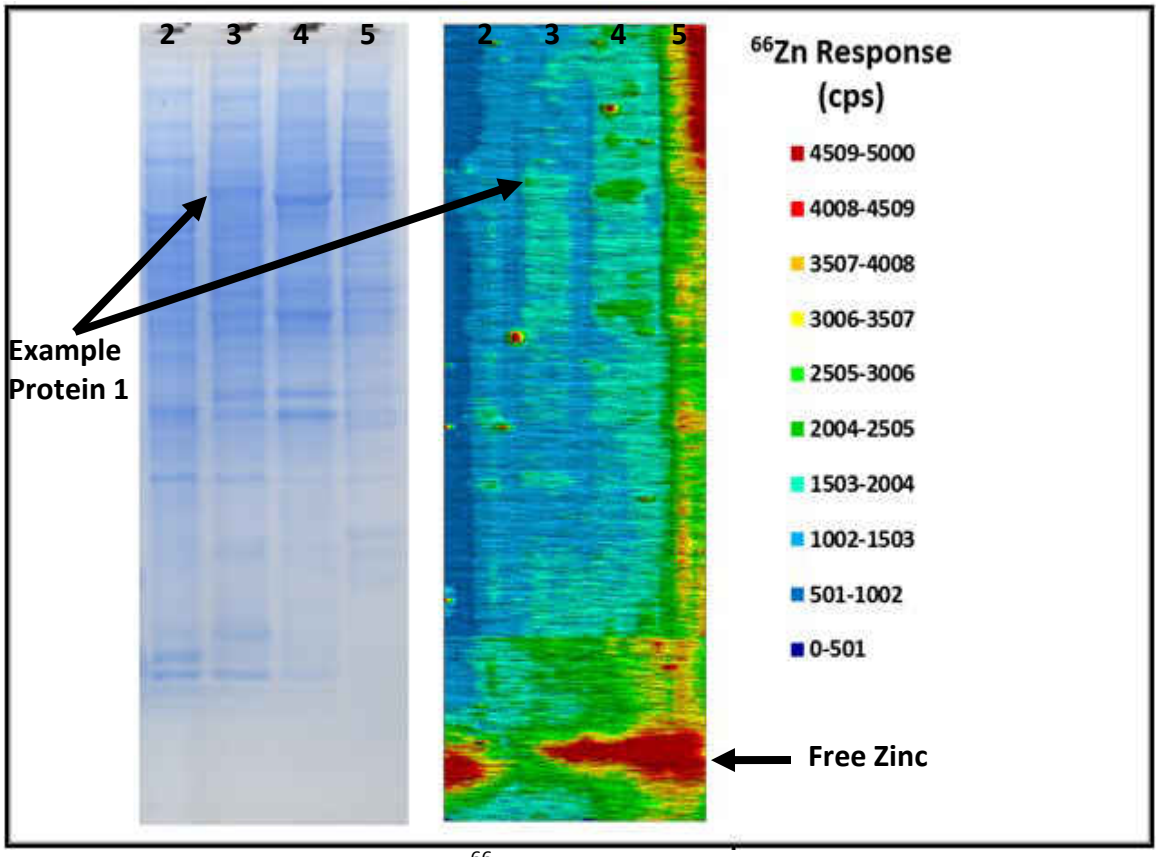

Figure 3.58 2D LA-ICP-MS image of ^{66}Zn content in control NSDS-PAGE gel. Coomassie stained gel image shown for reference.

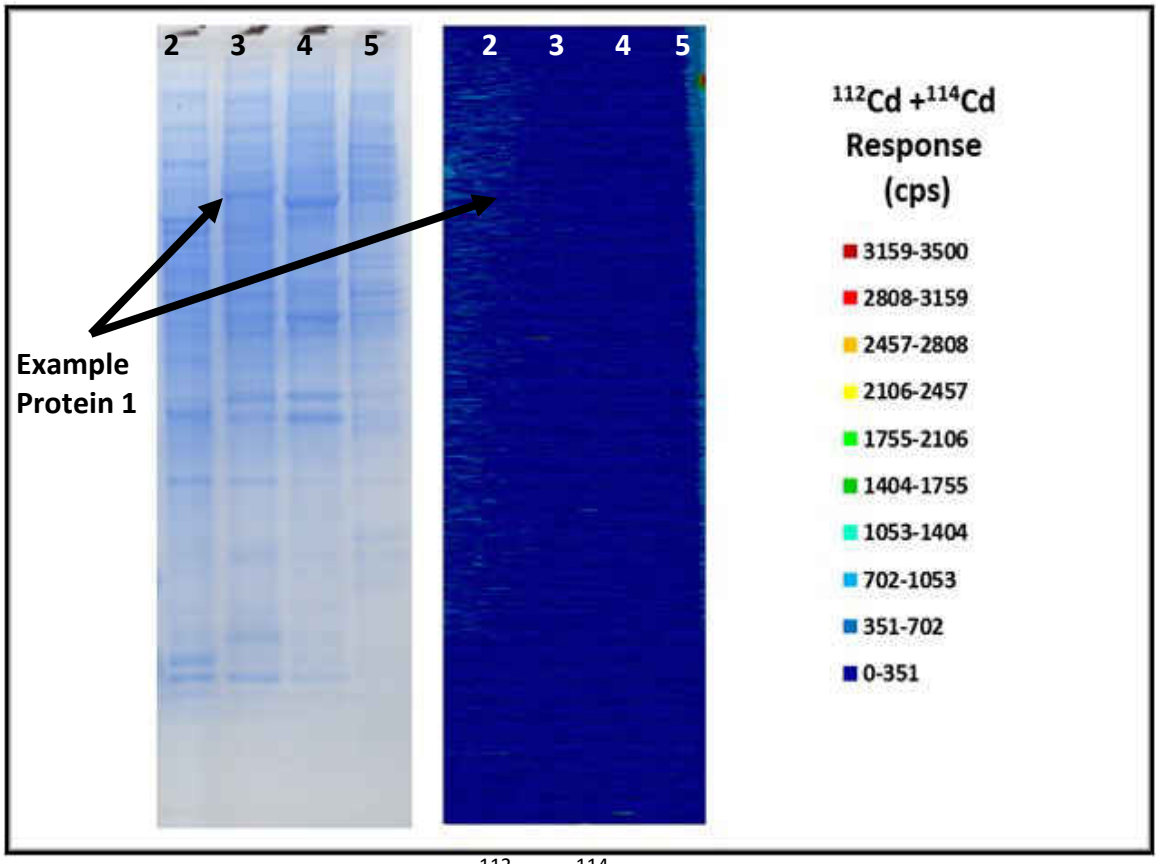

Figure 3.59. 2D LA-ICP-MS image of ^{112}Cd + ^{114}Cd content in control NSDS-PAGE gel. Coomassie stained gel image shown for reference.

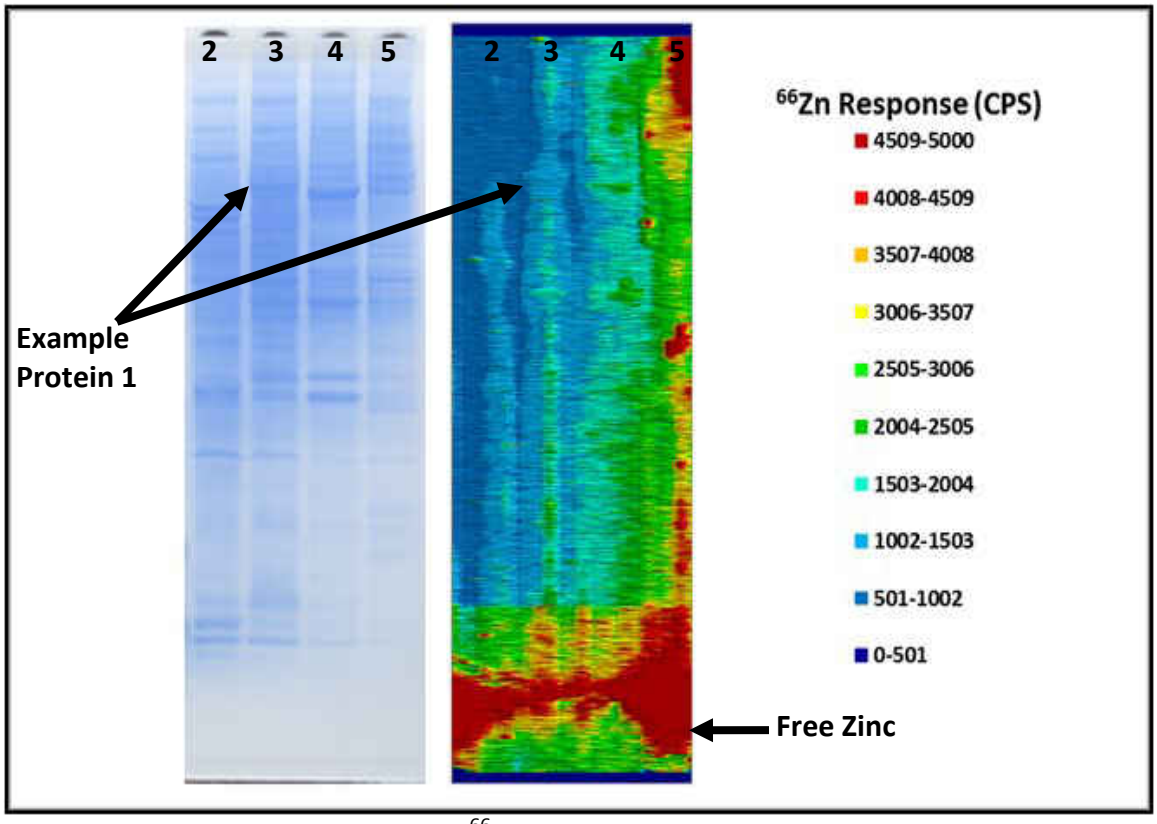

Figure 3.60 2D LA-ICP-MS image of ^{66}Zn content in fractionated proteome reacted with cadmium NSDS-PAGE gel. Coomassie stained gel image shown for reference.

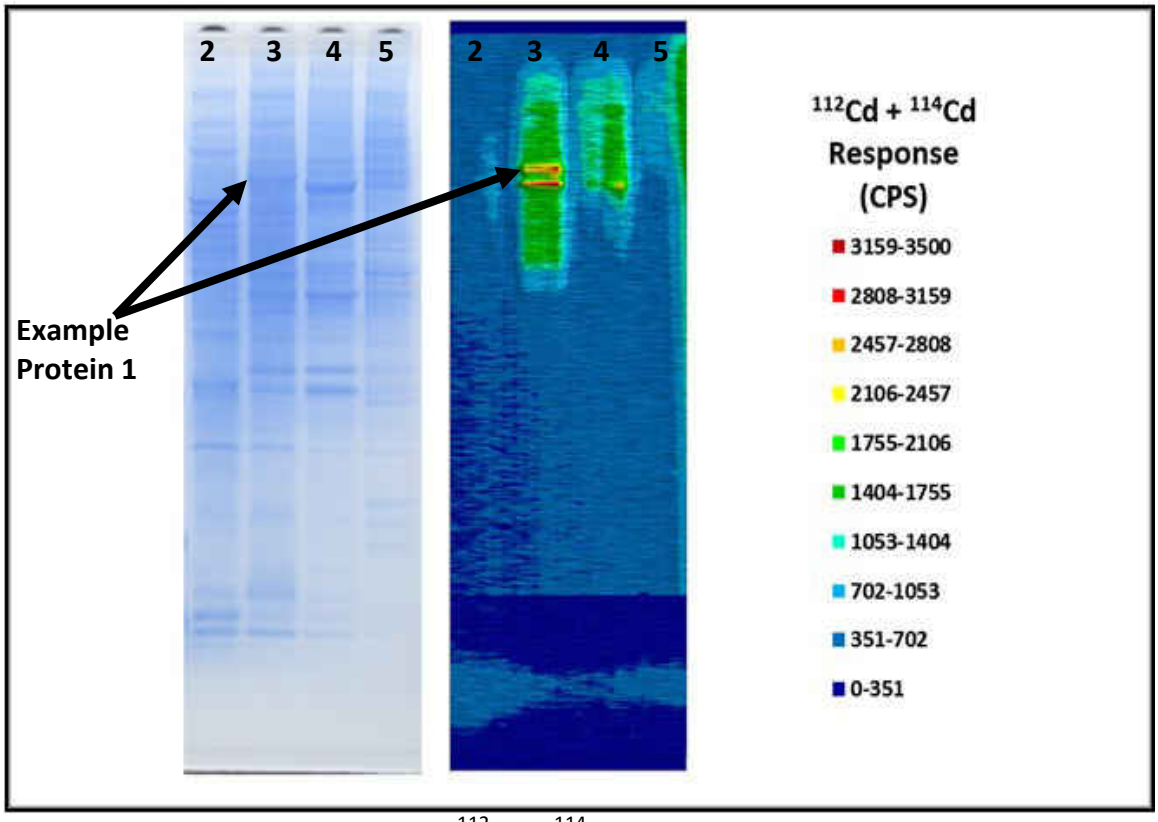

Figure 3.61 2D LA-ICP-MS image of ^{112}Cd + ^{114}Cd content in fractionated proteome reacted with cadmium NSDS-PAGE gel. Coomassie stained gel image shown for reference.

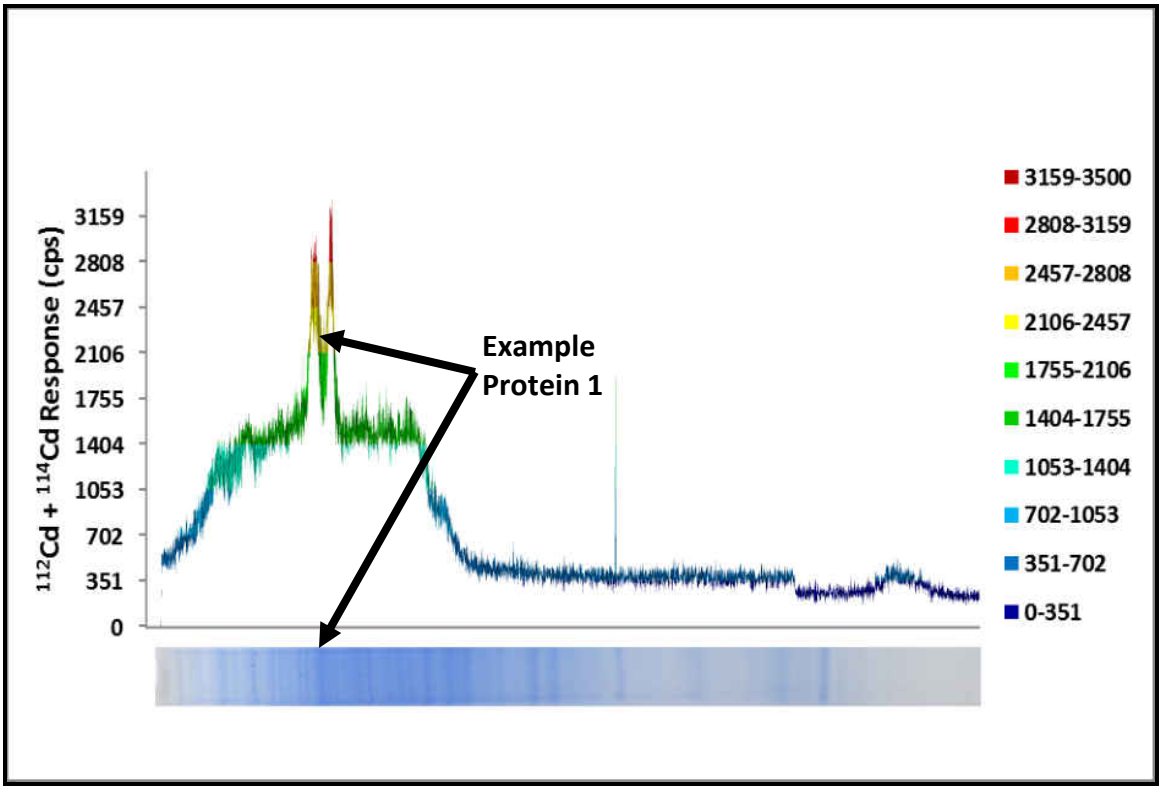

Figure 3.62 Profile view of LA-ICP-MS analysis of ^{112}Cd + ^{114}Cd in Lane 3 of Figure 3.61 (cadmium reacted proteome)

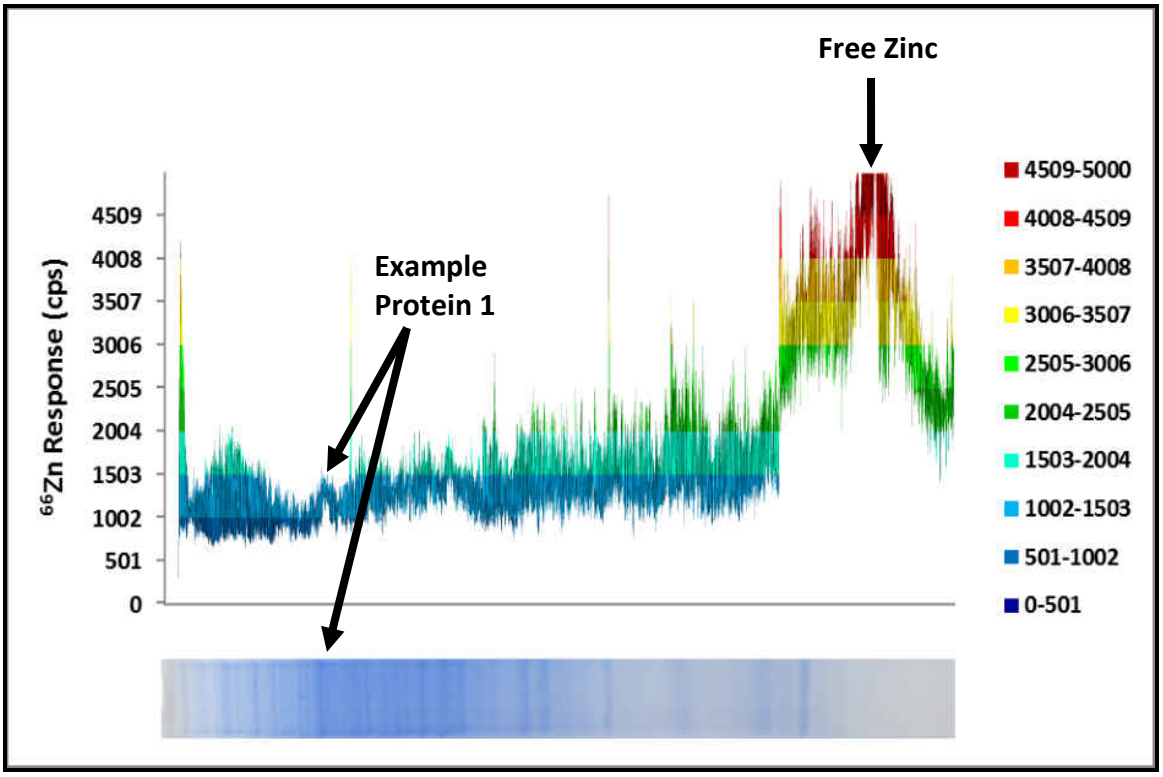

Figure 3.63 Profile view of LA-ICP-MS analysis of ^{66}Zn in Lane 3 of Figure 3.60 (cadmium reacted proteome)

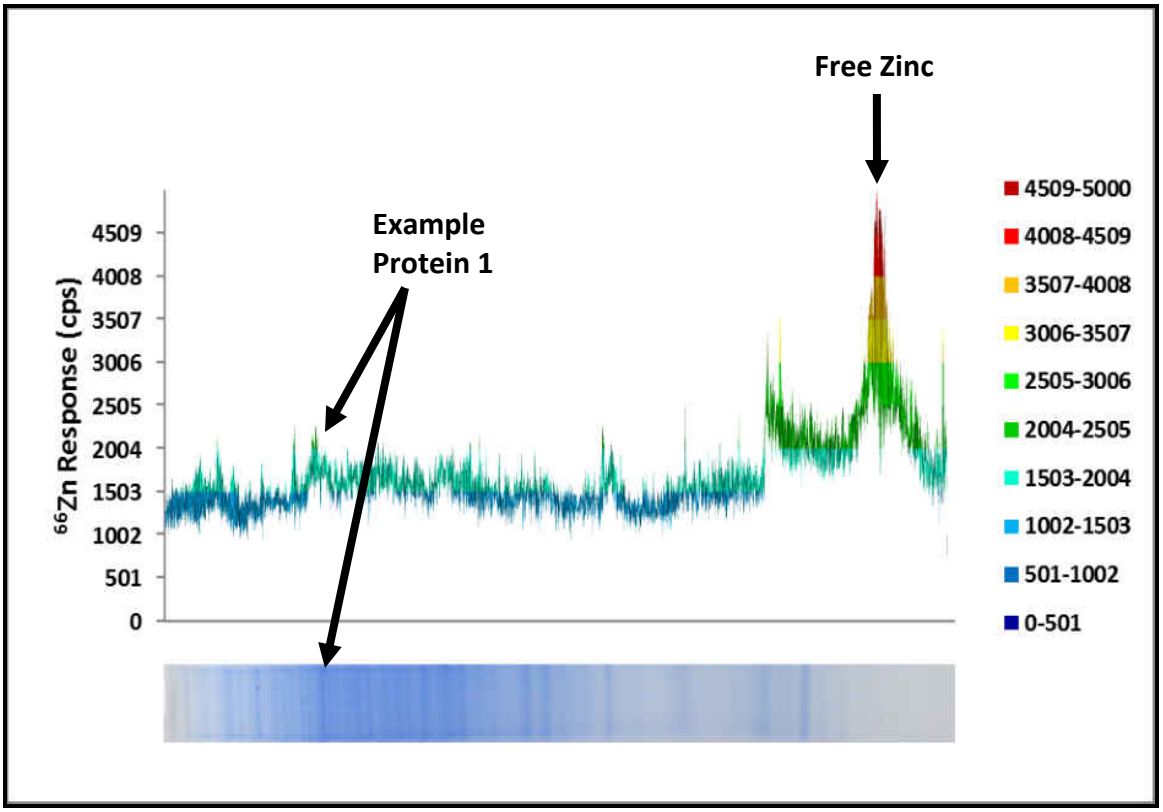

Figure 3.64 Profile view of LA-ICP-MS analysis of ^{66}Zn in Lane 3 of Figure 3.58 (control)

3.4.4. Determination of Mercury Localization in Zebra Fish Embryos

Zebrafish are a key model organism for the study of growth and development, and can be used for comparison to human growth and development. Exposure to mercury, particularly methyl mercury, in the early stages of development can cause developmental abnormalities[30]. Therefore, the study of where mercury becomes distributed in an organism during development can provide insight into the biochemical causes of developmental abnormalities. To determine if LA-ICP-MS could be utilized for the analysis of mercury and zinc in zebrafish exposed to methyl mercury prior to fertilization, a LA-ICP-MS method was developed which was suitable for analysis of ^{13}C,

^{64}Zn, and ^{202}Hg in dried zebrafish larvae. Imaging mercury distribution starting with an entire organism provides the starting point for 'top-down" analysis of metal distribution in an organism. The method parameters were optimized for maximum sensitivity and resolution by increasing the laser energy to 100 %, and decreasing the laser scan rate to 20 µm/sec., laser spot size to 10 µm, and laser scan spacing to 10 µm. Figure 3.65 shows the optical microscope image of two zebrafish embryos dried onto microscope slides in a similar orientation. The zebrafish on the right was exposed to 0.1 µM methyl mercury prior to being fertilized, whereas the zebrafish on the left was a control. There appeared to be no significant structural difference observed between the two zebra fish larvae in Figure 3.65. Laser ablation scan lines are shown to highlight the area of the slide and zebrafish that was ablated. Figure 3.66 shows the LA-ICP-MS analysis of ^{13}C in the zebra fish embryos. The darker pigmentations of the zebrafish from Figure 3.65 appeared to directly correlate to ^{13}C response from LA-ICP-MS analysis in Figure 3.66, which suggested that the darker pigmentation corresponded to tissues that were more dense. Figure 3.67 shows the distribution of ^{64}Zn in the two different zebrafish larvae. There appeared to be localized areas in the fish that contained larger amounts of zinc relative to the rest of the fish including the gut, spine, and head. In the fish exposed to methyl mercury, there appeared to be a larger amount of zinc present in the gut of the fish. Figure 3.68 shows the distribution of ^{202}Hg in the two zebrafish larvae. The control fish did not display any measurable ^{202}Hg. This observation indicated that there were no interferences from the sample matrix that were measured at mass 202. Therefore, it was determined that any response observed above the background at mass 202 was

due to the presence of ^{202}Hg. The fish that was exposed to methyl mercury showed that the mercury was distributed throughout the entire fish at a measureable amount. Interestingly, there were areas of the fish containing increased amounts of mercury relative to the rest of the fish. These areas included the gut, spine, brain, and eyes of the fish.

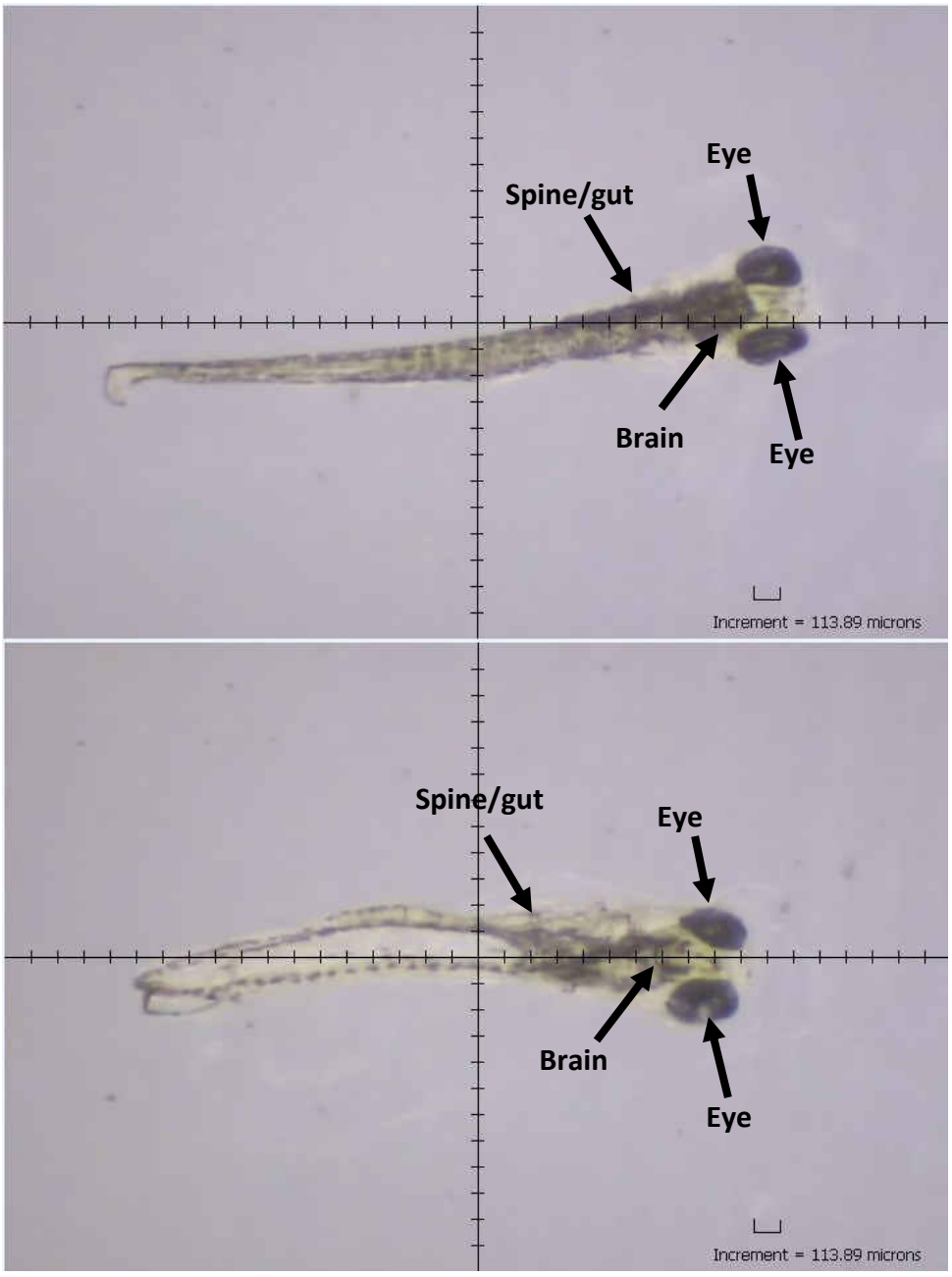

Figure 3.65 Optical microscope image of control (top) and 0.1 µM methyl mercury exposed (bottom) dried zebrafish larvae.

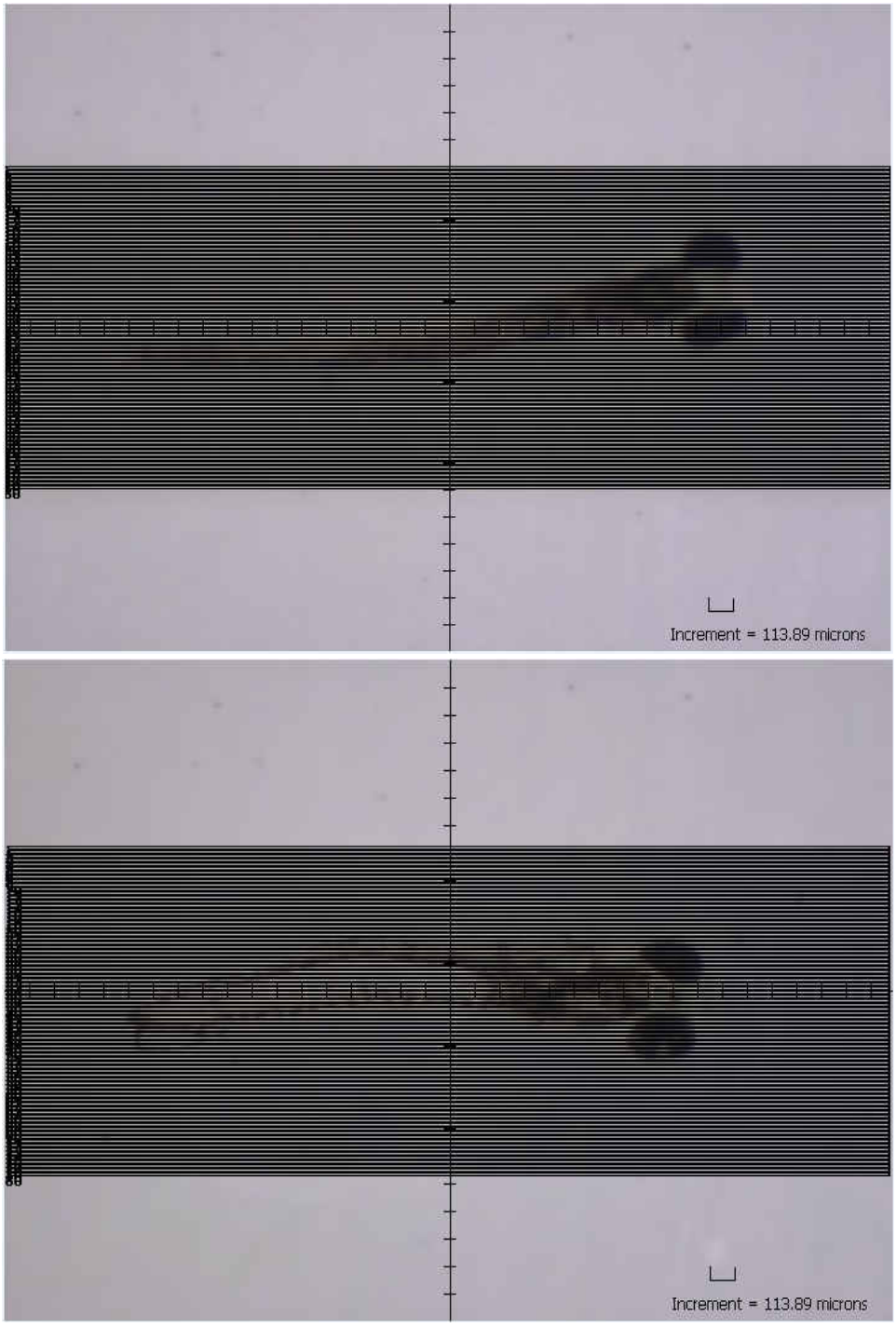

Figure 3.66 Optical microscope image of control (top) and 0.1 µM methyl mercury exposed (bottom) dried zebrafish larvae. Laser ablation area shown for reference.

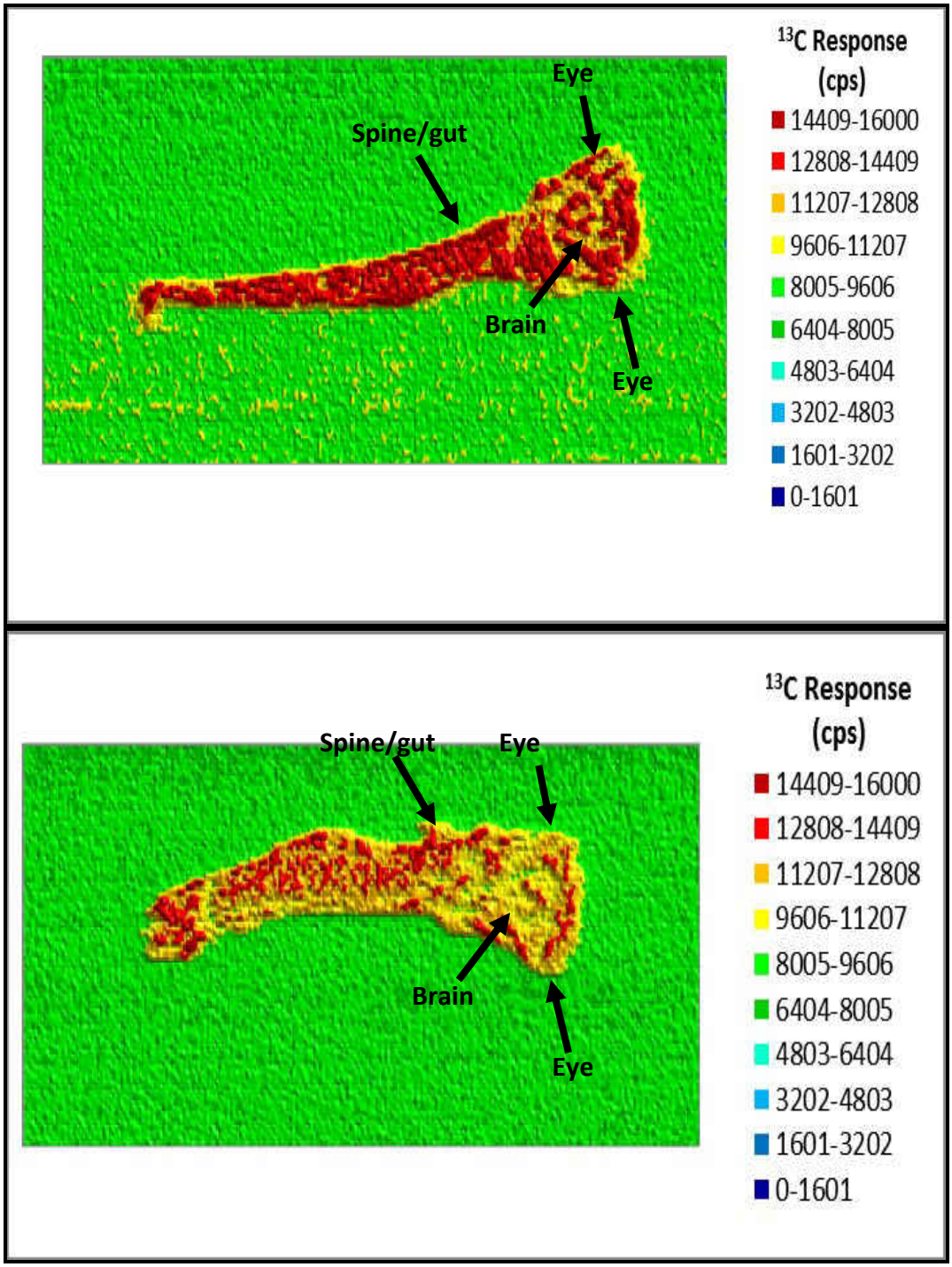

Figure 3.67 2D LA-ICP-MS analysis of ^{13}C in control (top) and 0.1 µM methyl mercury exposed (bottom) dried zebrafish larvae.

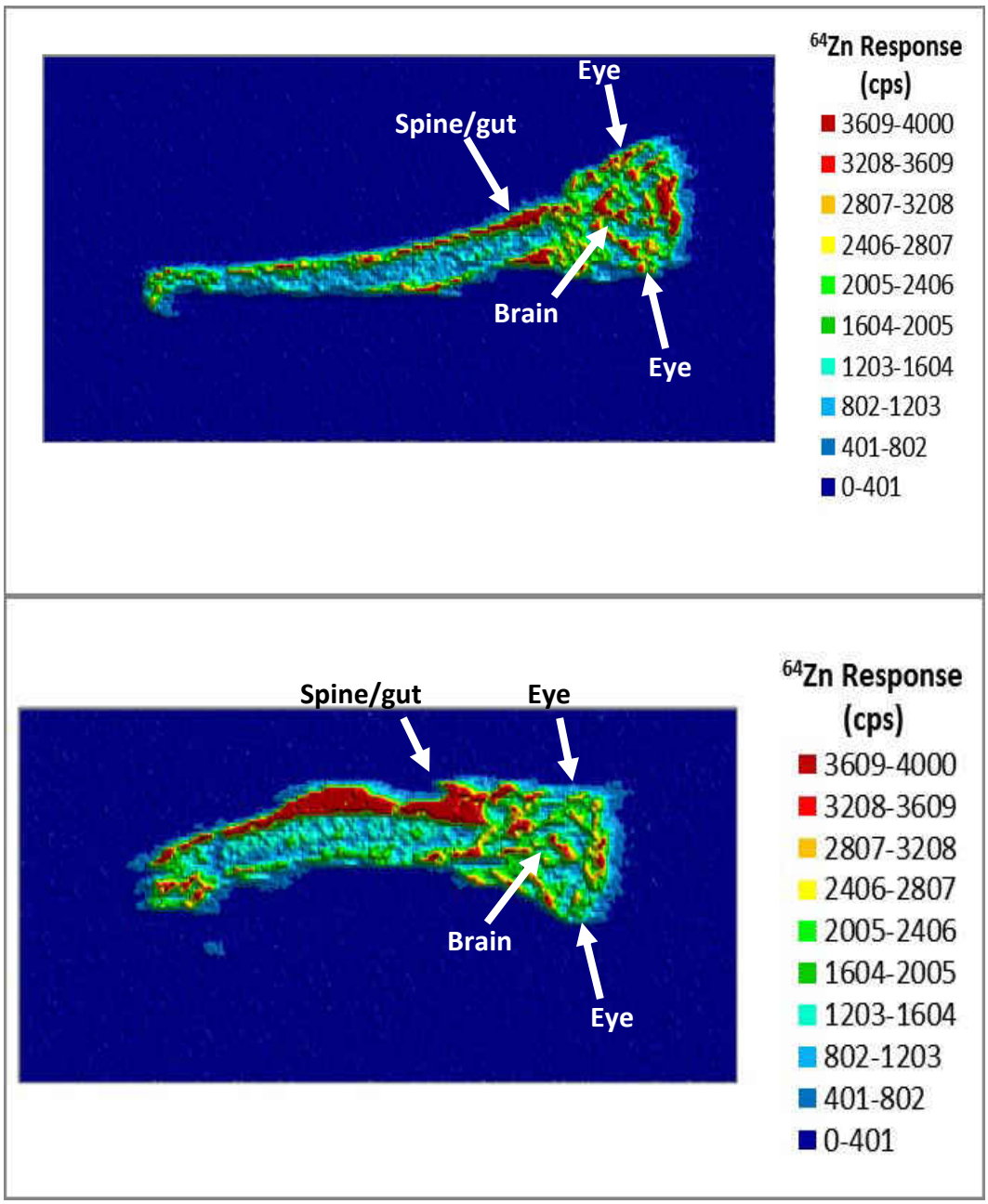

Figure 3.68 2D LA-ICP-MS analysis of ^{64}Zn in control (top) and 0.1 µM methyl mercury exposed (bottom) dried zebrafish larvae.

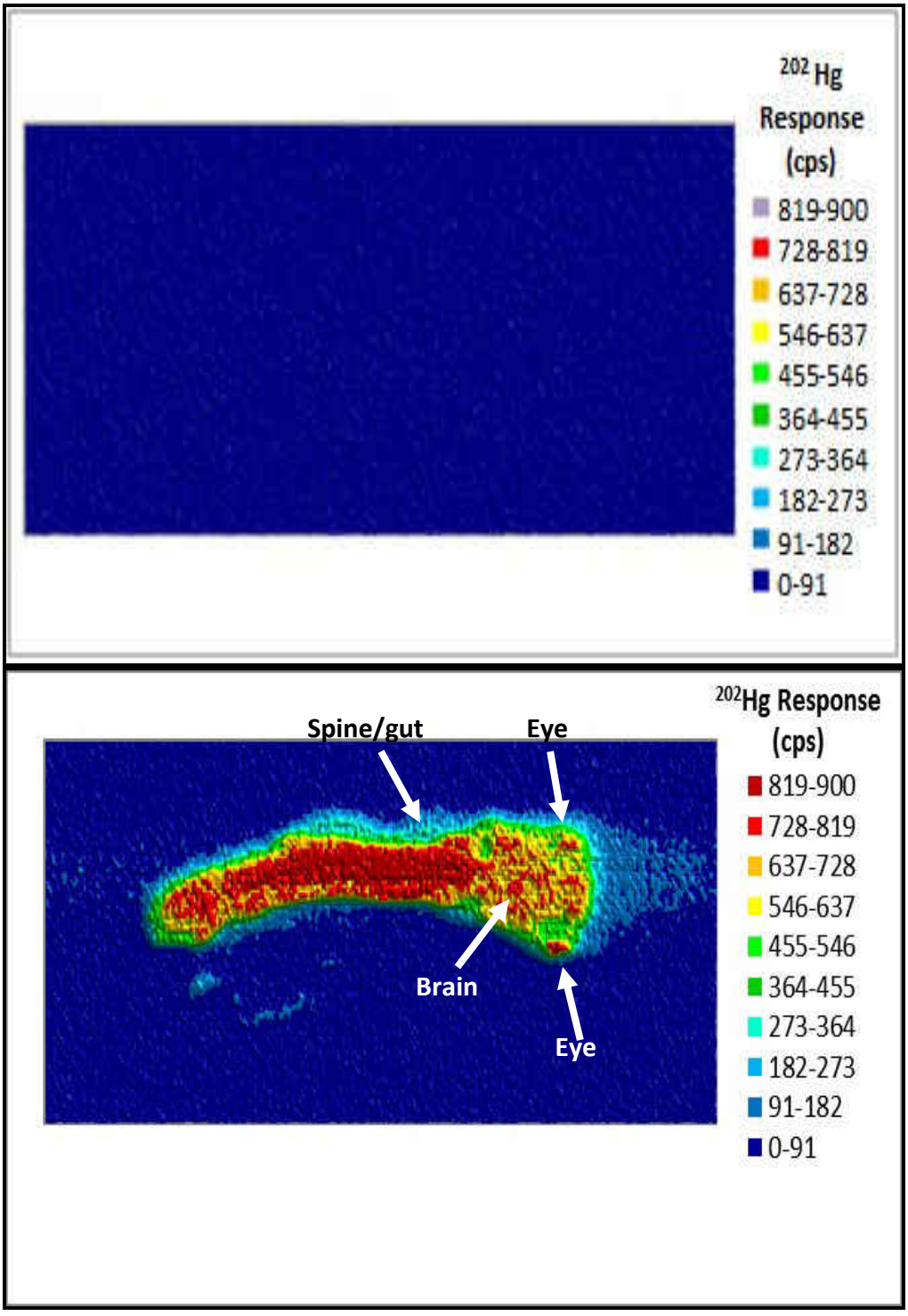

Figure 3.69 2D LA-ICP-MS analysis of ^{202}Hg in control (top) and 0.1 µM methyl mercury exposed (bottom) dried zebrafish larvae.

4. Discussion

In the emerging fields of proteomics and metallomics, a wide variety of analytical techniques are utilized [1-17]. One systematic approach begins with experiments performed on a cell culture and/or tissue, which is subsequently homogenized. The cell homogenate is then fractionated using liquid chromatography. Fractionated samples are further separated into an array of biomolecules using polyacrylamide gel electrophoresis. This array of biomolecules can then be analyzed using LA-ICP-MS to determine the metallomic inorganic information for each biomolecule in the array. Further analysis can also be performed to obtain the proteomic identity of each biomolecule using LC-MS coupled to genomic data base searches. Currently available analytical techniques, particularly PAGE and LA-ICP-MS, lack refinement for their use in metallomics and proteomics. In order to effectively explore the biochemical phenomena studied in metallomics and proteomics, PAGE methods needed to be refined to provide high resolution, while maintaining proteins' native structure and complement of metals. LA-ICP-MS methods needed to be refined to provide higher sensitivity, to allow the trace level analysis of metals present in biochemical samples, particularly, protein arrays separated on polyacrylamide gels.

PAGE has been a widely analytical technique utilized in the study of proteomics [1,4-7,12-17]. SDS-PAGE, provides a high resolution separation of proteins from complex proteomic samples [15-17]. However, current commercially available SDS-PAGE methods cannot be used to study metallo-proteins, due to the denaturing effects of the method, causing the loss of metals from proteins. BN-PAGE is a commercially available method for the separation of proteins [12-14]. However, BN-PAGE does not provide adequate resolution for the separation of proteins from a complex proteomic sample.

As a starting point in native electrophoresis, BN-PAGE was utilized to separate proteins from fractionated proteome samples despite it being known to have resolution limitations. Fractionated proteome samples were separated using BN-PAGE in section 3.1.5. Figure 3.11 shows that BN-PAGE did not provide adequate resolution in the separation of complex proteome samples. Only several protein bands appear as punctate bands on the stained gel. Rather, a majority of the stained gel was dominated by streaks of protein bands that were unresolved. Further analysis using LA-ICP-MS showed (Figure 3.12 and Figure 3.13) that the proteins' native complement of zinc was maintained. However, it appeared as a large, unresolved response, in which no designation of zinc to a particular protein band could be made. This lack of resolution in BN-PAGE is likely a result of there being no detergents present in any of the solutions. This lack of detergents causes

proteins to aggregate, and migrate as a variety of molecular weights throughout the gel as shown by a single protein (carbonic anhydrase) migrating as a series of multimers when separated by BN-PAGE (Figure 3.4). This further complicates the separation of an already complex proteomic sample.

As an alternative method, it was hypothesized that SDS-PAGE could be modified such that the retention of metals in metallo-proteins would be maintained, while providing high resolution separation. From experiments performed in section 3.1.6, SDS-PAGE provided a high resolution separation of proteins from the same fractionated proteome used in section 3.1.5 (Figure 3.14). Further analysis using LA-ICP-MS showed, surprisingly, that despite the denaturing conditions used in SDS-PAGE, numerous proteins were able to retain their native complement of zinc to some extent (Figure 3.15 and Figure 3.16). However, there was still a large loss of zinc from proteins, which migrated at the gel front.

When a critical evaluation of reagents and conditions utilized in commercially available SDS-PAGE kits was performed, and subsequently optimized, several key reagents and parameters were either removed or adjusted. From the experiment performed in section 3.3.1., heating was determined to be unnecessary to properly resolve proteins from a fractionated proteome sample. Upon comparison of the gels in Figure 3.37, there is no apparent improvement in resolution when samples are heated to 70 °C for 10 minutes prior to performing electrophoresis. It is well

known that heating proteins to high temperature causes denaturation, therefore the heating step was removed from the SDS-PAGE method. From the experiment performed in section 3.3.2, the reaction of zinc proteome with Invitrogen™ SDS-PAGE run buffer (50 mM MOPS, 50 mM TRIS Base, 0.1 % SDS, 1 mM EDTA, at pH 7.7) was shown to cause a 65.7 % loss of zinc from the proteome. This loss of zinc is largely due to the presence of 1 mM EDTA, a strong metal chelator, present in the buffer solution. In addition, the high concentration of SDS (0.1 %) could also have contributed to the loss of zinc from the proteome.

Experiments performed by Drew Nowakowski determined that several other denaturing parameters were not essential to the resolution of the SDS-PAGE method. These parameters included removing the 2.0 % SDS from the sample buffer, and 1 mM EDTA from the sample and run buffers. In addition, it was shown that SDS concentration in the run buffer could be lowered from 0.1 % to 0.0375 % without substantial loss of resolution. Also, the electrophoresis was performed at 4 °C to minimize protein degradation, and a lower voltage (150 V versus 200 V) was used. The culmination of these modifications to SDS-PAGE was referred to as native SDS-PAGE (NSDS-PAGE) in subsequent experiments.

To evaluate the ability of NSDS-PAGE to separate metallo-proteins while maintaining their native complement of metals, model proteins carbonic anhydrase (a zinc protein), alcohol dehydrogenase (a zinc protein), and superoxide dismutase (a copper, zinc protein) were separated using BN-PAGE and SDS-PAGE in addition to NSDS-PAGE for comparison. From the experiment performed in section 3.3.3., it was shown in Figure 3.39 that BN-PAGE was unable to provide adequate separation and resolution between SOD, ADH, and CA model proteins. If all three proteins were run on the same lane, the bands would overlap, causing one large protein streak to be visualized. The combination of the aforementioned method modifications in NSDS-PAGE led to the model proteins being well resolved from each other, while maintaining their native conformations as shown by SOD having migrated as a dimer in NSDS-PAGE versus two monomeric subunits in SDS-PAGE as shown in Figure 3.39. In addition, no fragmentation of CA appeared to occur when separated using NSDS-PAGE compared to SDS-PAGE. From the experiment in section 3.3.4 LA-ICP-MS analysis confirmed the maintenance of the native structure of SOD after electrophoresis by the retention of copper and zinc associated with the protein band. NSDS-PAGE provided a 95% retention of zinc, and 84% retention of copper associated with SOD protein band and was comparable to the amount of zinc and copper retained in the SOD protein band in the BN-PAGE gel. Comparatively, SDS-PAGE did not provide any retention of zinc, and only 27% retention of copper in SOD when compared to BN-PAGE. In summary, by lowering the run voltage from 200 V to 150 V, removing the metal chelator EDTA from the sample and run buffers,

lowering the SDS concentration from 0.1 % to 0.0375 % in the run buffers, removing SDS from the sample buffer, and eliminating the heating step, proteins were able to be separated with sufficient resolution, without compromising their native structures.

LA-ICP-MS in an analytical technique for the inorganic analysis of solid samples, and has been utilized in biochemical applications [3-5,7,8,11]. Experiments performed in section 3.1.2 showed a LA-ICP-MS was capable of detecting zinc and cadmium in the matrix of a protein spot on an acrylamide gel. Integrated responses for each isotope of cadmium and zinc used in the proteome spot, correlated directly with natural abundance percentages of each isotope as summarized in Table 3.1, with percent errors in measurement as low as 3.4 % for ^{67}Zn, and 0.8 % for ^{111}Cd. In addition, experiments in section 3.1.4 demonstrated that the LA-ICP-MS method was linear in the measurement of zinc in proteins on a polyacrylamide gel. The correlation coefficient for the measurement of zinc in a serial dilution of carbonic anhydrase (a model zinc protein) that had been separated using BN-PAGE was determined to be 89.3 % when the response from the entire gel lane was integrated, and 94.3 % when the response from a single protein band was integrated. In summary, the aforementioned experiments demonstrated that the LA-ICP-MS method was specific and linear for analysis on zinc proteins in a polyacrylamide gel matrix.

A critical evaluation is performed of the causes of poor detection limits and interferences when performing LA-ICP-MS analysis of zinc and copper in PAGE gels, as observed by Jiminez et. Al. The results indicate that the limitations arise from copper and zinc contamination of PAGE gels, and not the LA-ICP-MS analytical method. From the quantitative ICP-MS analysis of acid digested PAGE materials in section 3.2.1, PAGE gels were measured to be contaminated with 1.03 ppm of zinc, which is imaged by LA-ICP-MS as a high, non-homogenous background as shown in Figure 3.22, making the visualization of trace levels of zinc in proteome samples difficult. The level of contamination varied from 1.25 ppm to 2.5 ppm throughout the gel. The 1.25 ppm zinc standard spotted was the lowest level observed, which would account for the 3.15 ppm detection limit observed by Jiminez et al.

The use of western blotting gels onto nitrocellulose, and subsequent LA-ICP-MS analysis of the nitrocellulose, did not provide any improvement in the background level of contaminant zinc being measured as shown in Figure 3.27. Moreover, zinc contamination in the filter paper backing used to dry gels introduced additional contamination into PAGE gel analysis using LA-ICP-MS. According to Figure 3.20, 2D LA-ICP-MS analysis of a vacuum dried page gel showed that, in addition to the labile contaminant zinc which dominated the image of the gel, micro cracks in the gel were also imaged as zinc responses due to zinc contamination in the filter paper. However, as shown in Figure 3.24 and 3.29, the background ^{70}Zn was very low, due

to ^{70}Zn having a natural abundance of 0.60 %. This observation led to the hypothesis that if ^{70}Zn isotopes were used for cell cultures and standards, detection limits could be improved. In summary, current limitations in sensitivity for the detection of zinc in polyacrylamide gels was determined to be from contaminant zinc present in the polyacrylamide gel material. Therefore, modifications in sample preparation using a ^{70}Zn isotope were pursued, rather than further refinement of the LA-ICP-MS analytical method.

In order to eliminate the high background of zinc being measured by analyzing naturally abundant zinc isotopes such as ^{64}Zn (48.6 %), and ^{66}Zn (27.9 %) using LA-ICP-MS, cells were cultured using a rare isotope of zinc, ^{70}Zn. By using ^{70}Zn isotope to eliminate the high background of contaminant zinc measured, zinc standard spots were able to be visualized at trace level, with the lowest detected level readily visualized being 39 ppb. The relative detection limit and quantification of a spot with an initial concentration of 39 ppb is solution overestimates the actual amount of zinc being measured. During analysis, a small cross-section of the spot is actually ablated (200 µm). Given the total amount of ^{70}Zn present in the 0.5 µL spot of 39 ppb ^{70}Zn standard of 71 femto-moles, and that a 200 µm cross section ablated approximately 5 % of the spot, the actual amount of zinc being measured is 3.6 femto-moles.

From the experiment performed in section 3.3.5, the newly developed quantitative LA-ICP-MS method for the analysis of ^{70}Zn in fractionated proteome samples separated using NSDS-PAGE versus SDS-PAGE confirmed the increase in retained zinc in the context of proteome samples. The NSDS-PAGE gel showed a 122 % increase in protein-bound zinc in the NSDS-PAGE gel when compared to the SDS-PAGE gel (Figure 3.43). This increase in retained zinc appears to be underestimated upon visual comparison of the 2D LA-ICP-MS analyses, and is most likely due to the integration of the background response on the SDS-PAGE gel. Using ^{70}Zn isotope allowed zinc to be imaged at a relative level of 25 ppb – 50 ppb throughout the protein bands in the gel. This relative ppb level corresponds to amounts the low femto-mole range. In summary, the use of ^{70}Zn isotope in cultured cells for proteome samples, and spotted ^{70}Zn standards allowed for the quantitative LA-ICP-MS analysis of trace level zinc in proteome samples. This method was able to confirm the increase in retained zinc in proteome samples, which indicated a decrease in the amount of protein denaturation occurring during NSDS-PAGE when compared to SDS-PAGE. A key conclusion from experiments performed in section 3.3.5 was that although no single isolated zinc protein was observed, the limitation was no longer determined to be from the lack of sensitivity of the LA-ICP-MS method, interference from micro cracks in the gel matrix causing signal spikes, interfering contaminant zinc in the polyacrylamide gel, or poor resolution from the PAGE method. Rather, better separation using higher resolution chromatography,

and, or, using molecular weight cuts could provide adequate fractionation of complex proteomic samples, allowing for the visualization of isolated protein bands.

Having established methods suitable for the analysis of trace level zinc and cadmium in proteomic samples using NSDS-PAGE and LA-ICP-MS, several applications were performed.

TSQ is a zinc fluorescent sensor that has been widely utilized in cell microscopy to image cellular zinc [9,10,29]. A variety of conclusions have been drawn from these microscopy experiments at the cellular level, however, few papers discuss what is actually being imaged in these experiments with the exception of published work performed in Dr. David H. Petering's lab [9,10]. In the first application, NSDS-PAGE and LA-ICP-MS were used to identify a zinc protein that fluoresces upon reaction with the zinc fluorescent probe TSQ was performed in section 3.4.1. By fractionating proteome using DEAE IEX, separating fractionated proteome samples into a protein band array using NSDS-PAGE, imaging fluorescence of protein bands using TSQ in combination with a fluorescence gel documentation system, LA-ICP-MS analysis, and LC-MS analysis coupled to a genomic data base search allowed for the identification of a single protein which contained zinc, and reacted with TSQ from a cell proteome.

The protein was identified as HSP90, and had not previously been identified as a zinc protein[31].

This is not the first experiment to have utilized LA-ICP-MS in combination with a MS identification method to ultimately discover a protein which contained zinc that had not previously been documented as a zinc protein. In an experiment performed by Becker et al, Malate dehydrogenase, Beta-synuclein, and Protein FAM44B were identified as zinc containing proteins using LA-ICP-MS, all of which had not been previously labeled as such. Further verification of stoichiometric zinc binding in these proteins was not performed, making a definite conclusion about the observed zinc binding phenomena ambiguous. Due to the complexity and transient nature of metal trafficing processes in cells, many proteins may bind and utilize zinc have are not able to be identified by direct isolation and metal analysis. The NSDS-PAGE and LA-ICP-MS methods have the potential be used to reveal the numerous proteins from proteomes that bind zinc, which have not been previously known to bind zinc. However, further analysis of a potential zinc binding protein needs to be performed to confirm, stoichiometrically, the protein does in fact bind zinc.

A second application, was based on observations made in cellular microscopy experiments, in which cells were reacted with the zinc sensor TSQ resulting in

enhanced fluorescence, followed by the quenching of the enhanced fluorescence by the zinc chelator TPEN [9,10]. In the experiment performed in section 3.4.2., DEAE IEX fractionated proteome was separated into an array using NSDS-PAGE, reacted with TSQ and TPEN, followed by imaging using a fluorescence gel documentation system, and subsequent analysis of zinc content using LA-ICP-MS. The observation of fluorescent enhancement after reaction with TSQ at the cellular level was also observed at the proteomic level as shown in Figure 3.54. The enhanced fluorescence of protein bands after reaction with TSQ confirms the observation of the formation of TSQ-Zn-Protein adducts as demonstrated in previous proteomic experiments [9,10]. In addition, the observation of the quenching of the enhanced fluorescence from TSQ after reaction with TPEN at the cellular level and in in vitro proteomic experiments was also observed at the proteomic level as shown in Figure 3.54. In Figure 3.54, all protein bands that showed enhanced fluorescence upon reaction with TSQ, were no longer visible after reaction with TPEN. Subsequent analysis of zinc content in the control, TSQ reacted, and TSQ reacted followed by TPEN reacted gels, was performed using LA-ICP-MS. These experiments were performed prior to the development of the quantitative LA-ICP-MS method using ^{70}Zn standards and proteome from cells cultured in ^{70}Zn. The LA-ICP-MS data were not quantified. The proteome samples were obtained from cells cultured in a natural distribution of zinc isotopes and as a result, the responses observed were only relative, and could not be correlated to amounts of zinc present in the protein bands on the gel. The interpretation of the results was

further complicated due to the potential of contaminant zinc on the gel to cause interferences in the designation of zinc to a particular protein band. In summary, these results do not reveal whether the enhanced fluorescence from reaction with TSQ was quenched by the chelation of zinc from the protein bands, or by ligand substitution forming a TPEN-Zn-Protein adduct. The results from these experiments contributed to the necessity to develop the previously discussed quantitative LA-ICP-MS method.

Cadmium is a toxic metal, which is known to bind to several specific proteins cells, particularly, metallothionein [22-25]. In experiments performed by Mohammad Ali Namdarghanbari, a significant portion of the Zn-proteome of a cell has been shown to react with cadmium. In these experiments, the reaction of cadmium with the Zn-proteome showed cadmium binding to high molecular weight proteins. In addition, the reaction of cadmium with the proteome displaced zinc. In a third application, LA-ICP-MS was utilized to determine which proteins in fractionated proteome samples are reactive with cadmium, and whether cadmium reacts with zinc proteins causing metal exchange and displacement of zinc. In the experiment performed in section 3.4.3. proteome samples fractionated using DEAE IEX, were reacted *in vitro* with cadmium in a 1:1 zinc : cadmium ratio, separated into arrays using NSDS-PAGE, and subsequently analyzed for zinc and cadmium content using LA-ICP-MS. From comparison of the cadmium reacted proteome with the control

proteome in Figure 3.57, no apparent alteration on the protein array pattern was observed. Interestingly, this suggested that cadmium did not disrupt any structural interactions in the fractionated proteome samples. From the comparison of Figure 3.58 (control) and Figure 3.60, a decrease in the amount of zinc associated with protein bands occurs when fractionated proteome samples are reacted with cadmium. This displaced zinc migrated with the gel front as shown by a 20% increase in the amount of zinc at the gel front in Figure 3.60 (2,500 cps – 4,500 cps) compared to Figure 3.58 (3,000 cps – 5,500 cps). A specific example of a single protein in which the displacement of zinc after binding cadmium occurred is highlighted as "Example Protein 1" of Figures 3.58, 3.59, 3.60, 3.61, 3.62, and 3.63. These figures show that initially, the amount of zinc in the protein had a measured response of approximately 2,000 cps. Upon reaction with cadmium, the amount of zinc in "Example Protein 1" had a measured response of approximately 1,000 cps, and the amount of cadmium had a measured response of 2,800 cps. The difference in response of zinc before and after reaction with cadmium in "Example Protein 1" corresponds to a 50 % loss of zinc. In Figure 3.61, cadmium was shown to be bound to other isolated, punctate protein bands, showing that cadmium binds to a specific subset of proteins, and not non-specifically to a majority of proteins in the fractionated proteome samples. These results suggest that toxicity occurs from cadmium exposure in cells by disruption of zinc in a specific subset of proteins that react with cadmium. Further investigation of which proteins reacted with cadmium using the method discussed in 3.4.1 can provide additional insight into the

underlying biochemical mechanisms associated with cadmium exposure and subsequent toxicity. In summary, NSDS-PAGE and LA-ICP-MS can be utilized cooperatively to identify zinc binding proteins, zinc proteins that are reactive to TSQ, and proteins that react with cadmium.

Zebrafish are a model organism used in developmental studies, which can be compared to human development. Mercury has been shown to cause developmental abnormalities, particularly in the startle response, of developing and mature zebrafish[30]. To determine the underlying biochemical mechanisms related to developmental abnormalities resulting from exposure to mercury, LA-ICP-MS was utilized to determine the distribution of mercury in zebrafish larvae. A method development and application of LA-ICP-MS for imaging trace levels of mercury in microscopic zebra fish embryos exposed to methyl mercury was performed in section 3.4.4. The results show that non-lethal exposure of embryos to 0.1 µM methyl mercury can be detected and imaged using a high-resolution LA-ICP-MS method. By decreasing the laser spot size to 10 µm, decreasing the spacing between ablations to 10 µm, and decreasing the scan rate to 20 µm/second, high resolution elemental images using 2D LA-ICP-MS were obtained. In Figure 3.66, mercury was imaged using LA-ICP-MS and shown to be localized in the muscle tissue, eyes, and spinal cord of zebra fish embryo. The localization of mercury in the eyes and neurological tissues appears to be the underlying cause of the decreased startle

response in the developing and mature zebrafish. These findings at the organism level could be evaluated using proteomic samples and NSDS-PAGE followed by LA-ICP-MS to reveal which specific proteins are reactive with methyl mercury, connecting behavioral observations, biological observations, and biochemical observations to form an integrated "top-down" evaluation of methyl mercury toxicity in biological systems. Moreover, this same experimental approach could be used to evaluate metal toxicity of other toxic metals such as lead, chromate, cadmium, and uranium to name a few[35-37].

These newly developed methods in proteomics, metallomics, and toxic metal studies provide the means to unveil the complete metallo-proteome of various biological systems, their reactivity to various ligands, and their reactivity to various toxic metals. In addition, these methods can be applied to "top-down" experiments, liking observations at the organism level, to cellular observations, to underlying biochemical phenomena.

References

1. Lobinski, R.; Becker, J. S.; Haraguchi, H.; Sarkar, B., Metallomics: Guidelines for terminology and critical evaluation of analytical chemistry approaches (IUPAC Technical Report). *Pure Appl. Chem.* **2010**, 82 (2), 493-504.

2. Yannone, S. M.; Hartung, S.; Menon, A. L.; Adams, M. W.; Tainer, J. A., Metals in biology: defining metalloproteomes. *Current Opinion in Biotechnology* **2011**, 23, 1-7

3. Mounicou, S.; Szpunar, J.; Ryszard, L., Metallomics: the concept and methodology. *Chem. Soc. Rev.* **2009**, 38, 1119-1138

4. Jimenez, M. S.; Rodriguez, L.; Gomez, M. T.; Castillo, J. R., Metal-protein binding losses in proteomic studies by PAGE-LA-ICP-MS. *Talanta* **2010**, 81, 241-247

5. Becker, J. S.; Mounicou, S.; Zoriy, M. V.; Backer, J. S.; Lobinski, R., Analysis of metal-binding proteins separated by non-denaturing gel electrophoresis using matrix-assisted laser desorption/ionization mass spectrometry (MALDI-MS) and laser ablation inductively coupled plasma mass spectrometry (LA-ICP-MS). *Talanta* **2008**, 76, 1183-1188

6. Gallagher, S. R. and Wiley, E. A., *Current Protocols Essential Laboratory Techniques* (2008) Hoboken, NJ: John Wiley and Sons, Inc.

7. Becker, J.S.; Zoriy, M.; Wu, B.; Matusch, A.; Becker, J. S., Imaging of essential and toxic elements in biological tissues by LA-ICP-MS. *Journal of Analytical Atomic Spectrometry* **2008**, 23, 1275-1280

8. Moreno-Gordaliza, E.; Giesen, C.; Lazaro, A.; Esteban-Fernandez, D.; Humanes, B.; Canas, B.; Panne, U.; Tejedor, A.; Jakubowski, N.; Gomez-Gomez, M. M., Elemental Bioimaging in Kidney by LA-ICP-MS As a Tool to Study Nephrotoxicity and Renal Protective Strategies in Cisplatin Therapies. *Anal. Chem.* **2011**, 83, 7933-7940

9. Meeusen, J. W.; Nowakowski, A.; Petering, D. H., Reaction of Metal Binding Ligands with the Zinc Proteome: Zinc Sensors and TPEN. *Inorg. Chem.* **2012**, 51 (6), 3625-3632

10. Nowakowski, A. B. and Petering, D. H., Reactions of the fluorescent sensor, Zinquin, with the zinc-proteome: adduct formation and ligand substitution. *Inorg. Chem.* **2011**, 50 (20), 10124-10133

11. Binet, M. R. B.; Ma, R.; McLeod, C. W.; Poole, R. K., Detection and characterization of zinc- and cadmium-binding proteins in *Escherichia coli* by gel electrophoresis and laser ablation-inductively coupled plasma-mass spectrometry. *Analytical Biochemistry* **2003**, 318, 30-38

12. Sessler, N.; Krug, K.; Nordheim, A.; Mordmuller, B.; Macek, B., Analysis of the *Plasmodium falciparum* proteasome using Blue Native PAGE and label-free quantitative mass spectrometry. *Amino Acids* **2012**, 43, 1119-1129

13. Remmerie, N.; De Vijder, T.; Valkenborg, D.; Laukens, K.; Smets, K.; Vreeken, J.; Mertens, I.; Carpentier, C.; Panis, B.; De Jaeger, G.; Blust, R.; Prinsen, E.; Witters, E., Unraveling tobacco BY-2 protein complexes with BN PAGE/LC-MS/MS and clustering methods. *Journal of Proteomics* **2011**, 74, 1201-1217

14. Thangthaeng, N.; Sumien, N.; Forster, M. J.; Shah, R. A.; Yan, L. J., Nongradient blue native gel analysis of serum proteins and in-gel detection of serum esterase activities. *Journal of Chromatography* **2011**, 879, 386-394

15. Ndimba, B.; Rafudeen, S.; Gehring, C.; Meyer, Z.; Simon, W.; Chivasa, S.; Slabas, A., Proteomic identification of an hsp70.1 protein induced in *Arabidopsis* cells following hyperosmotic stress treatments. *South African Journal of Science* **2005**, 101, 449-453

16. Hulce, J. J.; Cognetta, A. B.; Niphakis, M. J.; Tully, S. E.; Cravatt, B. F., Proteome-wide mapping of cholesterol-interaction proteins in mammalian cells. *Nature Methods* **2013**, 10, 3, 259-263

17. Kamal, A. H. M.; Cho, K.; Choi, J. S.; Bae, K. W.; Komatsu, S.; Uozumi, N.; Woo, S. H., The wheat chloroplastic proteome. *Journal of Proteomics* **2013**, 1-17

18. Merriam-Webster Dictionary. Retrieved from http://www.merriam webster.com/dictionary/proteomics

19. Andreini, C.; Banci, L.; Bertini, I.; Rosato, A., Counting the zinc-proteins encoded in the human genome. *Journal of Proteome Research* **2006,** *5* (1), 196-201.

20. Bertini, I.; Rosato, A., From genes to metalloproteins: A bioinformatic approach. *European Journal of Inorganic Chemistry* **2007**, (18), 2546-2555.

21. Human Genome Sequencing, C., Finishing the euchromatic sequence of the human genome. *Nature* **2004,** 431 (7011), 931-945.

22. Margoshes, M.; Vallee, B. L., A CADMIUM PROTEIN FROM EQUINE KIDNEY CORTEX. *Journal of the American Chemical Society* **1957**, 79 (17), 4813-4814.

23. Petering, D. H., In Metallothioneins: Synthesis, Structure and Properties of Metallothioneins: Phytochelatins, and Metal-Thiolate Complexes, Stillman, M.; Shaw, C. F.; Suzuki, K. T., Eds. VCH: New York: 1992; pp 164-183.

24. Krepkiy, D.; Forsterling, F. H.; Petering, D. H., Interaction of Cd2+ with Zn finger 3 of transcription factor IIIA: Structures and binding to cognate DNA. *Chemical Research in Toxicology* **2004**, 17 (7), 863-870.

25. Petering, D. H.; Loftsgaarden, J.; Schneider, J.; Fowler, B., Metabolism of cadmium, zinc and copper in the rat kidney: The role of metallothionein and other binding sites. *Environmental Health Perspectives* **1984**, 54, 73-81

26. Joachim, K. and Detlef, G., Review of the State-of-the-Art Lase Ablation Inductively Coupled Plasma Mass Spectrometry. *Applied Spectroscopy* **2011**, 65 (5), 155-162

27. Mokgalaka, N.S. and Gardea-Torresdey, J. L., Laser Ablation Inductively Coupled Plasma Mass Spectrometry: Principles and Applications. *Applied Spectroscopy Reviews* **2006**, 41, 131-150

28. Montaser, Akbar, Inductively Coupled Plasma Mass Spectrometry (1998) USA: Wiley-VCH

29. Andrews, J. C.; Nolan, J. P.; Hammerstedt, R. H.; Bavister, B. D., Characterization of N-(6-methoxy-8-quinolyl)-p-toluenesulfonamide for the detection of zinc in living sperm cells. *Cytometry* **1995**, 21 (2), 153-9.

30. Carvan, M. ; Heiden, T. ; and Tomasiewicz, H., Chapter 1 the utility of zebrafish as a model for toxicological research. *Biochemistry and Molecular Biology of Fishes* **2005**, 6, 3-41

31. Ali, M. M. U.; Roe, S. M.; Prodromou, C.; Pearl, L. H., Crystal Structure of an Hsp90-Nucleotide-P23/Sba1 Closed Chaperone Complex. *Nature* **2006**, 440, 1013

32. Strandberg, B.; Tilander, B.; Fridborg, K.; Lindskog, S.; Nyman, P. O., The crystallization and x-ray investigation of one form of human carbonic anhydrase. *J Mol Biol* **1962**, 5, 583-4.

33. Lindskog, S.; Malmstrom, B. G., Metal binding and catalytic activity in bovine carbonic anhydrase. *J Biol Chem* **1962**, 237, 1129-37.

34. Lindskog, S., Structure and mechanism of carbonic anhydrase. *Pharmacol Ther* **1997**, 74 (1), 1-20.

35. Zhang, A.; Hu, H.; Sanchez, B. N.; Ettinger, A. S.; Park, S. K.; Cantonwine. D.; Schnass, L.; Wright, R. O.; Lamadrid-Figueroa, H.; Tellez-Rojo, M. M., Association between Prenatal Lead Exposure and Blood Pressure in Children. *Environmental Health Perspectives* **2012**, 120, 445-450

36. Holland, S. L.; Simon, A. V., Chromate toxicity and the role of sulfur. *Metallomics* **2011**, 3, 1119-1123

37. Tapia-Rodriguez, A.; Luna-Velasco, A.; Field, J. A.; Sierra-Alvarez, R.; Toxicity of Uranium to Microbial Communities in Anaerobic Biofilms. *Water Air Soil Pollut.* **2012**, 223, 3859-3868